

Effects of Long-Term Creep on the Integrity of Modern Wood Structures

by

Jacem Tissaoui

Dissertation submitted to the Faculty of the
Virginia Polytechnic Institute and State University
in partial fulfillment of the requirements for the degree of
Doctor of Philosophy
in
Civil Engineering

Approved:

Siegfried M. Holzer, Co-Chair

Joseph R. Loferski, Co-Chair

David A. Dillard

Surot Thangjitham

Don A. Garst

December, 1996

Blacksburg, Virginia

Keywords: Creep, Wood, Structures, Finite Element, TTSP

Effects of Long Term Creep on the Integrity of Modern Wood Structures

by
Jacem Tissaoui

S. M. Holzer, Co-Chairman
J. R. Loferski, Co-Chairman
(ABSTRACT)

Short-term creep tests in tension and in compression were conducted on southern pine, Douglas-fir, yellow-poplar, and Parallam™ samples at temperatures ranging between 20 and 80°C and at 6, 9 and 12% moisture content. The principle of time-temperature superposition was applied to form a master curve that extended for a maximum of 2 years. The horizontal shift factors followed an Arrhenius relation with activation energies ranging between 75 and 130 kJ/mole. It was not possible to superpose the compliance curves at 70 and 80°C, this is attributed to the presence of multiple components in wood with different temperature dependence.

Long-term creep tests were also conducted in tension and in compression at 20°C and 12% moisture content for over 2 years. The resulting compliance curves were fitted to the power law equation using a nonlinear fitting procedure. The results were compared with those of the short-term creep tests.

Finite element analysis was conducted on selected wood structures to determine the effect of creep on serviceability and stability.

Acknowledgments

I am very grateful to Dr. S. M. Holzer for his continued support, encouragement, and guidance. I also thank Dr. J. R. Loferski for serving as Co-Chairman and for his help with the experimental part. Thanks are due to Dr. D. A. Dillard for his valuable contributions and suggestions. I also thank Dr. S. Thangjitham, Dr. D. A. Garst, and Dr. M. P. Wolcott for serving on my committee and for their helpful comments.

I thank Dr. R. L. Youngs and Dr. A. A. Trani for their support, and the technicians especially Denson Graham and Harold Vandivort for the excellent job they did in making the experimental fixtures.

I also thank Raul Andruet, Samruam Tongtoe, and Amara Loulizi for their friendship and support.

Finally I am grateful to my wife Luz and son Yassine for making my life in Blacksburg enjoyable.

Table of Contents

1. INTRODUCTION.....	1
1.1 BACKGROUND	1
1.2 RESEARCH NEEDS.....	3
1.3 SCOPE AND OBJECTIVES	3
1.4 SIGNIFICANCE.....	4
2. LITERATURE REVIEW.....	5
2.1 GLASS TRANSITION TEMPERATURE OF POLYMERS.....	5
2.2 GLASS TRANSITION TEMPERATURES FOR WOOD.....	7
2.3 THE PRINCIPLE OF TIME-TEMPERATURE SUPERPOSITION.....	10
2.4 THE PRINCIPLE OF TIME-MOISTURE SUPERPOSITION.....	13
2.5 APPLICATION OF TTSP TO WOOD	20
2.6 APPLICATION OF TTSP TO THERMORHEOLOGICALLY COMPLEX MATERIALS.....	21
2.7 CREEP MODELS	24
2.8 FINITE ELEMENT ANALYSIS FOR CREEP.....	26
2.8.1 Creep Models.....	26
2.8.2 Computer Programs.....	30
2.8.3 Creep Stability.....	30
2.8.4 Creep Analyses.....	31
3. EXPERIMENTAL.....	32
3.1 DYNAMIC TESTS USING THE DMA.....	32
3.2 SHORT-TERM CREEP TESTS.....	32
3.3 LONG-TERM CREEP TESTS.....	41
4. RESULTS.....	45
4.1 DYNAMIC TESTS	45
4.1.1 Fixed frequency tests.....	45
4.1.2 Creep Tests.....	51
4.2 SHORT-TERM CREEP TESTS.....	52
4.2.1 Difficulties.....	52
4.2.2 Creep in tension.....	53
4.2.3 Creep in compression.....	62
4.2.4 Time-moisture superposition creep test.....	74
4.3 LONG-TERM CREEP TESTS.....	77
4.3.1 Creep in tension.....	78
4.3.2 Analytical Criterion for the application of TTSP to wood.....	88
4.3.3 Comparison between short-term and long-term results.....	94
4.4 FINITE ELEMENT ANALYSIS.....	95
4.4.1 Creep model using time hardening model.....	95
4.4.2 Creep model with user subroutine.....	96
4.4.3 Incorporation of the creep law from experimental analysis.....	97
4.4.4 Creep analysis checking.....	98
4.4.5 Analysis of a truss for creep.....	101
4.4.6 Finite element analysis for stability.....	105
5. CONCLUSIONS AND RECOMMENDATIONS	113
5.1 CONCLUSIONS.....	113
5.2 RECOMMENDATIONS.....	113
6. REFERENCES.....	115

List Of Illustrations

FIGURE 1.1 (A) CREEP, (B) STRESS RELAXATION, (C) RECOVERY.....	2
FIGURE 2.1 MODULUS (E) AS A FUNCTION OF TEMPERATURE FOR A TYPICAL AMORPHOUS POLYMER.....	6
FIGURE 2.2 STORAGE MODULUS (E') FOR MAPLE AND SPRUCE AT 10% MOISTURE CONTENT (KELLY ET AL. 1987)8	
FIGURE 2.3 LOSS TANGENT (TAN δ) FOR MAPLE AND SPRUCE AT 10% MOISTURE CONTENT (KELLY ET AL. 1987)..8	
FIGURE 2.4 GLASS TRANSITION TEMPERATURES OF IN-SITU LIGNIN (1) AND HEMICELLULOSE (2) AS A FUNCTION OF MOISTURE CONTENT (KELLY ET AL. 1987).....	9
FIGURE 2.5 CONSTRUCTION OF THE MASTER CURVE FROM EXPERIMENTAL MODULUS CURVES AT VARIOUS TEMPERATURES (AKLONIS AND MACKNIGHT 1983).....	11
FIGURE 2.6 EFFECT OF RELATIVE HUMIDITY AND TEMPERATURE ON RELATIVE CREEP OF UF CHIPBOARD, PLYWOOD, AND SCOTS PINE.....	13
FIGURE 2.7 COMPLIANCE CURVES FOR PVAC AT 0% MOISTURE CONTENT AND AT DIFFERENT TEMPERATURES (EMRI AND PAVSEK, 1992).....	15
FIGURE 2.8 MASTER CURVE FROM TTSP FOR PVAC AT 0% MOISTURE CONTENT (EMRI AND PAVSEK, 1992)...16	
FIGURE 2.9 COMPLIANCE CURVES FOR PVAC AT 20°C AND AT DIFFERENT MOISTURE CONTENTS (EMRI AND PAVSEK, 1992).....	17
FIGURE 2.10 MASTER CURVE FROM TMSP FOR PVAC AT 20°C (EMRI AND PAVSEK, 1992).....	18
FIGURE 2.11 RELAXATION MODULUS CURVES AT DIFFERENT TEMPERATURES FOR PVA (ONOGI ET AL, 1962)..18	
FIGURE 2.12 RELAXATION MODULUS CURVES AT DIFFERENT RELATIVE HUMIDITIES FOR PVA (ONOGI ET AL, 1962).....	19
FIGURE 2.13 MASTER CURVE FROM TMSP AT 20°C FOR PVA (ONOGI ET AL, 1962).....	19
FIGURE 2.14 SUPERPOSITION ON THE TIME AXIS FOR THERMORHEOLOGICALLY COMPLEX MATERIALS.....	23
FIGURE 2.15 SUPERPOSITION ALONG THE TEMPERATURE AXIS.....	24
FIGURE 2.16 TIME AND STRAIN HARDENING RESPONSES TO VARIABLE STRESS.....	29
FIGURE 3.1 TENSION TEST APPARATUS.....	34
FIGURE 3.2 CREEP APPARATUS (A) TENSION, (B) COMPRESSION.....	35
FIGURE 3.3 LOG TIME AXIS (SECONDS).....	37
FIGURE 3.4 MECHANICAL CONDITIONING OF SAMPLE 1 AT 25°C.....	38
FIGURE 3.5 MECHANICAL CONDITIONING OF SAMPLE 2 AT 25°C.....	39
FIGURE 3.6 MECHANICAL CONDITIONING OF SAMPLE 3 AT 25°C.....	40
FIGURE 3.7 (A) ACTIVE AND DUMMY SPECIMENS; (B) WHEATSTONE BRIDGE.....	41
FIGURE 3.8 SAMPLE ARRANGEMENT FOR THE LONG-TERM CREEP TESTS.....	43
FIGURE 3.9 LONG-TERM CREEP TEST SETUP.....	44
FIGURE 4.1 LOSS TANGENT FOR PAINTED AND UNPAINTED SOUTHERN PINE SAMPLES.....	46
FIGURE 4.2 LOSS TANGENT FOR PAINTED AND UNPAINTED DOUGLAS-FIR SAMPLES.....	47
FIGURE 4.3 LOSS TANGENT FOR YELLOW-POPLAR AT 5, 7, AND 9% MOISTURE CONTENTS.....	48
FIGURE 4.4 LOSS TANGENT FOR SOUTHERN PINE AT 13.0 AND 9% MOISTURE CONTENTS.....	49
FIGURE 4.5 LOSS TANGENT FOR DOUGLAS-FIR AT 12.5 AND 9.5% MOISTURE CONTENTS.....	50
FIGURE 4.6 COMPLIANCE CURVES FOR YELLOW-POPLAR AT 5% MOISTURE CONTENT.....	51
FIGURE 4.7 COMPLIANCE CURVES FOR YELLOW-POPLAR AT 7% MOISTURE CONTENT.....	52
FIGURE 4.8 (A) COMPLIANCE AND (B) MASTER CURVES FOR YELLOW-POPLAR AT 6% MOISTURE CONTENT (TENSION).....	55
FIGURE 4.9 HORIZONTAL SHIFT FACTORS (TENSION).....	55
FIGURE 4.10 MASTER CURVE AND POWER LAW FIT (TENSION).....	56
FIGURE 4.11 TEMPERATURE AND RELATIVE HUMIDITY DURING THE TEST.....	57
FIGURE 4.12 COMPLIANCE AND MASTER CURVES FOR SOUTHERN PINE AT 6% MOISTURE CONTENT (TENSION). 57	
FIGURE 4.13 HORIZONTAL SHIFT FACTORS FOR SOUTHERN PINE, DH=74.6 KJ/MOLE.....	58
FIGURE 4.14 COMPLIANCE AND MASTER CURVES FOR YELLOW-POPLAR AT 6% MOISTURE CONTENT (TENSION)59	
FIGURE 4.15 HORIZONTAL SHIFT FACTORS FOR YELLOW-POPLAR, DH=128.0 KJ/MOLE.....	60
FIGURE 4.16 COMPLIANCE AND MASTER CURVES FOR FIRST AT 6% MOISTURE CONTENT (TENSION).....	61
FIGURE 4.17 HORIZONTAL SHIFT FACTORS, DH=90.7 KJ/MOLE.....	62

FIGURE 4.18 (A) COMPLIANCE AND (B) MASTER CURVES FOR DOUGLAS-FIR AT 9% MOISTURE CONTENT (COMPRESSION).....	64
FIGURE 4.19 HORIZONTAL SHIFT FACTORS (COMPRESSION).....	65
FIGURE 4.20 MASTER CURVE AND POWER LAW FIT (COMPRESSION).....	65
FIGURE 4.21 TEMPERATURE AND RELATIVE HUMIDITY DURING THE TEST.....	66
FIGURE 4.22 COMPLIANCE AND MASTER CURVES FOR SOUTHERN PINE AT 9% MOISTURE CONTENT (COMPRESSION).....	67
FIGURE 4.23 HORIZONTAL SHIFT FACTORS FOR SOUTHERN PINE AT 9% MOISTURE CONTENT, H = 108.7 KJ/MOLE.....	68
FIGURE 4.24 COMPLIANCE AND MASTER CURVES FOR DOUGLAS-FIR AT 9% MOISTURE CONTENT (COMPRESSION).....	69
FIGURE 4.25 HORIZONTAL SHIFT FACTORS FOR DOUGLAS-FIR AT 9% MOISTURE CONTENT, H= 109.0 KJ/MOLE.....	70
FIGURE 4.26 COMPLIANCE AND MASTER CURVES FOR PARALLAM™ AT 9% MOISTURE CONTENT (COMPRESSION).....	71
FIGURE 4.27 HORIZONTAL SHIFT FACTORS FOR PARALLAM™ AT 9% MOISTURE CONTENT,.....	72
FIGURE 4.28 COMPLIANCE AND MASTER CURVES FOR THE YELLOW-POPLAR SAMPLE.....	74
FIGURE 4.29 COMPLIANCE AND MASTER CURVES FOR THE KILN DRIED SOUTHERN YELLOW PINE SAMPLE (MC _{REF} = 5.21%).....	75
FIGURE 4.30 COMPLIANCE AND MASTER CURVES FOR THE AIR DRIED SOUTHERN YELLOW PINE SAMPLE (MC _{REF} = 5.21%).....	76
FIGURE 4.31 ACTUAL (SYMBOLS) AND POWER LAW FIT (SOLID LINE) FOR THREE SOUTHERN PINE SPECIMENS IN TENSION.....	78
FIGURE 4.32 NORMALIZED COMPLIANCE CURVES FOR THREE SOUTHERN PINE SPECIMENS IN TENSION.....	79
FIGURE 4.33 ACTUAL (SYMBOLS) AND POWER LAW FIT (SOLID LINE) FOR TWO YELLOW-POPLAR SPECIMENS IN TENSION.....	80
FIGURE 4.34 NORMALIZED COMPLIANCE CURVES FOR TWO YELLOW-POPLAR SPECIMENS IN TENSION.....	81
FIGURE 4.35 ACTUAL (SYMBOLS) AND POWER LAW FIT (SOLID LINE) FOR THREE SOUTHERN PINE SPECIMENS IN COMPRESSION.....	82
FIGURE 4.36 NORMALIZED COMPLIANCE CURVES FOR THREE SOUTHERN PINE SPECIMENS IN COMPRESSION... 83	83
FIGURE 4.37 ACTUAL (SYMBOLS) AND POWER LAW FIT (SOLID LINE) FOR FOUR YELLOW-POPLAR SPECIMENS IN COMPRESSION.....	84
FIGURE 4.38 NORMALIZED COMPLIANCE CURVES FOR FOUR YELLOW-POPLAR SPECIMENS IN COMPRESSION... 85	85
FIGURE 4.39 ACTUAL (SYMBOLS) AND POWER LAW FIT (SOLID LINE) FOR FOUR DOUGLAS-FIR SPECIMENS IN COMPRESSION.....	86
FIGURE 4.40 NORMALIZED COMPLIANCE CURVES FOR FOUR DOUGLAS-FIR SPECIMENS IN COMPRESSION..... 87	87
FIGURE 4.41 COMPARISON OF THE LONG-TERM CREEP IN COMPRESSION AND IN TENSION FOR (A) SOUTHERN PINE AND (B) YELLOW-POPLAR.....	88
FIGURE 4.42 CREEP CURVES FOR YELLOW-POPLAR IN TENSION AT 9% MOISTURE CONTENT.....	89
FIGURE 4.43 FITTED CREEP CURVES FOR YELLOW-POPLAR (TTSP).....	90
FIGURE 4.44 $\frac{d \log D}{d \log t}$ VS. LOG T FOR YELLOW-POPLAR (TTSP).....	91
FIGURE 4.45 $\frac{d \log D}{d \log t}$ VS. LOG T FOR YELLOW-POPLAR (TMSP).....	92
FIGURE 4.46 $\frac{d \log D}{d \log t}$ VS. LOG T (TMSP).....	93
FIGURE 4.47 NORMALIZED SHORT-TERM AND LONG-TERM COMPLIANCE CURVES FOR SOUTHERN PINE IN COMPRESSION.....	94
FIGURE 4.48 NORMALIZED SHORT-TERM AND LONG-TERM COMPLIANCE CURVES FOR YELLOW-POPLAR IN TENSION.....	95
FIGURE 4.49 ABAQUS AND EXPERIMENTAL RESULTS FOR A TRUSS ELEMENT IN TENSION.....	100
FIGURE 4.50 ROOF TRUSS.....	101
FIGURE 4.51 DISPLACEMENT AT MIDDLE OF BOTTOM CHORD.....	103

FIGURE 4.52 CREEP DEFLECTION AS A PERCENTAGE OF ELASTIC DEFLECTION.....	104
FIGURE 4.53 GEOMETRY OF THE A-FRAME (CROSS SECTIONAL AREA = 1 IN ²).....	105
FIGURE 4.54 LOAD DEFLECTION PATH AT THE APEX.....	105
FIGURE 4.55 LONG TERM RESPONSE OF THE FRAME UNDER 50% OF SHORT TERM CRITICAL LOAD.....	106
FIGURE 4.56 (A) GEOMETRY AND (B) CROSS SECTION OF THREE HINGED ARCH.....	108
FIGURE 4.57 CREEP DISPLACEMENTS AT THE APEX.....	108
FIGURE 4.58 VARAX DOME GEOMETRY.....	110
FIGURE 4.59 BUCKLED SHAPE OF THE DOME.....	111
FIGURE 4.60 VERTICAL DISPLACEMENT AT THE DOME APEX.....	112

List of Tables

TABLE 3.1 RELATIVE HUMIDITY REQUIRED TO MAINTAIN A 12% MOISTURE CONTENT.....	36
TABLE 3.2 NUMBER OF SAMPLES IN THE LONG-TERM CREEP TEST.....	41
TABLE 4.1 MOISTURE LOSS DURING FIXED FREQUENCY TEST (25 TO 80°C AT 2°C / MINUTE).....	45
TABLE 4.2 MOISTURE LOSS DURING FIXED FREQUENCY TEST FOR PAINTED SAMPLES (25 TO 80°C AT 2°C / MINUTE).....	45
TABLE 4.3 POWER LAW PARAMETERS FOR SOUTHERN PINE, YELLOW-POPLAR, AND DOUGLAS-FIR AT 6% MOISTURE CONTENT IN TENSION.....	62
TABLE 4.4 POWER LAW PARAMETERS FOR SOUTHERN PINE, DOUGLAS-FIR, AND PARALLAM™ AT 6% MOISTURE CONTENT.....	72
TABLE 4.5 POWER LAW EQUATION PARAMETERS FOR TENSION FROM LONG-TERM TESTING.....	77
TABLE 4.6 POWER LAW EQUATION PARAMETERS FOR COMPRESSION FROM LONG-TERM TESTING.....	77
TABLE 4.7 CREEP PARAMETERS USED IN FINITE ELEMENT ANALYSIS OF THE VARAX DOME.....	111

1. INTRODUCTION

1.1 Background

Viscoelastic materials exhibit properties that are common to both perfect solids and perfect liquids. As a result, the stress is proportional to the strain, the rate of strain, and possibly higher time derivatives of strain; when the stress is linearly proportional to strain, the material is termed linearly viscoelastic (Sharma 1965). A constitutive equation for such materials must correctly represent the behavior under well known conditions of stress and strain. These conditions are creep, stress relaxation, recovery, constant rate stressing, and constant rate straining (Williams 1980). Creep is the continued deformation under a constant stress while stress relaxation is the reduction in stress with time under a prescribed strain. Recovery occurs when the strain decreases as the stress is removed (Figure 1.1).

Because wood is a viscoelastic material at normal operating stress, temperature, and moisture content (Van Der Put 1989), it is susceptible to creep which can lead to serviceability and strength reduction problems. Although the creep behavior of wood has been extensively studied, no long-term creep model (50 years) exists. Current design practices (NDS 1986; AITC 1985) account for creep by magnifying the dead load deflections using empirical factors. Creep in wood structures can lead to serviceability problems due to excessive deformations or to safety problems due to strength reduction. Modern wood structures such as lattice domes and arches are particularly prone to instability (snap-through or torsional instability). Long-term creep can lead to instability by magnifying the short-term deflections.

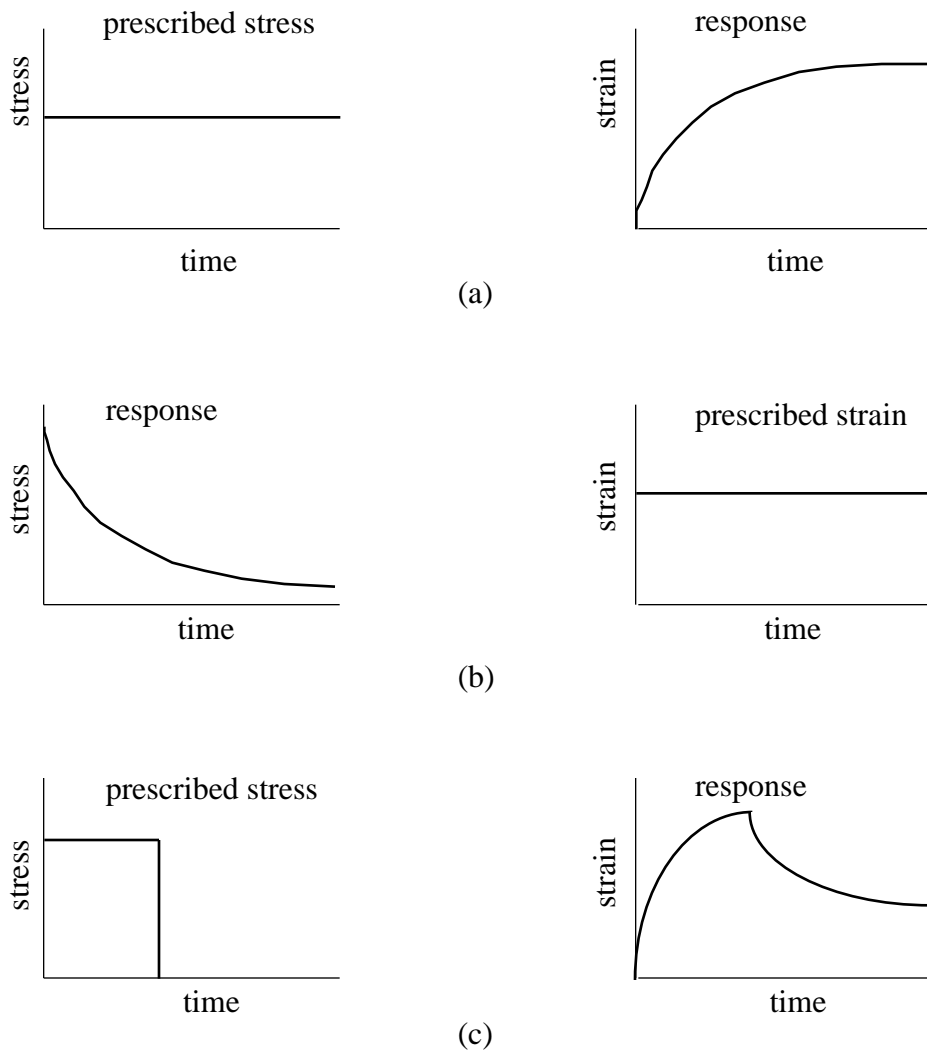


Figure 1.1 (a) creep, (b) stress relaxation, (c) recovery.

1.2 Research Needs

As reliability based design replaces traditional design practices, a long-term creep law for wood becomes necessary to account for the time-dependent behavior of wood. However, most of the creep data was obtained from bending tests which represent member behavior rather than material behavior (Holzer et al. 1989). There is also a lack of information about the long-term behavior of structural composite lumber. For example, in a report on creep rupture testing of Parallam™ at MacMillan Bloedel Ltd., Bledsoe et al. (1990) emphasize that static testing alone cannot guarantee the long-time performance of composite materials. Two Parallam™ products that were obtained using different pressing strategies had different creep and creep rupture behavior in spite of their similar moduli of rupture.

Moreover, in the 1991 proceedings of the NATO advanced research workshop on reliability-based design of engineered wood structures (Bodig 1992), the group on material resistance considerations identified the long-term behavior of structural composite lumber as an area where research is needed:

"Improvements must be sought in our knowledge of the long-term behavior of non-lumber materials. This information could help improve structural modeling, and also clarify questions of the linkages between strength degradation and creep, as well as the interaction between environmental effects, threshold levels for strength, upper limits of creep deformations, etc."

Furthermore, Leichti et al. (1990) cite the lack of information about the long-term behavior and durability of structural wood composites as the main reason why designers are reluctant to use them in primary structural applications.

The principle of time-temperature superposition (TTSP) can be used to obtain a long-term creep law from a series of short-term tests at different temperatures. Although the principle has been used for man-made polymers, very little research has been conducted to investigate its applicability to wood.

1.3 Scope and Objectives

The main goal of the study is to investigate the long-term behavior of plane and spatial wood structures. To achieve this goal, the following is needed:

- 1• To determine whether and under what conditions TTSP is valid for wood and wood composites. For this study, two common structural softwoods, southern yellow pine (*Pinus spp.*) and Douglas-fir (*Pseudotsuga menziesii*), a hardwood, yellow-poplar (*Liriodendron tulipifera*), and a structural composite lumber, parallel strand lumber (Parallam™) were tested.
- 2• To obtain long term creep laws for different types of wood and modern wood composites by using TTSP to construct master curves from short-term creep tests.
- 3• To verify the long term creep laws obtained by comparing them to those in the literature and to long-term creep test results.
- 4• To use the creep laws obtained to conduct finite elements analyses on some simple and complex wood structures.

1.4 Significance

The principles of time-temperature superposition and time-moisture superposition will be used to develop master curves to predict the long-term behavior of solid lumber and structural composite lumber for various temperatures and moisture contents. This can be useful for conducting creep studies on structural members or systems using finite element analysis. Furthermore, the procedure can be used to compare the long-term behavior of different structural composite lumber products. This could also be a useful tool in the development and evaluation of new composites.

2. LITERATURE REVIEW

A great body of literature exists on the topic of creep in wood; however, very little research was conducted to study the application of TTSP to wood. This literature review is first focused on transitions in wood and the application of TTSP to wood. Then creep modeling, creep analysis using finite element analysis, and instability due to creep are addressed.

2.1 Glass transition temperature of polymers

The behavior of polymers is strongly dependent on temperature. Figure 2.1 shows the typical behavior of an amorphous polymer undergoing a temperature increase. At low temperatures, the polymer is in a glassy phase characterized by high modulus of relaxation values and brittle behavior. The only molecular motion possible is vibration around fixed positions because the thermal energy is insufficient to surmount the barriers to rotation and translation (Aklonis and MacKnight 1983). As the temperature is increased, more energy is available and rotation and translation become possible. The polymer then behaves as a resilient leather characterized by a sharp drop in the relaxation modulus. This region is known as the transition region and the temperature as the glass transition temperature (T_g). Following the transition region, the modulus reaches a plateau region followed by flow for linear polymers and a slight increase in modulus for crosslinked polymers.

Several methods are available for determining the glass transition temperature of polymers. Dilatometry, calorimetry (Differential scanning calorimetry), and dynamic (mechanical, electrical, and thermal) methods have been used to determine T_g of polymers. The results obtained from different tests vary depending on the parameters used. Some of the factors affecting T_g are the heating/cooling rate and the plasticizer content (e.g., water in wood).

The behavior of complex polymer systems such as polymer blends is not as simple as that of a simple polymer. Polymer blends such as wood, are characterized by multiple transition temperatures corresponding to the different components of the polymer.

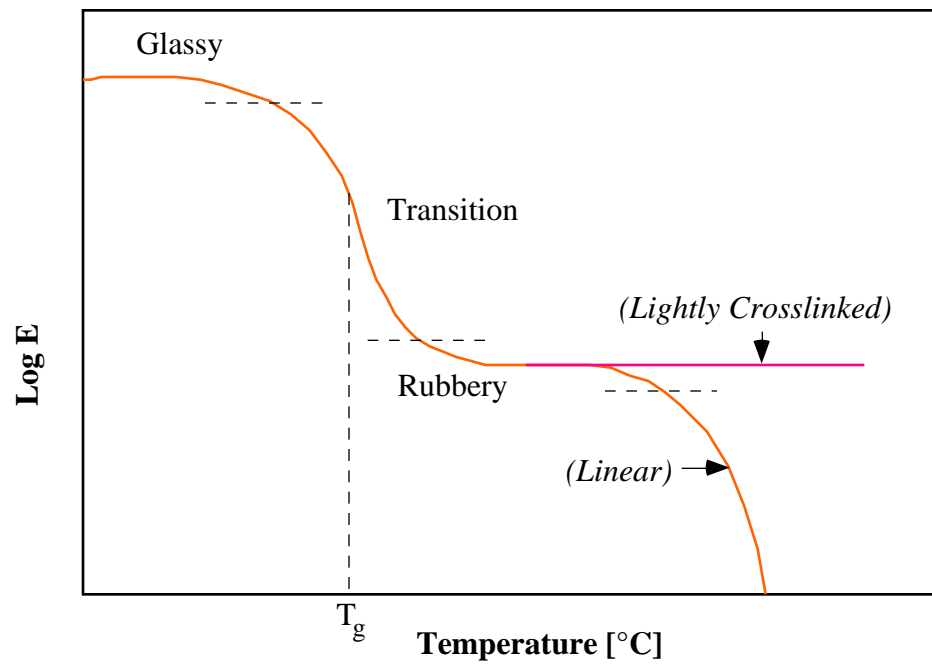


Figure 2.1 Modulus (E) as a function of temperature for a typical amorphous polymer.

2.2 Glass transition temperatures for wood

Wood is a bio-composite consisting of three structural components: cellulose, hemicellulose, and lignin. Cellulose molecules are long chains of glucose units which lie parallel to each other to form crystals; within the crystalline regions of cellulose, there are regions of amorphous cellulose. Hemicellulose is a branched amorphous polymer consisting of two carbohydrate polymers. Lignin is a complex three-dimensional phenolic polymer characterized by its water repellency (Bodig and Jayne 1982). The three constituents are similar to a fiber composite with the crystalline cellulose constituting the fiber component and the amorphous cellulose, lignin and hemicellulose, forming the matrix (Desh and Dinwoodie 1981); the hemicellulose acts as a binding agent between the cellulose and the lignin.

Two methods have been used to determine the glass transition temperatures of hemicellulose and lignin: the first consists of testing extracted lignin and hemicellulose (Sakata and Senju 1975, Irvine 1984), while the second consists of in-situ testing (Salmèn 1984, Kelly et al. 1987). Kelly et al. used a Polymer Laboratories' Dynamic Mechanical Thermal Analyzer (DMTA) to study the storage modulus (E') and the loss tangent ($\tan \delta$) for two species of wood, sitka spruce (*Picea sitchensis*) and sugar maple (*Acer saccharum*), with different diluents. The specimens were tested at temperatures between -140 and 150 °C with a heating rate of 5°C/min, a frequency of 1Hz, and a strain level of 1%. The authors determined three transition regions (Figures 2.2, 2.3): the first is a transition at temperatures between -90 and -110°C, followed by a shoulder δ_2 between 10 and 60°C and a peak δ_1 between 80 and 100°C. The values of the transition temperatures δ_1 and δ_2 at various moisture contents were fit to the Kwei model and the results are shown in Figure 2.4. At 0% moisture content, the glass transition temperature of both lignin and hemicellulose is assumed to be 200°C, a temperature near which degradation takes place. The glass transition temperature of lignin decreases with increasing moisture content but starts to reach a plateau at 70°C near 10 to 15% moisture content. The Tg of hemicellulose, however, continues to decrease with increasing moisture content with a value of -20°C near 30% moisture content.

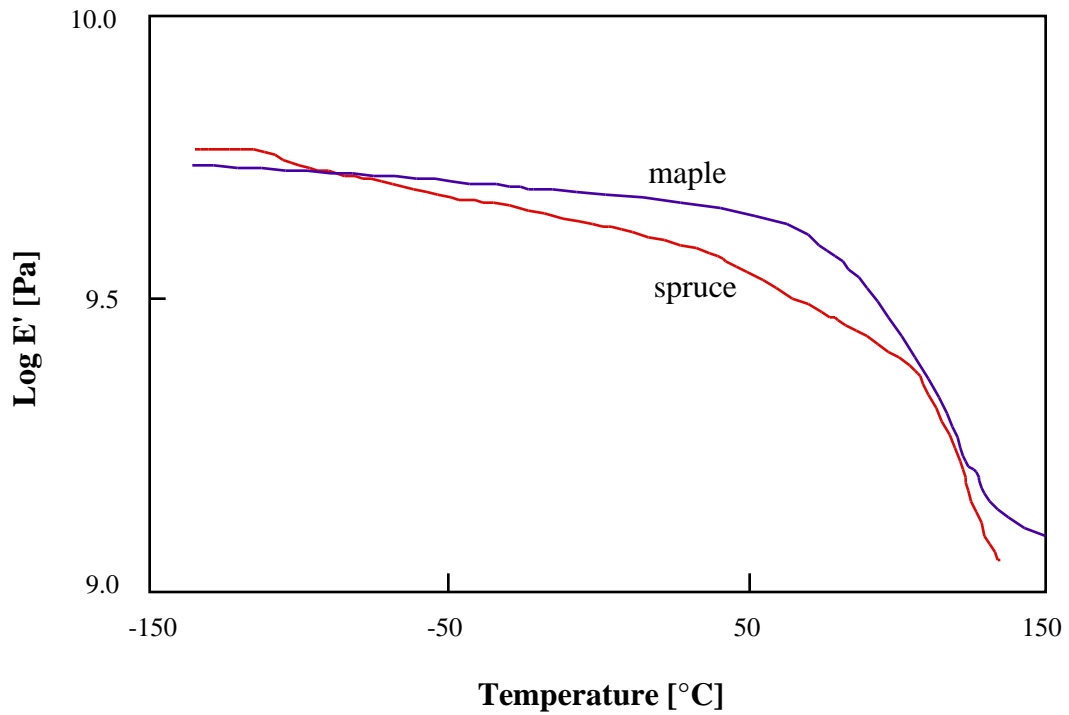


Figure 2.2 Storage Modulus (E') for maple and spruce at 10% moisture content (Kelly et al. 1987)

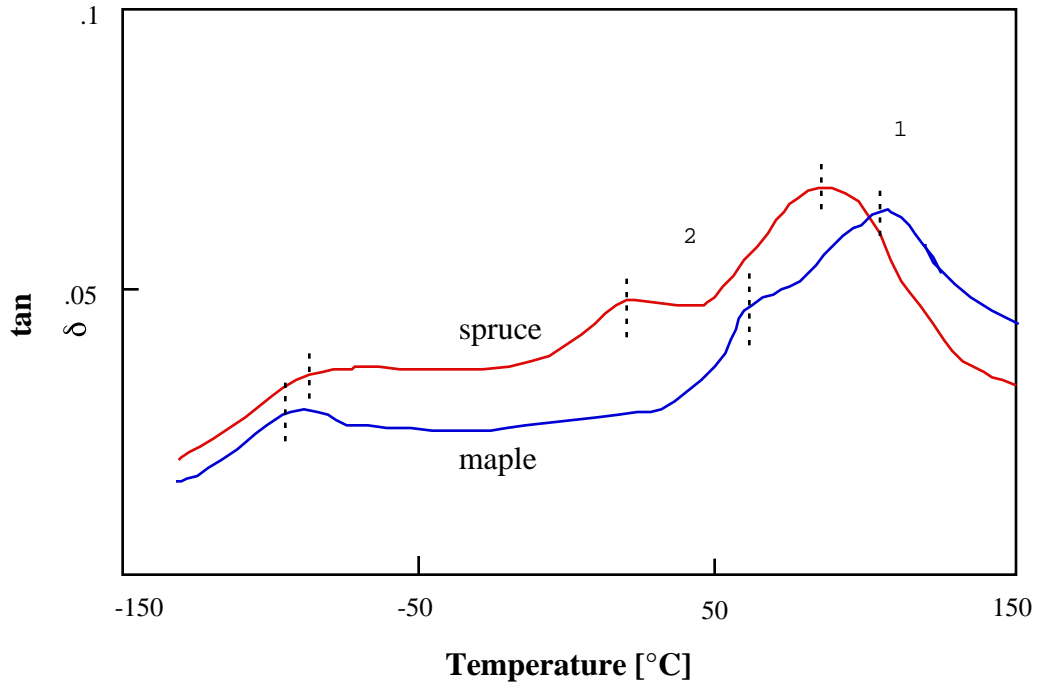


Figure 2.3 Loss Tangent ($\tan \delta$) for maple and spruce at 10% moisture content (Kelly et al. 1987)

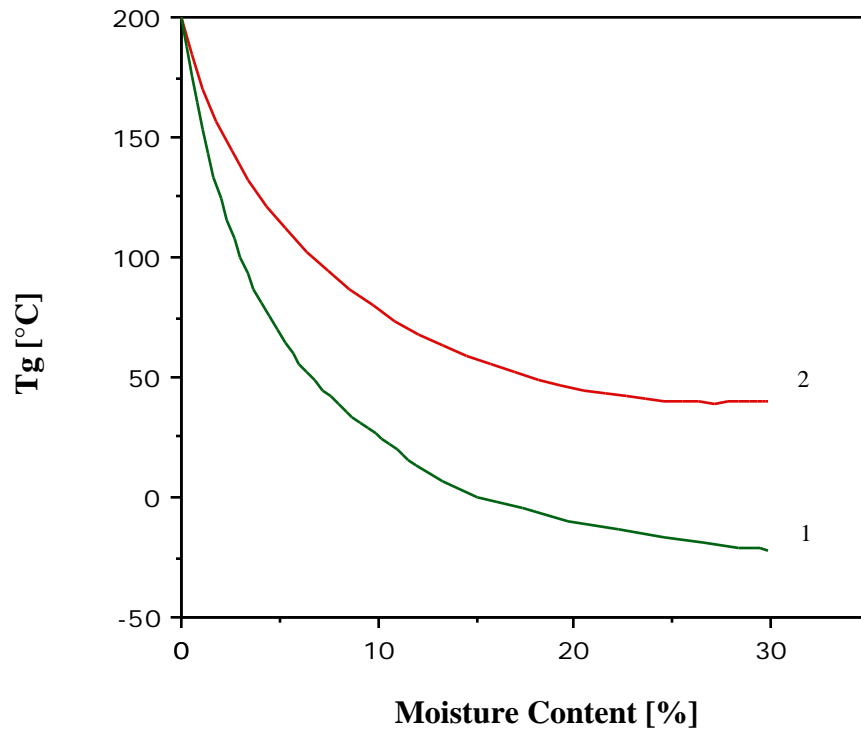


Figure 2.4 Glass transition temperatures of in-situ lignin ($\alpha 1$) and hemicellulose ($\alpha 2$) as a function of moisture content (Kelly et al. 1987).

2.3 The principle of time-temperature superposition

To determine the long-term behavior of polymers, one can either conduct experiments for an extended period of time or use the principle of time-temperature superposition to construct a master curve from a number of short-term creep tests at different temperatures.

The principle of time-temperature superposition has been used for a number of years to describe long-term behavior of polymers. The experimental procedure is well established; it is explained by Aklonis and Macknight (1983). Since the modulus of a polymer depends on temperature as well as time, one can measure the response at constant temperatures and variable time, then horizontally shift the curves to form a master curve in a logarithmic scale (figure 2.5). A reference temperature T_0 is chosen and the modulus/compliance vs. time curves for temperatures different than the reference temperature are horizontally shifted in such a manner that they join to form a smooth curve called the master curve. The mathematical formulation is expressed as

$$E(T_0, t) = E(T_1, t/a_T) \quad (2.1)$$

Because of the inherent change in the modulus and density with temperature, the curves need to be shifted vertically in order to match. Equation 2.1 is modified to account for the vertical shifting. This leads to the relations

$$\frac{E(T_0, t)}{\rho(T_0)T_0} = \frac{E(T_1, t/a_T)}{\rho(T_1)T_1} \quad (2.2)$$

$$E(T_0, t) = \frac{\rho(T_0)T_0}{\rho(T_1)T_1} E(T_1, t/a_T) \quad (2.3)$$

Ferry (1980) proposed criteria for the application of the principle of time-temperature superposition. The first one is that adjacent curves match exactly over a reasonable distance. The second criterion is that the same values of the shift factor a_T must superpose all the viscoelastic functions. Finally, the shift factor's dependence on temperature should follow established relations. The shift factor follows either of two forms, the WLF equation or an Arrhenius relation. The WLF equation

$$\text{Log} a_T = \frac{-C_1 T - T_g}{C_2 + T - T_g} \quad (2.4)$$

is associated with transition, plateau, and terminal regions of the time scale. The constants C_1 and C_2 depend on the polymer; however, universal values of 17.4 and 51.6 for C_1 and C_2 respectively are commonly used (Aklonis and Macknight 1983).

In the glassy region, the horizontal shift factors follow an Arrhenius relation of the form

$$a_T = \exp \left[-\frac{E}{R} \left(\frac{1}{T} - \frac{1}{T_{ref}} \right) \right] \quad (2.5)$$

$$\text{Log} a_T = -\frac{E}{2.303R} \left(\frac{1}{T} - \frac{1}{T_{ref}} \right) \quad (2.6)$$

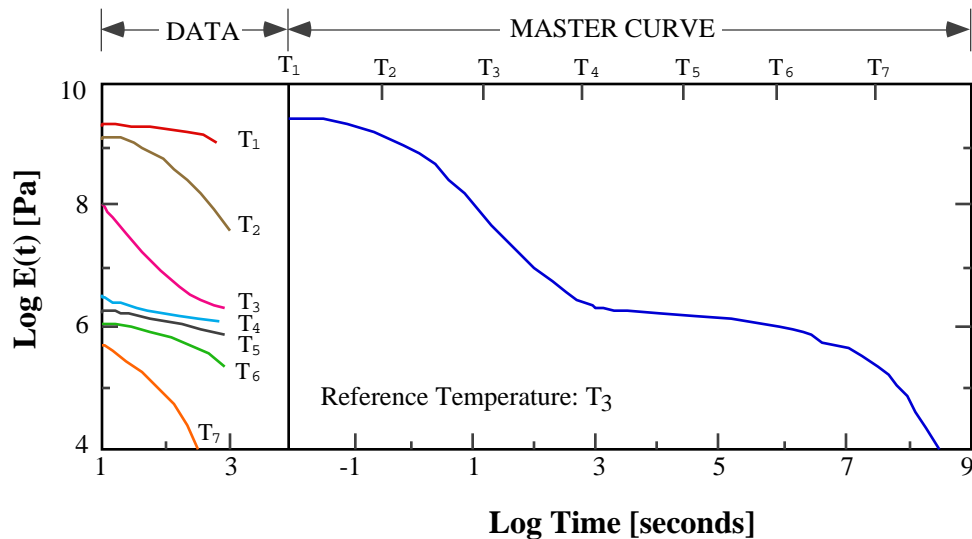


Figure 2.5 Construction of the master curve from experimental modulus curves at various temperatures (Aklonis and MacKnight 1983).

where

E	Activation energy	[Kcal/mole]
R	Gas constant	1.986 cal/mole/K
T	Temperature	K
T _{ref}	Reference temperature	K

Povolo and Fontelos (1987) proposed a more rigorous approach to determine whether TTSP is successful by studying the curves to determine if they are related by scaling. Letting (x,y;T) describe a set of curves in the (x,y) plane at different temperatures(e.g., creep compliance vs. time at different levels of temperature), then TTSP can be applied if the curves can be described by the following equation

$$g (Ax + By + C h(T)) = ax + by + c h(T) + d \quad (2.7)$$

where g is a real continuous and differentiable function; A, B, C, D, a, b, c, d are real constants; and h(T) is a real function of the temperature. The translation path is given by

$$y/x = \frac{Ac - Ca}{Cb - Bc} \quad (2.8)$$

To avoid the graphical procedure usually used to obtain the master curve, Yen and Williamson (1990) used an analytical approach to determine the horizontal and vertical shift factors. The Findley (1944) power law equation

$$\epsilon = \epsilon_0 + mt^n \quad (2.9)$$

is used to express the creep strain as a function of the instantaneous strain ϵ_0 , the transient creep m, and the time exponent n.

It is then assumed that the time exponent is independent of stress and temperature and the creep curves are fit to the Findley equation using the time exponent value from a reference temperature T_0 :

$$\epsilon(T,t) = \epsilon_0(T) + m(T)t^n \quad (2.10)$$

Using TTSP, the creep strain can be expressed as function of the parameters at the reference temperature.

$$\epsilon(T,t) = a_v [\epsilon_0(T_0) + m(T_0)(t/a_T)^n] \quad (2.11)$$

The horizontal and vertical shift factors are obtained by Equating (2.10) and (2.11) and separating the variables as follows:

$$a_V = \rho(T) / \rho(T_0) \tag{2.12}$$

$$a_T = [\rho(T) m(T_0) / \rho(T_0) m(T)]^{1/n}$$

This method yields good results as long as the time exponent is independent of the temperature; however, at high temperatures, the Findley equation with the time exponent from the reference temperature does not fit the experimental data very well (Yen and Williamson, 1990).

2.4 The Principle of Time-Moisture Superposition

Figure 2.6 shows the effect of varying moisture content and temperature on the creep behavior of solid wood as well as two wood composites (Dinwoodie, 1989). An increase in moisture accelerates creep, especially at relative

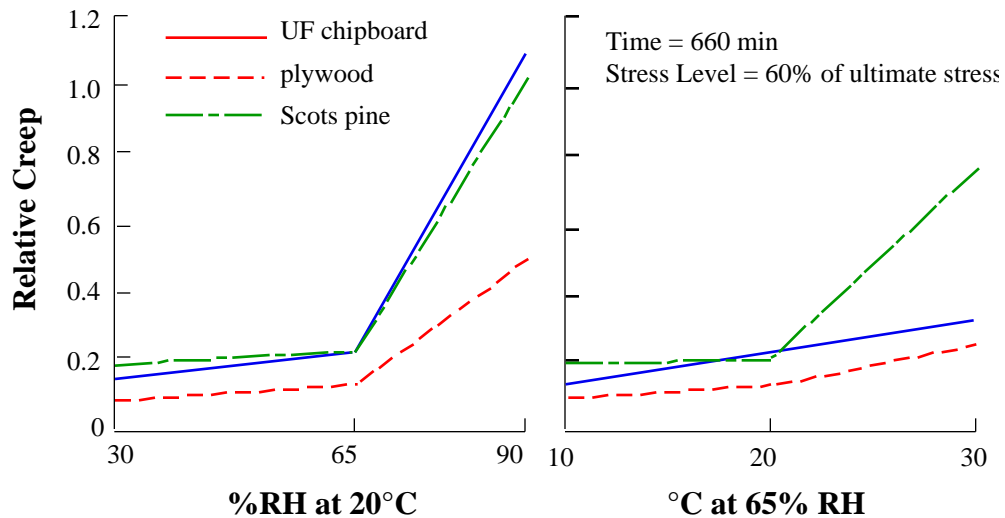


Figure 2.6 Effect of relative humidity and temperature on relative creep of UF chipboard, plywood, and Scots pine.

humidities above 65%. This creep acceleration due to increased moisture content leads to the possibility of applying a time-moisture equivalence scheme similar to time-temperature superposition where the temperature would be kept constant and the moisture content changed. Studies have been conducted to assess the applicability of the principle of time-moisture superposition to some polymers. Emri and Pavsek (1992) conducted time-temperature and time-moisture superposition experiments on polyvinyl acetate (PVAc) of medium molecular weight and a glass transition temperature of 30°C. The master curves at 20°C and zero moisture content were nearly identical. For the time-temperature experiment, samples were tested in torsion at zero moisture content at temperatures of 20, 26.4, 28.4, 30.6, 32.3, 34.4, and 35.8°C. Figure 2.7 shows the shear compliance curves and figure 2.8 shows the corresponding master curve. Similarly, torsion tests were conducted at 20°C and at moisture contents of 0, 0.74, 1.05, 1.29, 1.81, and 2.72%. The compliance curves are shown on figure 2.9 and the master curve on figure 2.10. Superimposing the two master curves shows that they are nearly identical; this leads the authors to conclude that the principle of time-moisture superposition can be applied to PVAc under the conditions considered in their experiments.

In an earlier study to check the applicability of the principle of time-moisture superposition to crystalline polymers, Onogi et al. (1962) conducted stress relaxation tests on polyvinyl alcohol (PVA) and nylon 6 films at various temperatures and moisture contents. For the PVA film with crystallinity of 36.0 and 47.3%, time-temperature superposition could not be applied, even with vertical shifts. Figure 2.11 shows the relaxation modulus curves at 0% relative humidity and temperatures of 20, 40, 60, 80, and 100°C. However, it was possible to superpose the relaxation modulus curves at 20°C and relative humidities of 0, 33, 45, 60, 65, and 75%, although the curves at the low and high humidities did not superpose very well. Figure 2.12 shows the relaxation curves and figure 2.13 shows the master curve.

For nylon 6 film, stress relaxation tests were conducted at 0% relative humidity and at temperatures ranging between 25 and 77°C. The curves at temperatures higher than 50°C superposed well while the curves at temperatures less than 50°C could not be superposed.

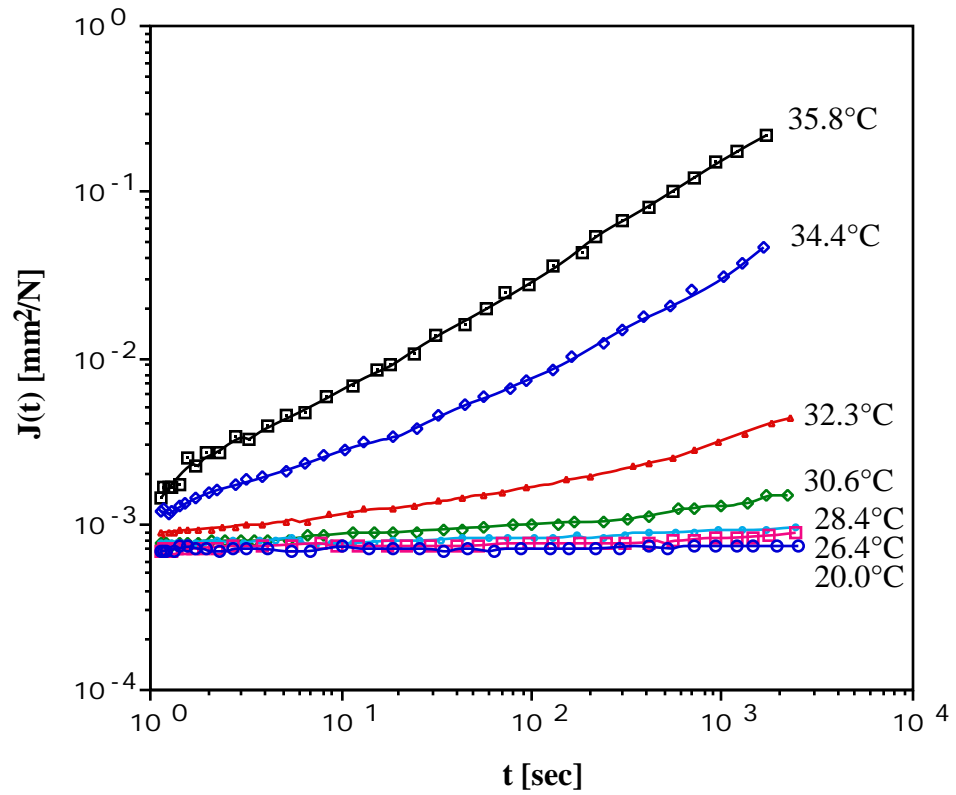


Figure 2.7 Compliance curves for PVAc at 0% moisture content and at different temperatures (Emri and Pavsek, 1992).

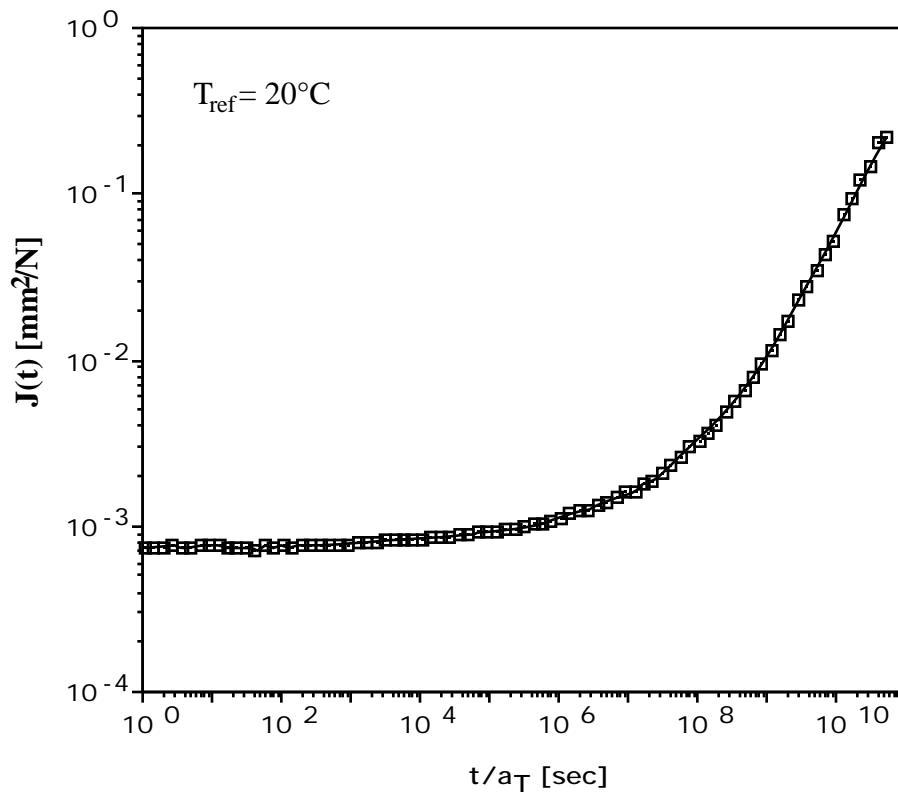


Figure 2.8 Master curve from TTSP for PVAc at 0% moisture content (Emri and Pavsek, 1992).

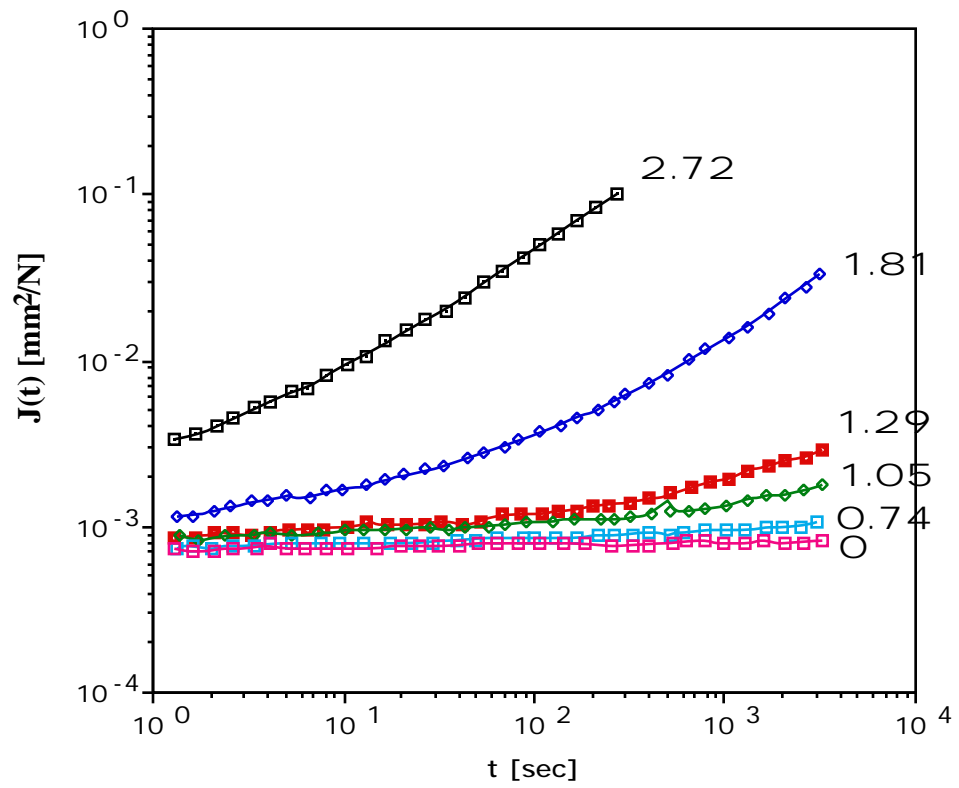


Figure 2.9 Compliance curves for PVAc at 20°C and at different moisture contents (Emri and Pavsek, 1992).

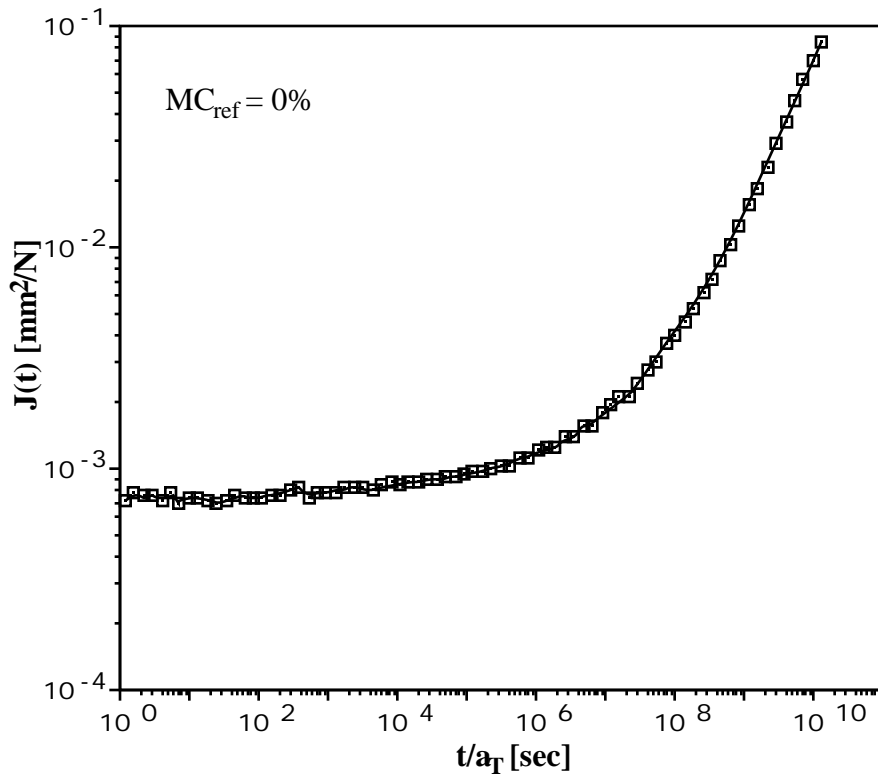


Figure 2.10 Master curve from TMS for PVAc at 20°C (Emri and Pavsek, 1992).

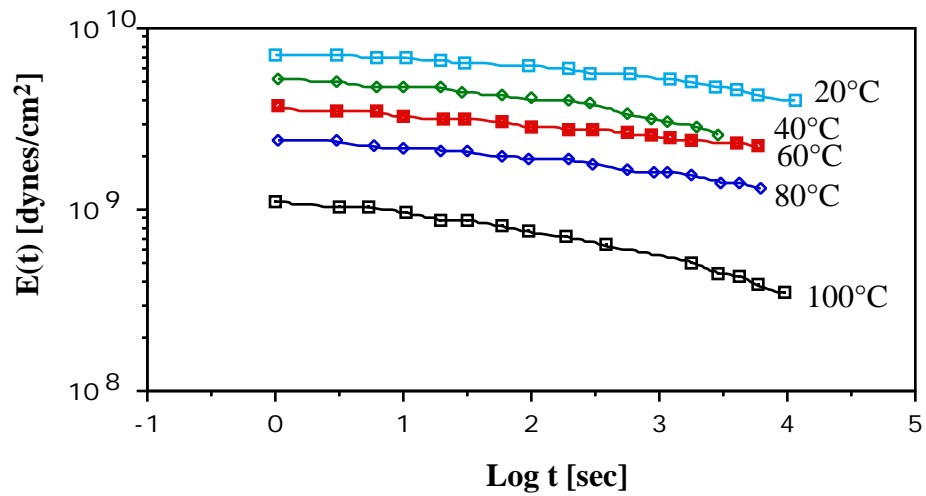


Figure 2.11 Relaxation modulus curves at different temperatures for PVA (Onogi et al, 1962).

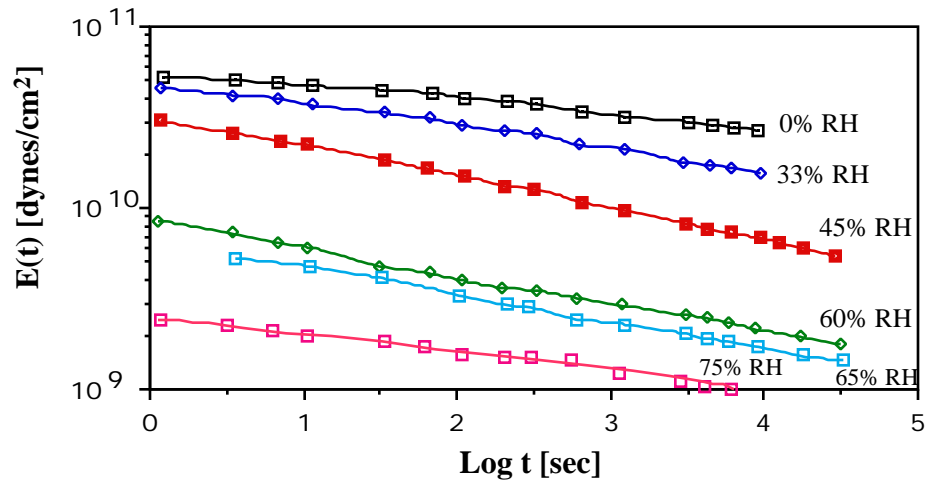


Figure 2.12 Relaxation modulus curves at different relative humidities for PVA (Onogi et al, 1962).

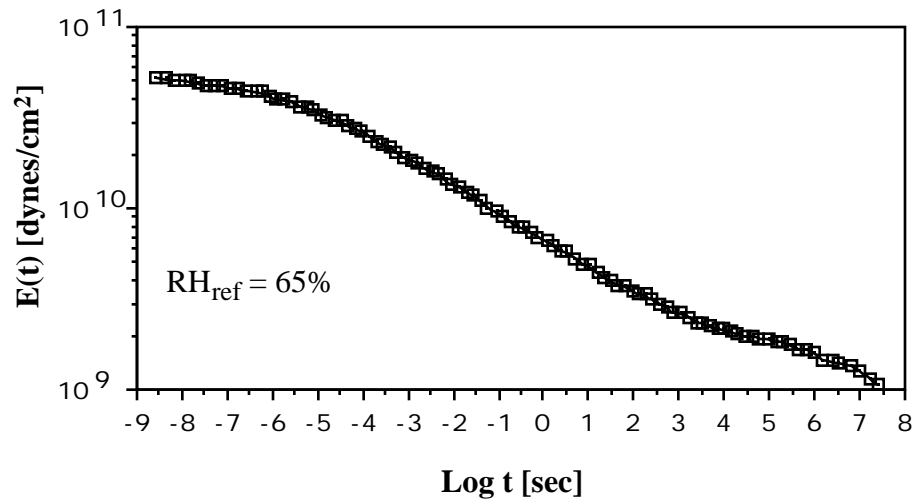


Figure 2.13 Master curve from TMSP at 20°C for PVA (Onogi et al, 1962).

For the time-moisture superposition tests, the samples were tested at 25°C and at relative humidities of 0, 6, 19, 33, 43, 52, 64, 76, and 86%. The curves superposed well except at lower humidities. The authors conclude that it is possible to apply the principle of time-moisture superposition provided the material is in the transition region.

2.5 Application of TTSP to wood

One of the key assumptions behind the principle of time-temperature superposition is that the material does not undergo any chemical or physical changes as a result of the temperature change (Ferry 1980). For wood two possible changes may occur: the first one is a moisture content change, and the second one is a change in the crystallinity of the cellulose. By maintaining the appropriate relative humidity in the testing chamber, it is possible to maintain a constant moisture content under a constant temperature. Also, Van der Put (1989) suggests that change in cellulose crystallinity is very small within a reasonable temperature range.

The previous criteria do not guarantee the quantitative accuracy of the results. Plazek (1965) suggests that the method is only valid in a limited region of time and temperature. When attempting to apply the principle of time-temperature superposition to wood, we are faced with three main obstacles:

(1) Under normal operating conditions, wood behaves in a glassy manner. In the glassy region, time effects are very small; this leads to large vertical shifts which do not conform to a pre-determined relation unlike the transition region where the $T_0 \propto 1/T$ correction factor is used (Ferry, 1980). In a study on glassy poly(methyl methacrylate), McCrum and Morris (1964) found that the shift factor follows an Arrhenius relation with a small activation energy (17 Kcal).

(2) Wood is highly crystalline; the cellulose in wood is about 70% crystalline. In a study on high density polyethylene, Nakayasu et al. (1961) report that simple superposition by horizontal shifting was ineffective; applying the temperature correction factor did not help. The authors concluded that it was possible to superpose the curves by applying two sets of shift factors corresponding to two different mechanisms.

(3) Wood is a polymer blend with multiple transition zones: wood consists of cellulose, lignin, and hemicellulose. These components depend differently on temperature. Fesko and Tschoegl (1971, 1974) studied the application of time-temperature superposition to thermorheologically complex polymers, such as styrene/butadiene/styrene block copolymers, and suggested a method of superposition which accounts for the different temperature dependencies of the components.

Although these wood properties limit the applicability of TTSP to wood, they do not render the method invalid for wood. Many attempts have been made to study the effect of temperature on wood; however, few attempts were made

to apply the principle of time-temperature superposition to wood. Davidson(1962) conducted creep recovery experiments in bending and concluded that time-temperature superposition should be used with caution because wood is thermorheologically complex. However, Salmèn (1984) was successful when he applied the principle to saturated wood samples at temperatures ranging from 20 to 140°C. In a study to determine the transition temperatures of the amorphous components in wood, Kelly et al. (1987) were able to apply the principle of time-temperature superposition to wood saturated with non-aqueous diluents. Gamalath (1991) superposed compliance curves obtained from creep tests in compression for southern pine samples at temperatures between 20 and 60°C. Along with horizontal shifting, vertical shifts were needed to obtain a smooth master curve; the horizontal shift factors followed an Arrhenius relation with an activation energy of 30Kcal/mole.

Recently, a group of French researchers published the results of a study on time-temperature superposition application to wood (Le Govic et al. 1987, 1989). Creep tests in bending were conducted and the principle of time-temperature superposition was applied to obtain a compliance master curve. The curve was then fitted to a power law model. Seventy two French spruce (*picea exeisa*) samples were tested in bending at temperatures of 25, 55, 65 and 75°C, at a 12% moisture content, and load levels of 40, 30, 20 and 10% of the average short term ultimate loads. The horizontal shift factors followed an Arrhenius relation with an activation energy of 162 kJ/mole (38.7Kcal/mole). Although the study produced a compliance master curve for over 60 years, compliance and master curves were not smooth and there is no mention of possible vertical shifts.

In order to successfully apply the principle of time-temperature superposition to wood, a good understanding of the procedures used for synthetic polymers with properties similar to wood is necessary. The following two sections review the application of TTSP to crystalline and thermorheologically complex materials.

2.6 Application of TTSP to thermorheologically complex materials

When a material is thermorheologically complex, the horizontal shift factor depends on time in addition to temperature. This is illustrated in figure 2.14 where the compliance curves at T_1 and T_r , where $T_r < T_1$, cannot be superposed using a single shift factor. This is similar to superposing compliance curves for thermorheologically simple materials as a function of

temperature at various times (figure 2.15). If the shift factors follow the WLF relation then the temperature shift factor is given by

$$T = \frac{C_2 \log(t / t_r)}{C_1 - \log(t / t_r)} \quad (2.13)$$

Fesko and Tschoegl (1971) derived equations (2.13, 2.14) for determining the shift factors as a function of time; however, these equations cannot be integrated which lead the authors to use a technique developed by Takayanagi (1965) which requires knowledge of the mechanical properties of the components and their temperature functions:

$$\frac{\log D(t)}{\log t} = \frac{\log D[t / a_T(t)]}{\log t / a_T(t)} \quad 1 - \frac{\log a_T(t)}{\log t} \quad (2.14)$$

$$\frac{\partial \log a_T(t)}{\partial T} = - \frac{\partial D(T)}{\partial T} \frac{D[t / a_T(t)]^{-1}}{\log t / a_T(t)} \quad (2.15)$$

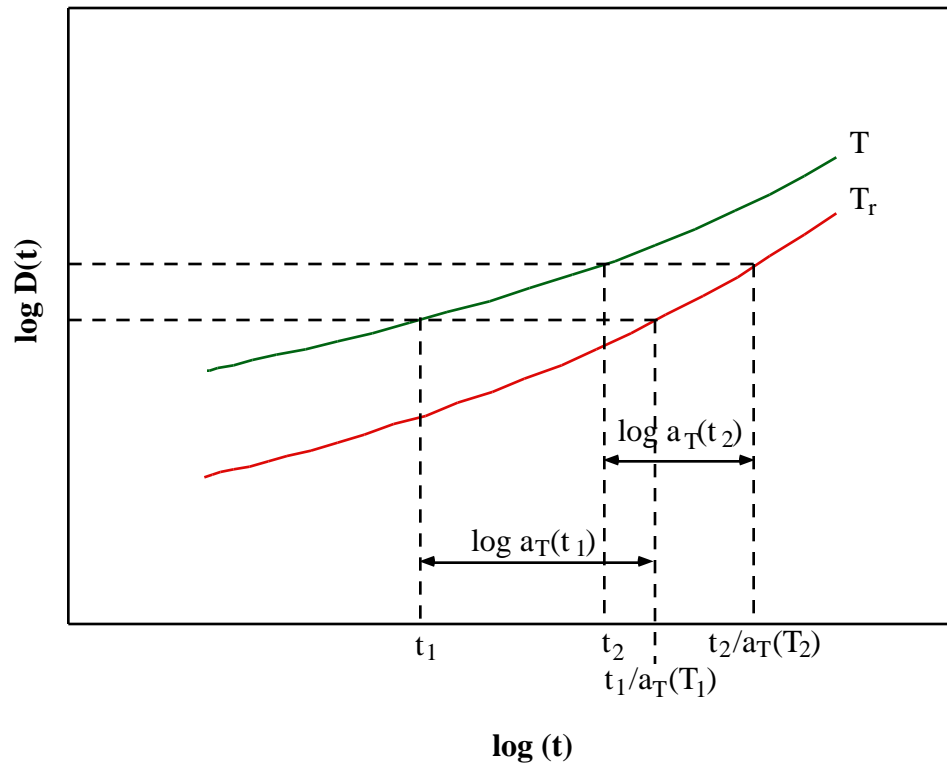


Figure 2.14 Superposition on the time axis for thermorheologically complex materials.

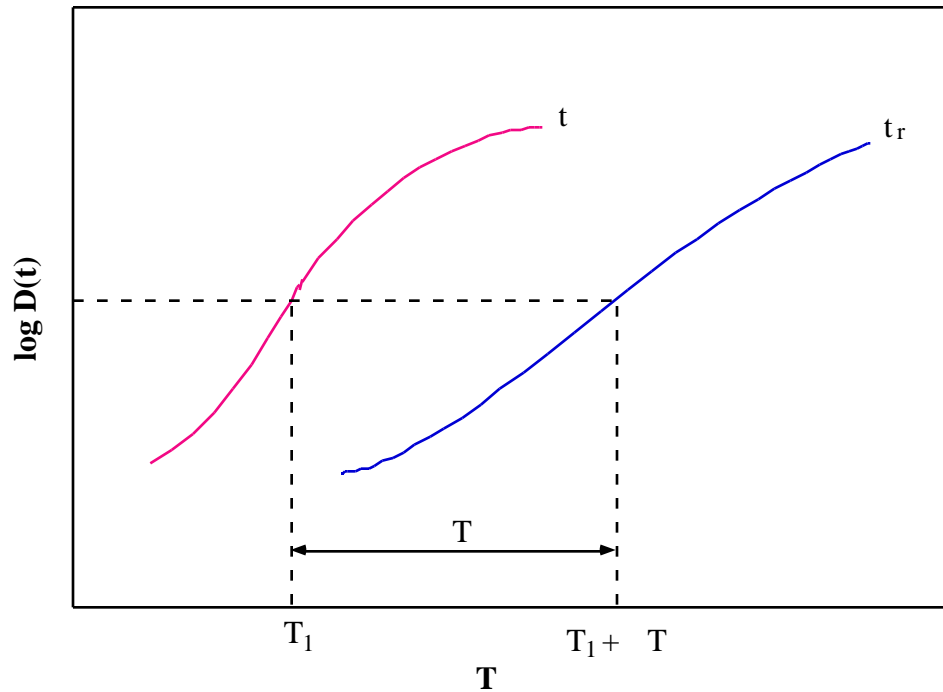


Figure 2.15 Superposition along the temperature axis.

Wood is a complex bio-composite material with many properties that make the application of time-temperature superposition a challenge. However, similar studies on various thermorheologically complex polymers have been successfully conducted. Obtaining a master curve is not a guarantee of the validity of TTSP. Long-term tests will be needed to assess the validity of the method.

2.7 Creep Models

Gressel (1984) classified commonly used creep equations into mechanical, empirical, temperature, and molecular models. Empirical models are the most commonly used because of their simplicity; in particular the power law model

$$\varepsilon(t) = \frac{1}{E}(1 + at^b) \quad (2.16)$$

first applied to wood by Clouser (1959), is frequently used.

Because the constant a has units of t^{-b} , equation 2.13 can be modified to yield

$$\varepsilon(t) = \frac{1}{E} \left(1 + A \frac{t}{\rho} \right)^b \quad (2.17)$$

$$\varepsilon(t) = \frac{1}{E} \left(1 + \frac{t}{\tau} \right)^b \quad (2.18)$$

where $\tau = \rho A^{\frac{1}{b}}$

A and b are dimensionless constants while ρ and τ have the dimensions of time. The variable τ is the doubling time or the time required to reach twice the instantaneous deformation. The power law function has the following implications (Nielsen 1984): Creep develops very rapidly at the beginning then the rate approaches zero at long times

Nielsen (1984) suggests that the time exponent in the power law model is independent of the environmental conditions. However the retardation time depends on the temperature and humidity conditions as well as the angle between the load and the grain directions. A range for the time exponent is given by Nielsen (1984):

Parallel to grain: 1/5 to 1/4
 Perpendicular to grain: 1/4 to 1/3

Le Govic et al. (1987) suggest the following model:

$$D(t,T) = D_0 \left(1 + \frac{t}{\tau_0} \right)^k \exp \frac{-kW}{RT} \quad (2.19)$$

Where D_0 is the instantaneous compliance, W is the activation energy from the Arrhenius relation, and τ_0 is the retardation time at infinite temperature. The parameters from LeGovic's study are:

$D_0 = 0.5866 \times 10^{-4} \text{ MPa}^{-1} = 4.0455 \times 10^{-7} \text{ in}^2/\text{lb}$
 $W = 162.66 \text{ kJ/mole} = 38.7 \text{ Kcal/mole}$
 $k = 0.112$
 $\tau_0 = 1.22 \times 10^{-16} \text{ s}$

The activation energy of 38.7 kJ/mole is comparable to the one found by Gamalath (1991). Le Govic (1989) suggests that although the power law model is widely used, an exponential law would be more suitable for building codes.

Such exponential laws were proposed for the EUROCODE 5. Specifically, for bending

$$\varepsilon(t - t_0) = \frac{\sigma}{E} \left[1 + 0.65 \left(1 + 0.65 \left(1 - e^{-(t-t_0)} \right) \right) \right] \quad (2.20)$$

and for compression

$$\varepsilon(t - t_0) = \frac{\sigma}{E} \left[1 + 0.30 \left(1 + 0.30 \left(1 - e^{-(t-t_0)} \right) \right) \right] \quad (2.21)$$

Huet and Navi (1990) proposed a model which accounts for the multitransitional nature of wood. This model consists of a series of modified Kelvin elements where the dashpots are replaced by a power law creep model. Each element has unique parameters that correspond to each transition.

2.8 Finite Element Analysis for Creep

The finite element method is a powerful and well established tool for stress analysis. Therefore, when researchers became interested in solving creep problems numerically, they turned to the finite element method rather than finite difference and direct integration methods (Kraus, 1980). The subject of finite element analysis has been addressed by many authors such as Zienkiewicz (1971) and Bathe (1982).

2.8.1 Creep Models

In statically indeterminate structures, such as space frames and lattice domes, the creep differences within the structure cause extensive long-term stress redistributions, even under constant loads. Therefore, creep laws must be formulated for variable stresses. Moreover, any creep analysis must proceed in an incremental manner with suitable time steps, and iteration within time steps is frequently required to satisfy the creep law and assure convergence (Bathe, 1982). In the one-dimensional case, the creep strain can be expressed as a function of the stress, temperature, and time:

$$\varepsilon^c = f(\sigma, T, t) \quad (2.22)$$

It is usually assumed that these effects are independent, then the creep strain can be expressed as (Kraus, 1980)

$$\varepsilon^c = \sum_{i=1}^n f_i(T) g_i(\sigma) h_i(t) \quad (2.23)$$

This allows for more than one term in the expression. In order to account for the change in stress or temperature, two options are available. The first is the equation of state, or rate-type, formulation where the creep strain depends on the present state and the second is the hereditary, or integral-type, formulation where the response depends on the entire loading history. Although the hereditary model would yield better results (Kraus, 1980), it is not commonly used because it requires extensive storage and more elaborate material testing. The equation of state approach is widely used because it is easy to incorporate into available computer programs. Procedures have been developed to convert the hereditary integral into a state equation (Chan 1983; Kabir 1976; Nilson 1982). This has been accomplished, for example, by expanding the compliance function in a Dirichlet series (Kabir 1976):

$$D(\tau, t - \tau, T) = \sum_{i=1}^m a_i(\tau) \left[1 - e^{-\lambda_i \phi(T)(t-\tau)} \right] \quad (2.24)$$

where $a_i(\tau)$ is a scale factor depending on the time of loading, λ_i are exponential constants, and $\phi(T)$ is the temperature shift function.

In order to use the equation of state formulation, the Bailey-Norton law is commonly used:

$$\varepsilon^c = A \sigma^m t^n \quad (2.25)$$

where A, m, and n depend on temperature; also m is greater than one and n is a fraction. The rate of creep strain is obtained by differentiating the above equation with respect to time; this is referred to as the time-hardening formulation of the equation of state:

$$\dot{\varepsilon}^c = A \sigma^m n t^{n-1} \quad (2.26)$$

Solving Eq. 2.25 for time, we obtain

$$t = \frac{\varepsilon^c}{A \sigma^m}^{\frac{1}{n}} \quad (2.26)$$

which when introduced into the time hardening equation produces the strain-hardening formulation of the equation of state:

$$\dot{\epsilon}^c = A\sigma^m n \frac{\epsilon^c}{A\sigma^m}^{\frac{n-1}{n}} = A^{\frac{1}{n}} \sigma^{\frac{m}{n}} n \epsilon^c{}^{\frac{n-1}{n}} \quad (2.27)$$

Although the time and strain hardening formulations are derived from the same equation, they yield different results when the applied stress is not constant, as illustrated in Figure 2.16. For time hardening, when the stress changes from σ_3 to σ_4 , the strain is resumed on the σ_4 curve at the time of change whereas for strain hardening, the strain resumed where it stopped on the σ_3 curve. Kraus (1980) states that based on experimental results, the strain hardening formulation gives better results; this is also noted by Bushnell (1977).

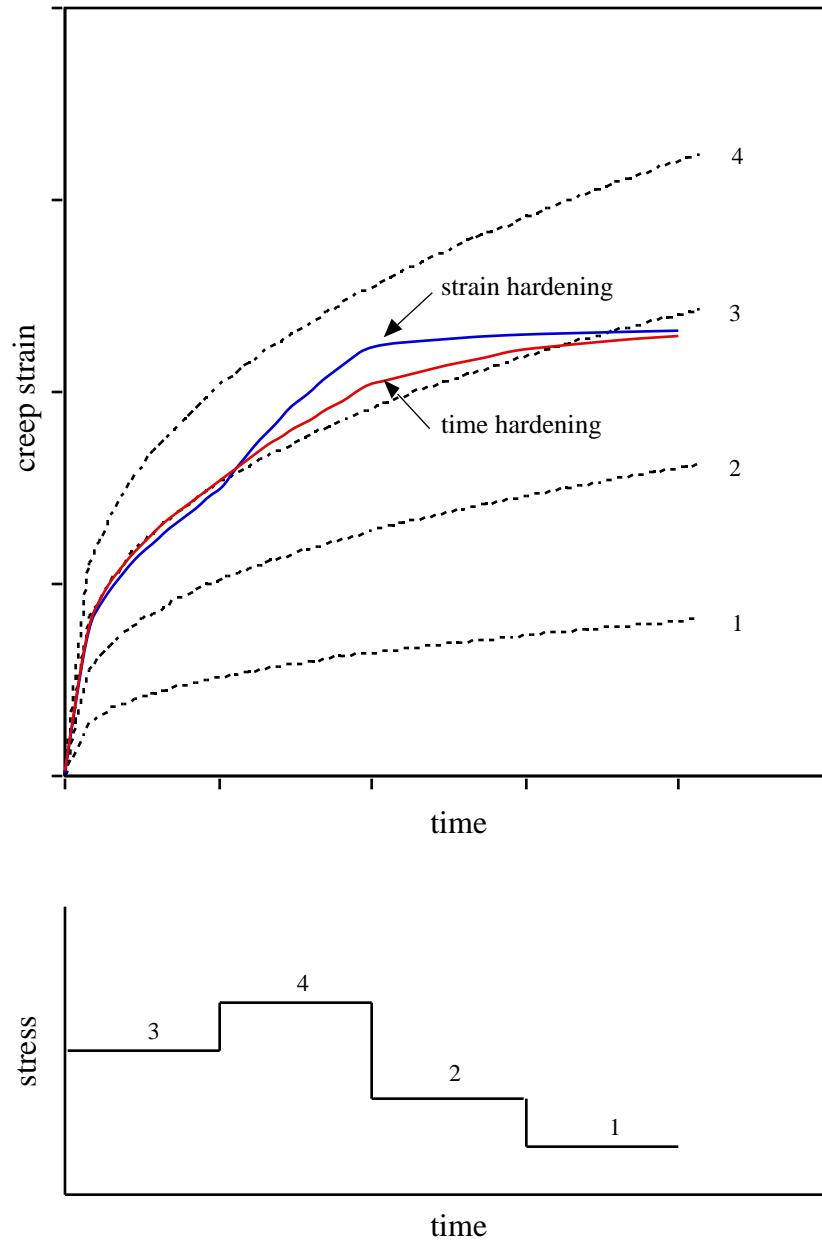


Figure 2.16 Time and strain hardening responses to variable stress.

2.8.2 Computer Programs

With few exceptions, finite element computer programs for the analysis of creep problems are based on the initial strain method (Boyle and Spence 1983; Bushnell 1977; Kraus 1980; Nickell 1974). The initial strain method was motivated by the similarity of creep problems to thermal stress problems (Greenbaum and Rubinstein 1968; Mendelson et al. 1959; Zienkiewicz and Watson 1966), where the method was first proposed.

A shortcoming of early applications, the requirement of small time steps to achieve convergence (Nickell 1974), has been overcome by the subincrementation of time steps and effective time integration algorithms (Bushnell 1977; Snyder and Bathe 1981; Zienkiewicz and Cormeau 1974). In addition, the initial strain method can be used to investigate the effect of structural imperfections (e.g., lack-of-fit problems caused by fabrication errors) or flaws in connections. This will be useful in large assemblies of elements such as lattice domes. Moreover, it permits one to represent the effect of creep in connections as a structural imperfection.

For this study, ABAQUS, a commercial finite element program was used. It has powerful nonlinear analysis capabilities that allow for automatic time integration and iteration. For linear elastic materials, creep properties can be assigned either by supplying the constants for the Bailey-Norton law or by using a special subroutine that computes the creep strain increment at each iteration. The last method allows for introduction of temperature and moisture effects.

2.8.3 Creep Stability

According to Britvec (1973), a body is stable if it tends to regain its original state after being disturbed by an external effect. To determine if a column is stable, an infinitesimal velocity is applied at time $t=0$. The column is stable if the motion decreases with time and is unstable otherwise. For elastic members and systems, the problem consists of finding the critical load for which the system becomes unstable. For viscoelastic materials, however, the problem becomes more complicated as the critical load depends on time and on the magnitude of the applied impulse for nonlinear creep. The finite element method can be used to determine the time to failure by checking the tangent stiffness matrix along the equilibrium path. The system is stable if the stiffness matrix is positive definite and unstable otherwise.

2.8.4 Creep Analyses

The finite element method will be used to study the effect of long-term creep on columns, arches, and lattice domes. Of primary interest is the extent to which creep can reduce the load-carrying capacity. The possibility of creep buckling of arches and lattice domes will be investigated.

3. EXPERIMENTAL

The purpose of the experimental study is: (1) to use the principle of time-temperature superposition to develop a power law model for long-term creep, and (2) to compare the resulting master curve to long-term creep curves. The power law model will then be used to conduct finite element analyses on simple and complex wood structures.

3.1 Dynamic tests using the DMA

A TA Instruments DMA (Dynamic Mechanical Analyzer) was used to detect transitions and to conduct creep tests at temperatures between 25 and 80°C. The DMA has the advantage of quickly giving results, however, it does not allow for control of the moisture content of the sample. The DMA was used in two modes: fixed frequency and creep.

Fixed frequency. In fixed frequency tests, the sample is bent at a predetermined frequency and the storage compliance, loss modulus, and loss tangent are recorded as the temperature is increased at a specified rate. A frequency of 1 Hz and a temperature rate of 2°C/minute were used.

Creep. Creep experiments on the DMA are simple to perform. The sample is mounted in the grips and the grips are tightened using screws. The constant stress is prescribed by assigning an initial displacement (0.1 - 0.3 mm). The sample creeps for 15 minutes then recovers for 45 minutes. The temperature is then increased by a predetermined amount and the process is repeated until a maximum temperature is reached. The data is read and manipulated by the on-line computer system and the results can be displayed as the experiment progresses.

3.2 Short-term creep tests

Short-term creep tests in tension and in compression were conducted to obtain creep compliance curves at different temperatures while maintaining a constant moisture content. The following test parameters were used.

Specimens. Southern yellow pine, Douglas-fir, yellow-poplar, Parallam™ were tested. These species were chosen to reflect the current trends in wood usage. Southern yellow pine and Douglas-fir are used extensively as lumber and as materials for several wood composites such as glulam. Yellow-poplar is used in Parallam, laminated veneer lumber and other products. Parallam™ is a structural composite lumber product gaining popularity because of its availability in large sizes.

Size. Specimen dimensions are a compromise between the load magnitude that can be applied and the size that would be representative of the species. For tension the size chosen is 0.25 x 0.5 x 12 in. The size for the compression test is 0.75 x 0.75 x 4 in.

Number of specimens. The number of specimens is subject to two conflicting restrictions. On one hand, wood is a variable material which requires testing many specimens for statistical accuracy, on the other hand, the time available for the tests is limited and so is the availability of the equipment. For this study, 12 samples of each species were tested.

Load. Wood is considered to behave in a linear viscoelastic manner for loads below 50% of the ultimate load (Schniewind 1968, Nielsen 1984). Schaffer (1983) describes the behavior of wood as nonlinear regardless of the load level; however, he states that at low stresses, linear behavior can be a good approximation of the behavior and Boltzmann's superposition principle applies for stresses up to 40% of the short-term strength. Le Govic (1988) gives limits for linear behavior of 30-35% of the short-term strength for bending and up to 50% of the short-term strength for tension. To insure that behavior of test specimens remains within the linear range, loads in the 20 to 25% range of the short-term ultimate strength were.

Testing apparatus. Creep experiments are very sensitive because the deformations are very small. Because each sample is loaded and unloaded several times, any perturbation to the sample can adversely affect the results. Each sample is mounted to grips and the load is applied and removed using a hydraulic jack (Figure 3.1). Figure 3.2 shows the tension and compression specimen holders which were designed and built for this project.

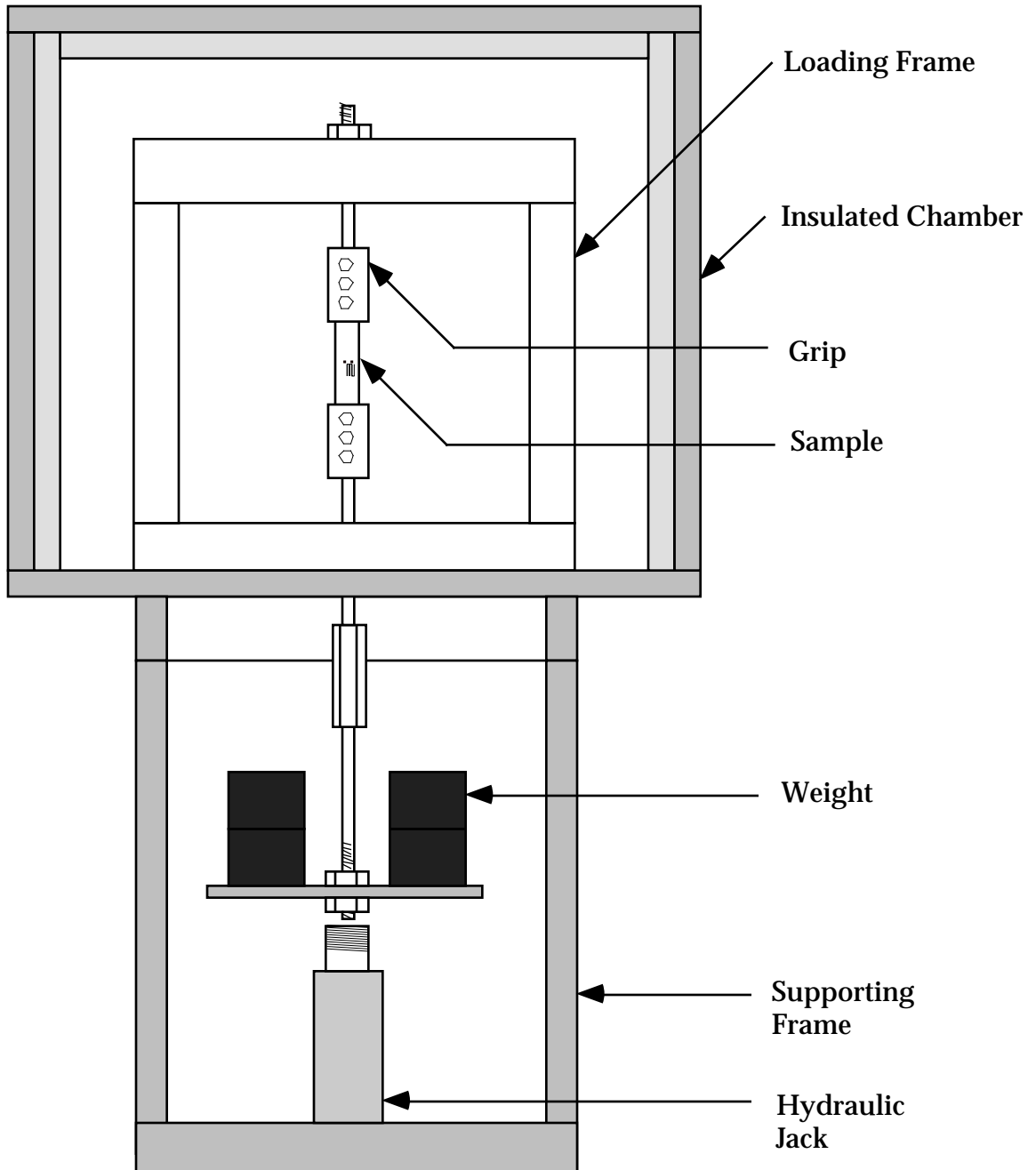


Figure 3.1 Tension test apparatus

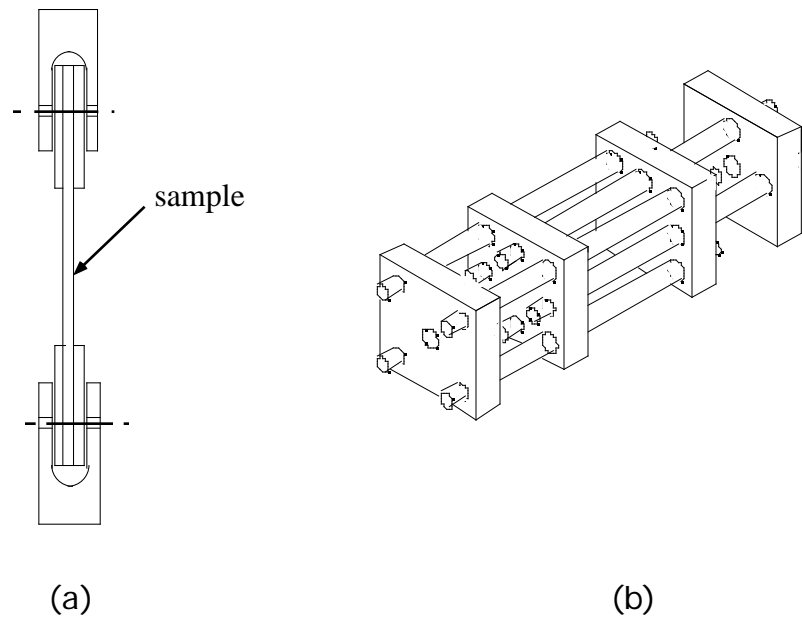


Figure 3.2 Creep apparatus (a) tension, (b) compression.

Environmental conditions. The testing apparatus is housed in an insulated chamber, conditioned air is circulated through the chamber to maintain a constant 12% moisture content. The temperatures used are 20, 30, 40, 50, 60, 70, and 80°C. The relative humidity required to maintain a 12% moisture content can be calculated using the Hailwood-Horobin model (Simpson 1971). Table 3.1 shows the corresponding values of temperature and relative humidity to maintain 6, 9, and 12% moisture contents. The primary target EMC for the test specimens in this study will be 9% MC to reflect the average EMC for most of the country. Additionally, specimens were tested at 6 and 12% EMC for three reasons: (1) There is a historic precedence for reporting

wood properties at a standard 12% MC since this is an easy condition to achieve and the results will be readily comparable with the results of others; (2) 12% MC represents the upper range EMC of normal interior exposure for wood products and the average for protected exterior exposure (Oviatt, 1968); (3) the additional EMC levels will enhance our understanding of the application and suitability of the time-temperature superposition principle to wood.

Table 3.1 Relative humidity required to maintain a 12% moisture content.

Temperature °C	Temperature (Dry bulb) °F	Relative Humidity for 6 % MC	Relative Humidity for 9 % MC	Relative Humidity for 12 % MC
20.0	68.0	29.2	48.7	64.5
25.0	77.0	29.8	49.6	65.4
30.0	86.0	30.7	50.8	66.5
35.0	95.0	31.8	52.2	67.7
40.0	104.0	33.1	53.7	69.0
45.0	113.0	34.6	55.4	70.4
50.0	122.0	36.2	57.2	71.8
55.0	131.0	38.0	59.0	73.3
60.0	140.0	40.0	60.9	74.9
65.0	149.0	42.0	62.9	76.4
70.0	158.0	44.2	64.8	77.9
75.0	167.0	46.4	66.7	79.4
80.0	176.0	48.7	68.7	80.9

Test duration. Figure 3.3 shows the log time axis for times ranging from 1 second to 50 years. Depending on the horizontal shift factors, a creep period of as little as 4 hours can be sufficient to extrapolate to 50 hours. A creep duration of six to twelve hours is chosen. Another consideration for the duration of the creep test is that the load is not applied instantly, but over a period of time (ramp load). Nielsen (1984) suggests a test duration of 1-10 days

to account for ramp loading. A recovery period of three times the creep period is used to recover most of the creep deformation. In her study, Gamalath (1991) used a creep period of 17 hours and a recovery period of 40 hours.

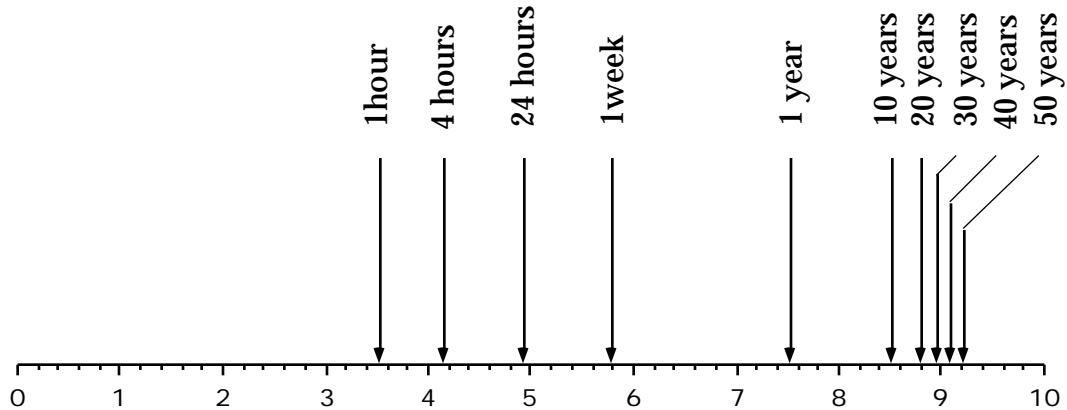


Figure 3.3 Log time axis (seconds)

Mechanical Conditioning. The wood specimens used in the creep experiments were not subjected to significant loads prior to the tests. The specimens need to be mechanically conditioned to obtain consistent results. In his creep recovery experiments, Davidson (1962) used a mechanical conditioning program that consisted of six 10-hour creep tests at 60°C followed by a recovery period of two weeks. The specimens were also conditioned at every temperature decrement for two days. In this study, the specimens were subjected to repeated cycles of creep and recovery until the compliance curves were reasonably close. To determine the effect of mechanical conditioning, three southern pine samples were tested in tension at 25°C for 4 hours of creep and 20 hours of relaxation, the results are shown in figures 3.4, 3.5, and 3.6. It can be concluded that one or two cycles are enough to get close results.

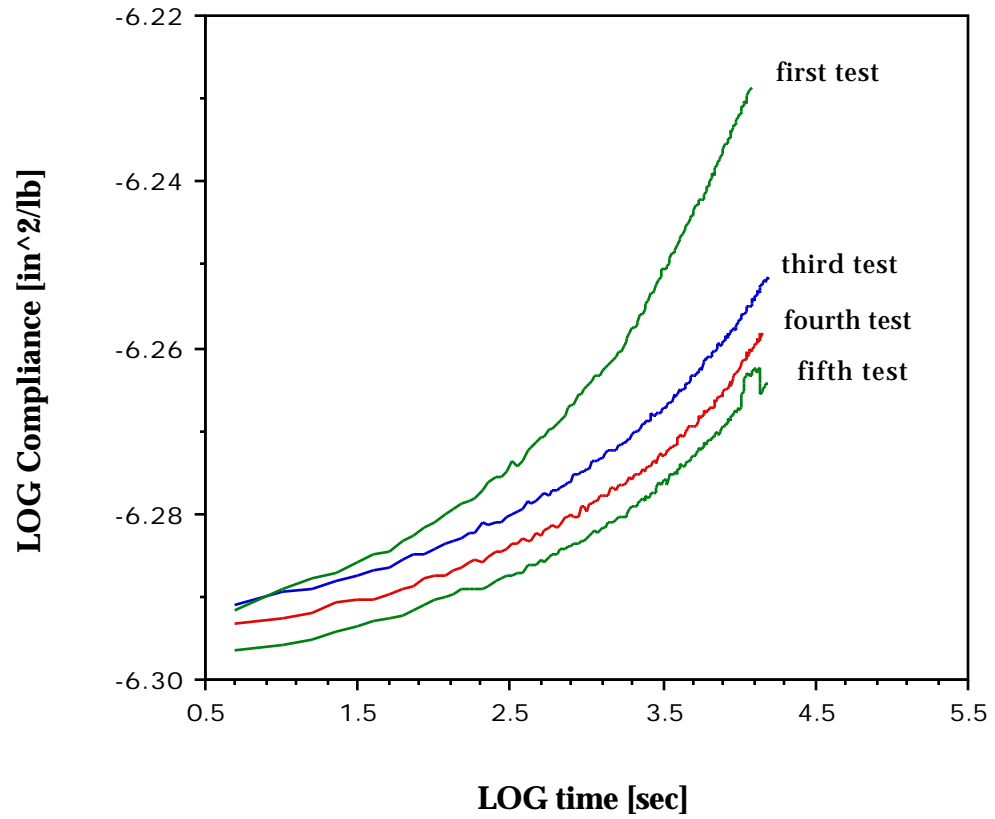


Figure 3.4 Mechanical conditioning of sample 1 at 25°C.

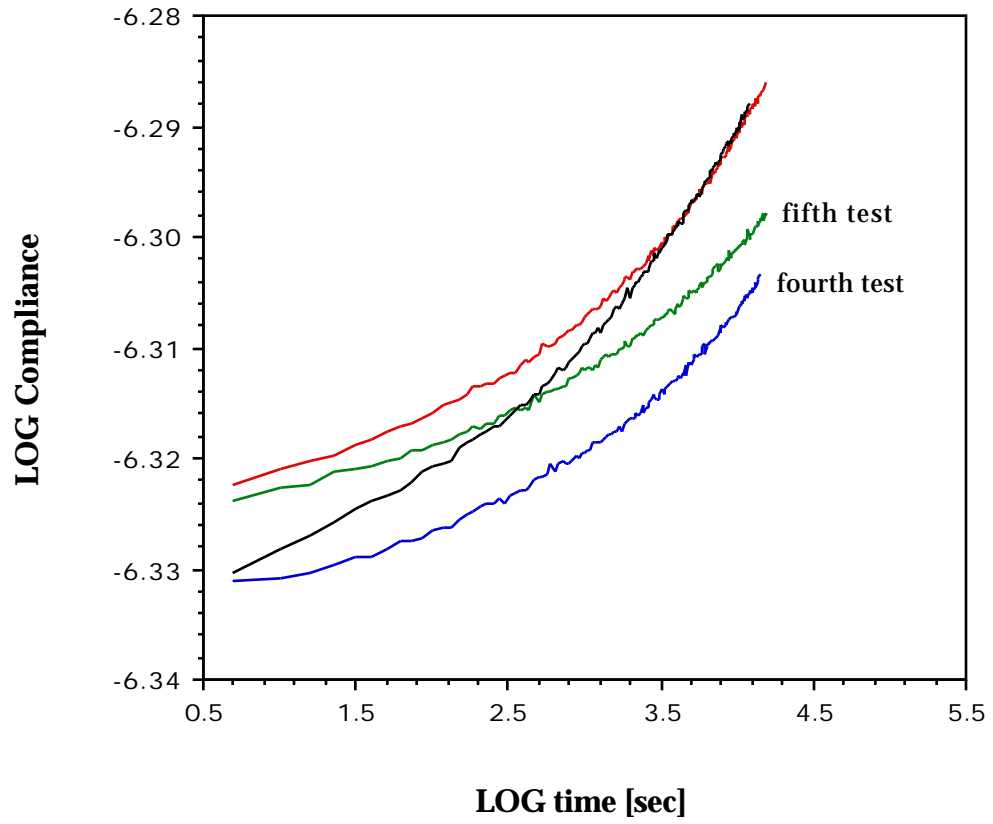


Figure 3.5 Mechanical conditioning of sample 2 at 25°C.

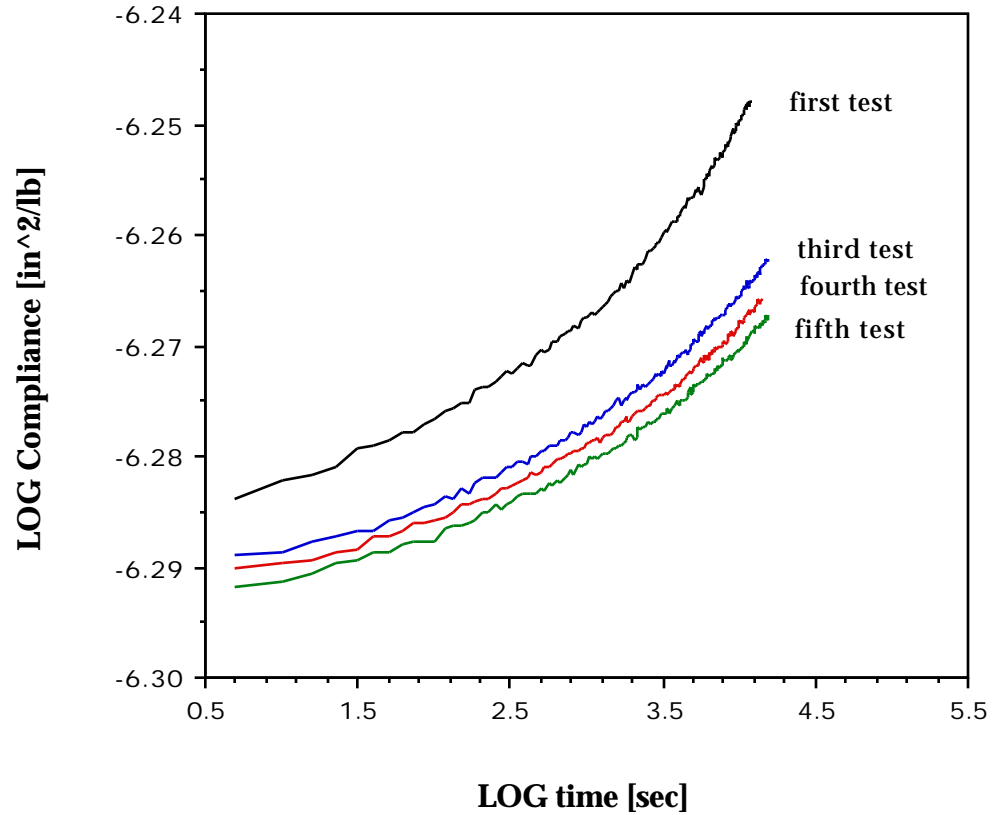
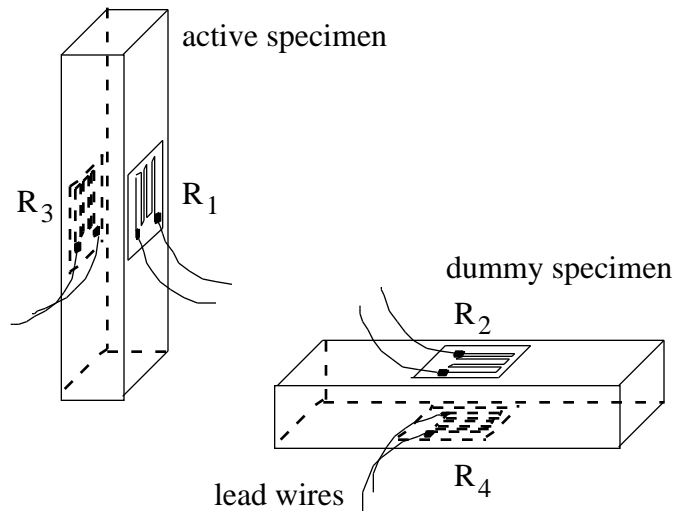
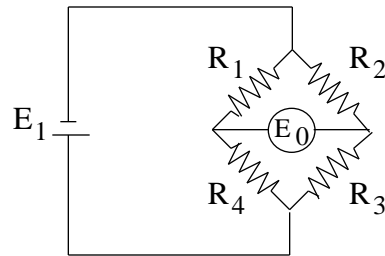


Figure 3.6 Mechanical conditioning of sample 3 at 25°C

Strain measurement and data acquisition. The strain is measured using 350Ω strain gages connected in a Wheatstone bridge as shown in figure 3.7. Two strain gages are mounted on the specimen and the other two on a dummy specimen to account for self heating of the strain gages due to the poor thermal conductivity of wood. The bridge output voltage is measured and converted to strain using an Hewlett Packard data acquisition system.



(a)



(b)

Figure 3.7 (a) active and dummy specimens; (b) Wheatstone bridge.

3.3 Long-term creep tests

Long-term creep tests in tension and in bending were conducted to serve as a basis for comparison with the results from short-term creep tests. The tests were conducted in an air-conditioned room with an equilibrium moisture content of 12%. Three species were tested in tension and in compression.

3.2 shows the number of samples for each species while figure 3.8 and 3.9 show the sample arrangement.

Table 3.2 Number of samples in the long-term creep test.

Species	number of samples in compression	number of samples in tension
Yellow-poplar	4	3
Douglas-fir	4	0
Southern yellow pine	4	4

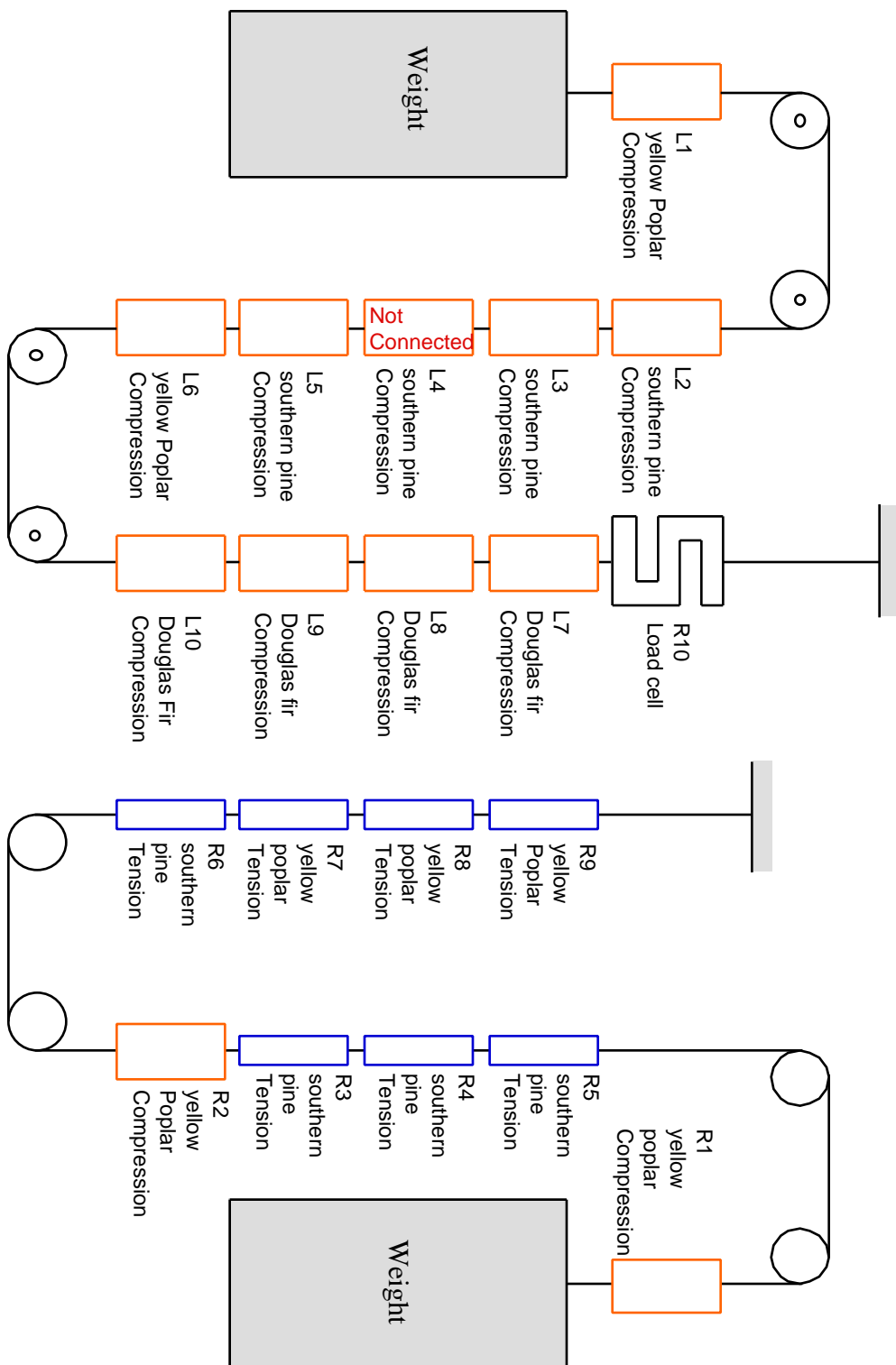


Figure 3.8 Sample arrangement for the long-term creep tests.

The sample holders for tension and compression were the same as the ones used in the short-term experiments. The strain was read using two strain indicators and two switch and balance units, readings were taken at increasing time intervals. A load cell was used to monitor the load to insure that there was no reduction in load due to friction at the pulleys.

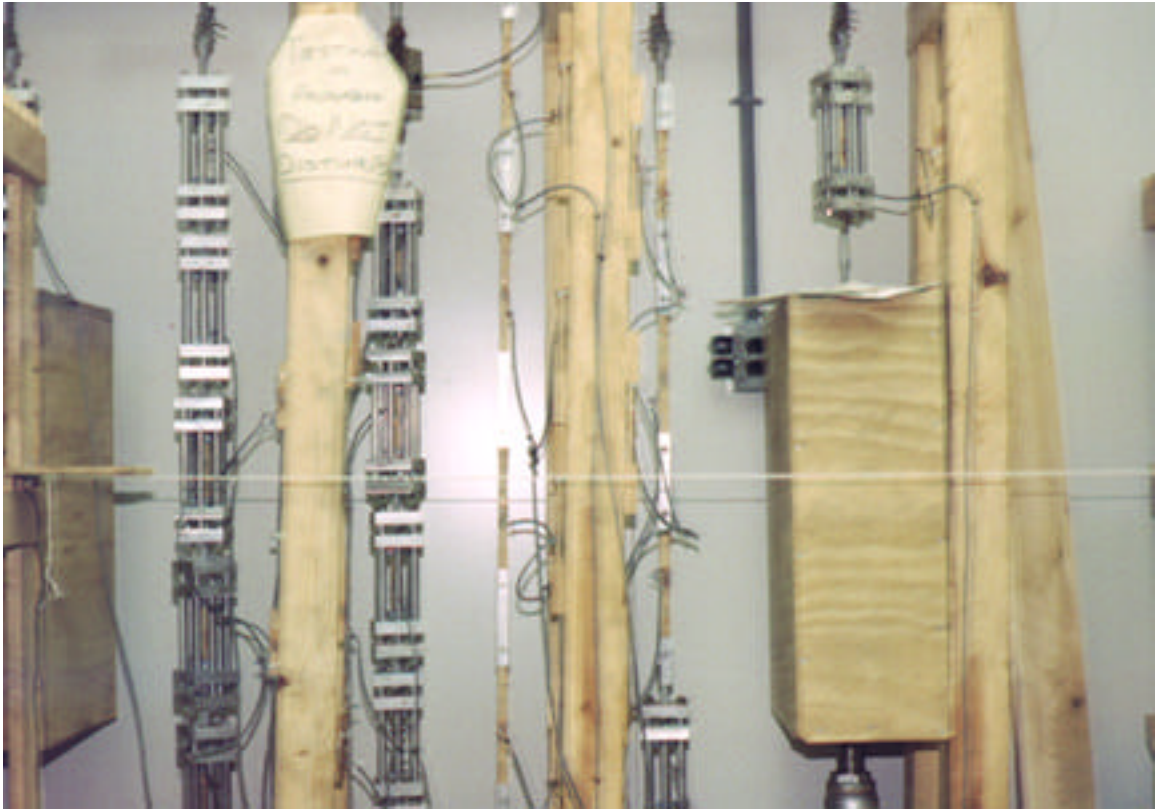


Figure 3.9 Long-term creep test setup.

4. RESULTS

4.1 Dynamic tests

4.1.1 Fixed frequency tests

It was observed in preliminary experiments that the wood samples would lose most of their moisture during the test, this lead to incorrect results since the wood behavior depends greatly on moisture content. To quantify the amount of moisture loss, some samples were weighed before and after the test, then dried and weighed again to measure the moisture contents before and after the test. Typical results are shown in Table 4.1.

Table 4.1 Moisture loss during fixed frequency test (25 to 80°C at 2°C / minute).

Species	Starting moisture content (%)	ending moisture content (%)
southern pine	13.0	4.8
Douglas-fir	11.4	4.3

This reduction in moisture will not allow for the accurate detection of transitions. To reduce moisture loss, the samples were painted with aluminum paint which is a good moisture barrier. Although some moisture was lost it was very small relative to the unpainted samples; typical results are shown in Table 4.2.

Table 4.2 Moisture loss during fixed frequency test for painted samples (25 to 80°C at 2°C / minute).

Species	Starting moisture content (%)	ending moisture content (%)
Southern pine	13.0	12.5
Douglas-fir	11.4	10.8

The effect of painting the samples on the fixed frequency test results can be seen for southern pine and Douglas-fir samples in figures 4.1 and 4.2 The southern pine and Douglas-fir samples had starting moisture contents 13.0 of and 11.4%, respectively.

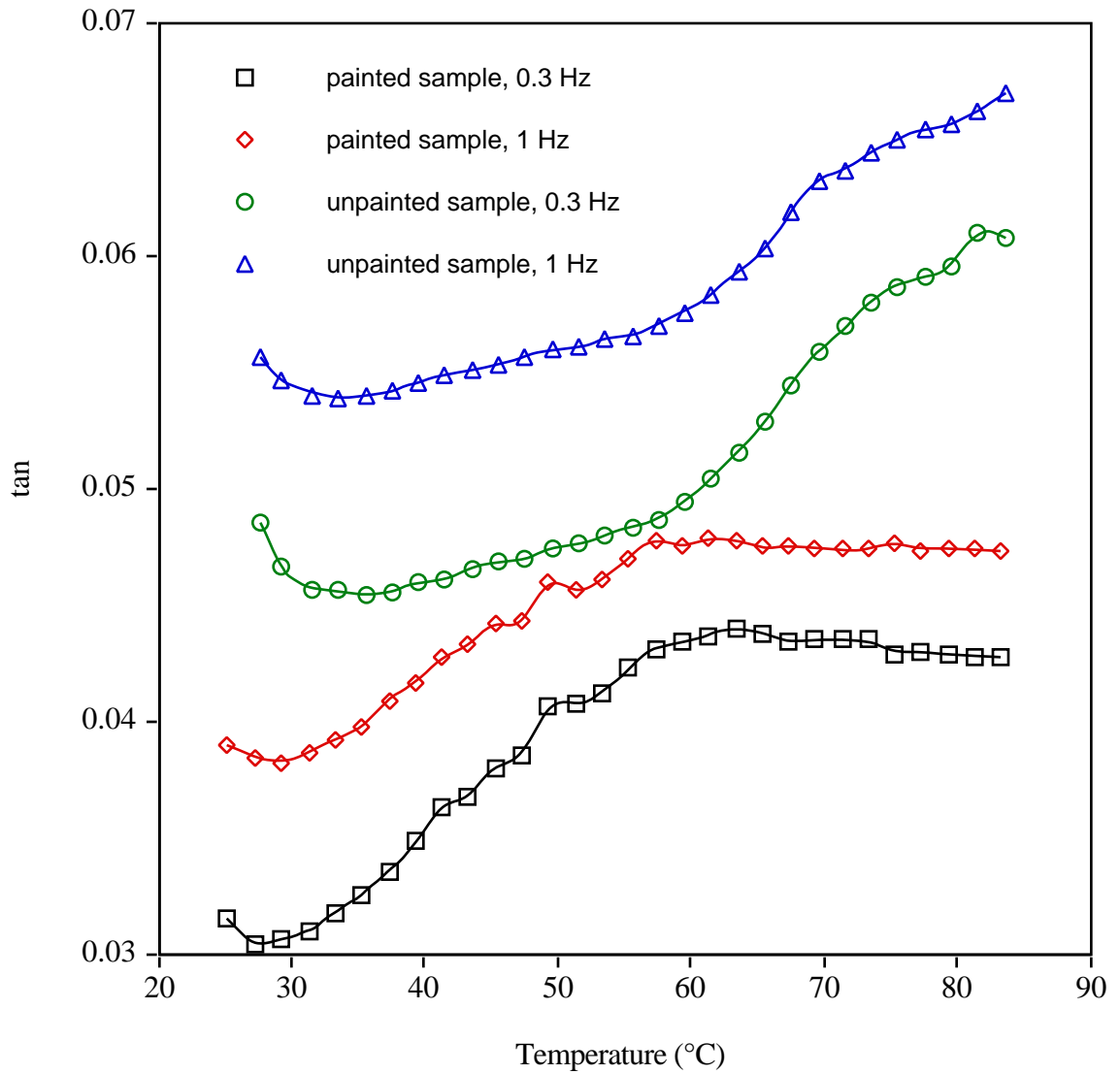


Figure 4.1 Loss tangent for painted and unpainted southern pine samples.

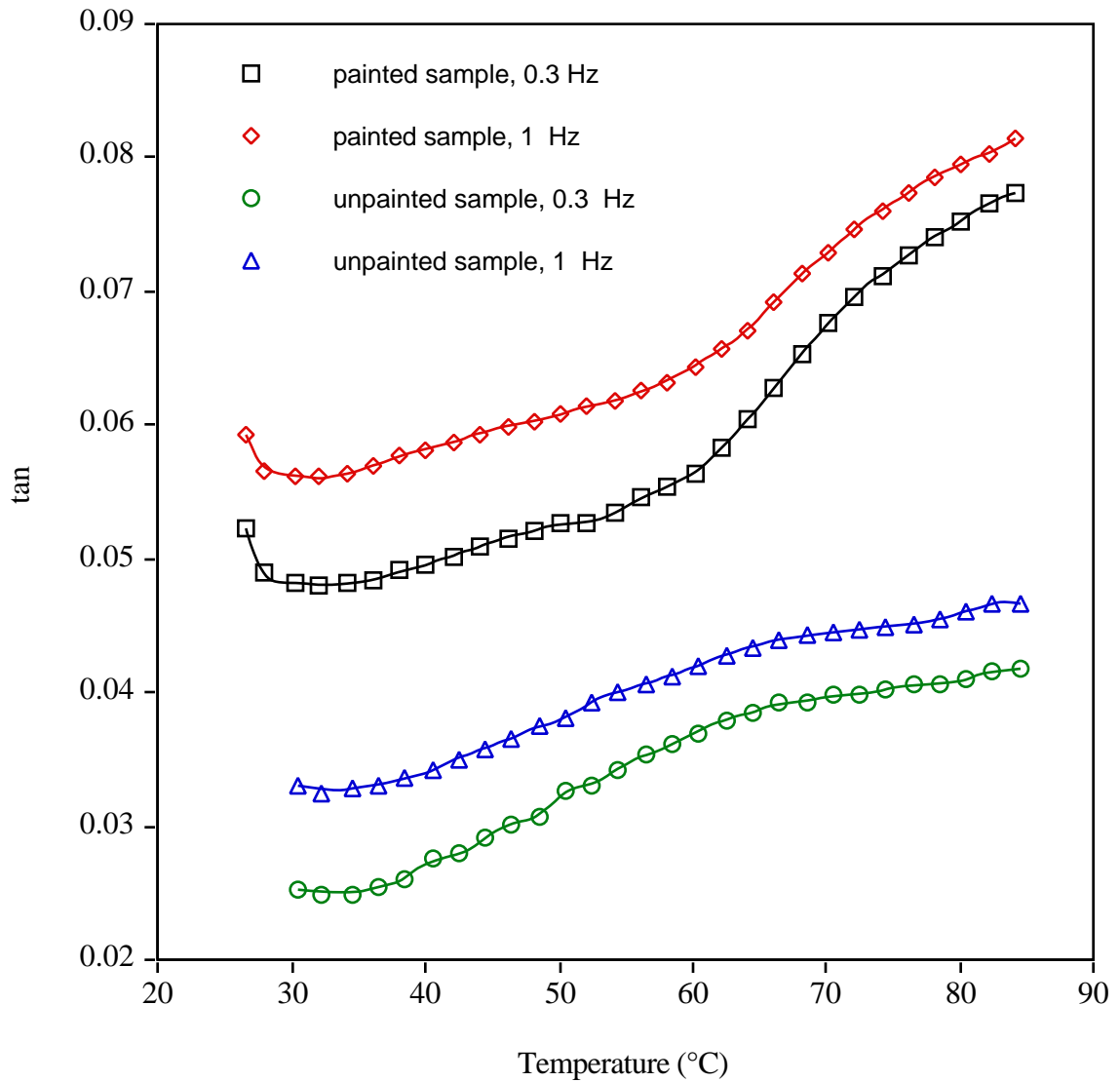


Figure 4.2 Loss tangent for painted and unpainted Douglas-fir samples.

Moisture loss from the samples results in higher transition temperatures; for southern pine the difference is at least 20°C. It should be noted however that the loss tangent for the painted samples is about half that of the unpainted samples, this may indicate that the paint is influencing the response.

Once the moisture loss problem was resolved several tests were conducted to determine any transitions in samples of southern pine, Douglas-fir, and yellow-poplar at different moisture contents. Once the samples reached the desired equilibrium moisture content, they were painted and tested soon after the paint was dry. The results at frequencies of 1 Hz at 5, 7, and 9% moisture content are shown in figure 4.3 for yellow-poplar. At 5% m.c. there is a

transition at 70°C. At 7% m.c. the transition is at 60°C, whereas at 9% m.c. there is a transition at 65°C.

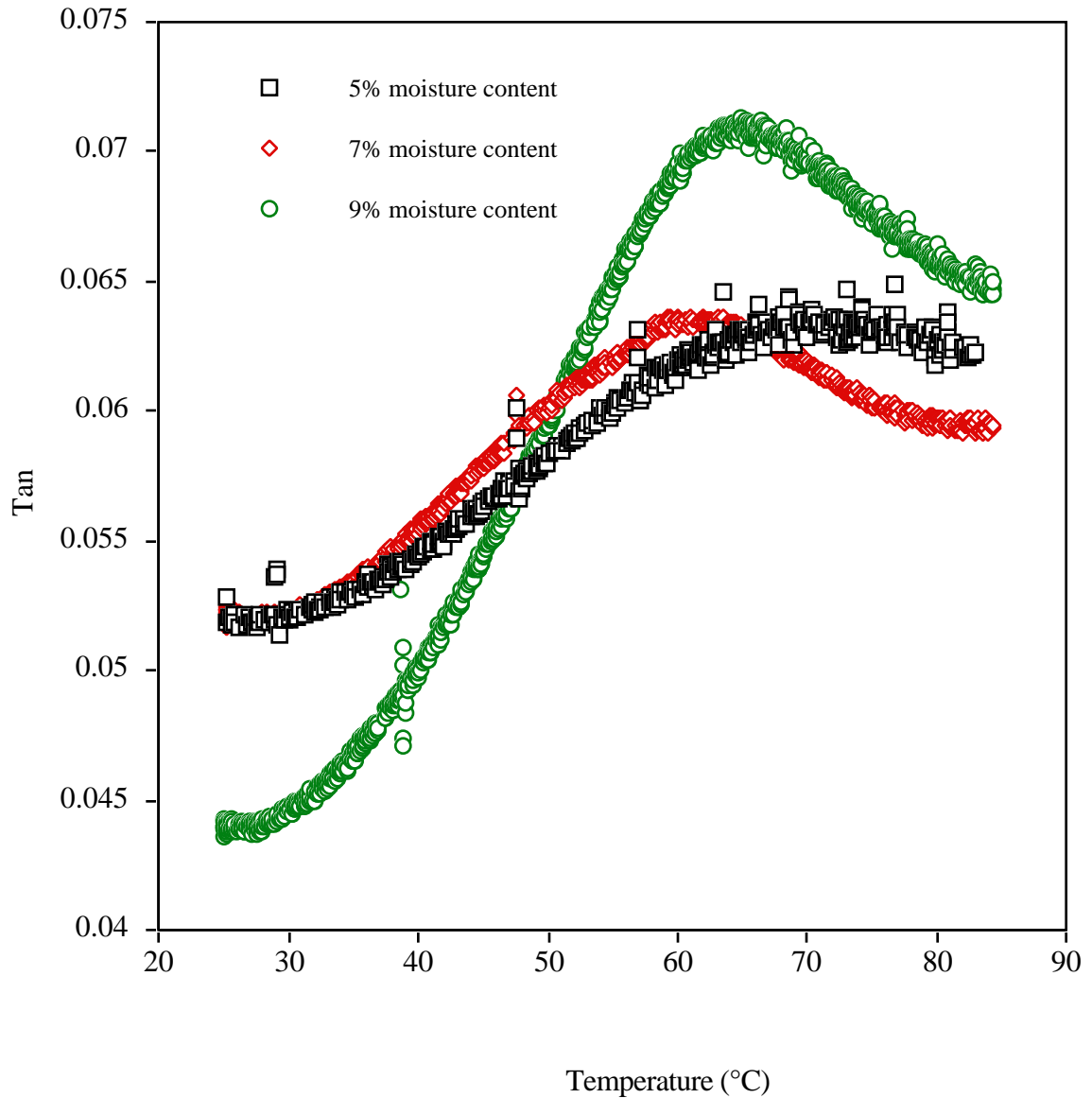


Figure 4.3 Loss tangent for yellow-poplar at 5, 7, and 9% moisture contents.

For southern pine (figure 4.4) and Douglas-fir (figure 4.5), the transitions begin around 70°C and extend beyond the maximum test temperature.

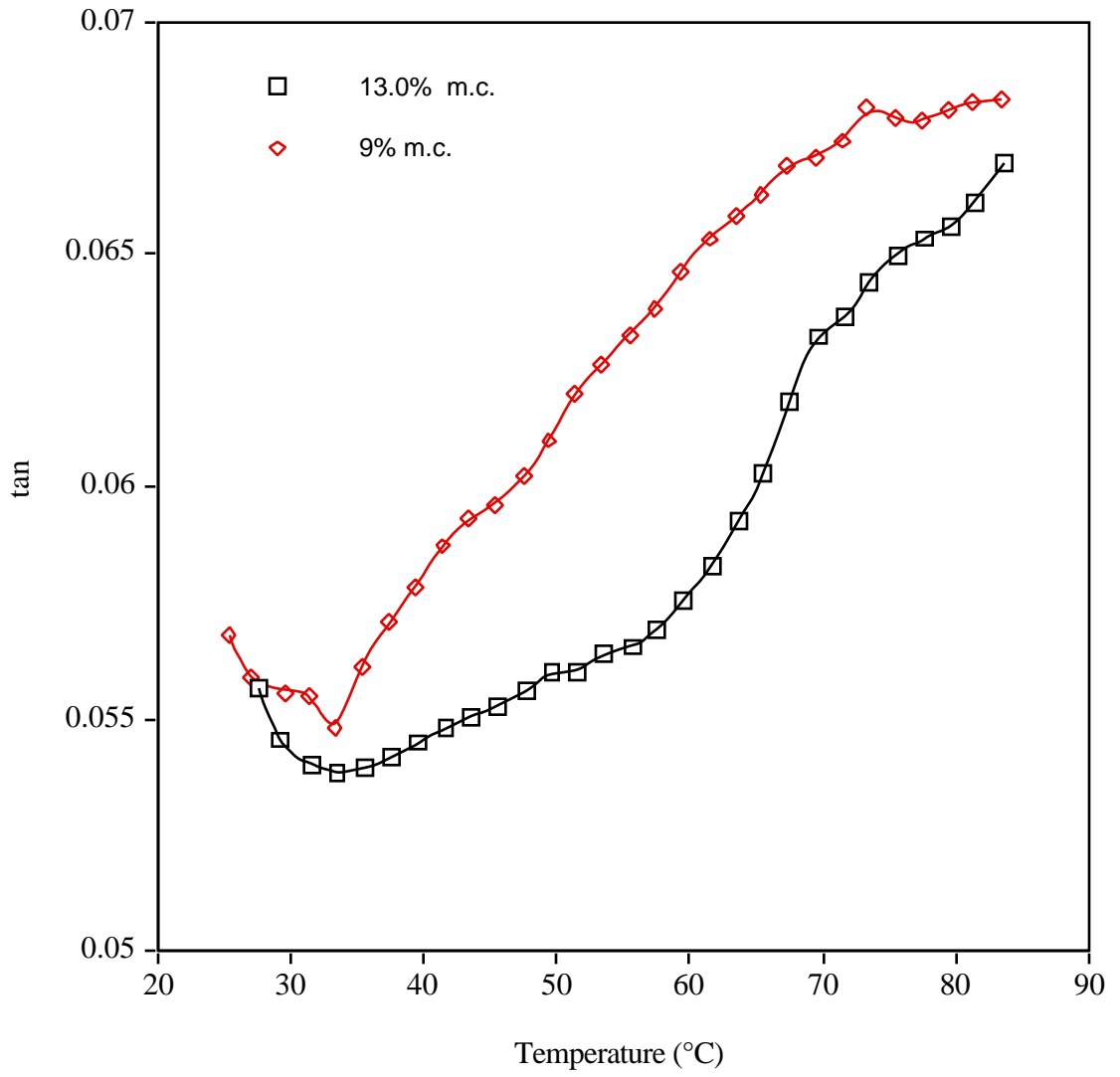


Figure 4.4 Loss tangent for southern pine at 13.0 and 9% moisture contents.

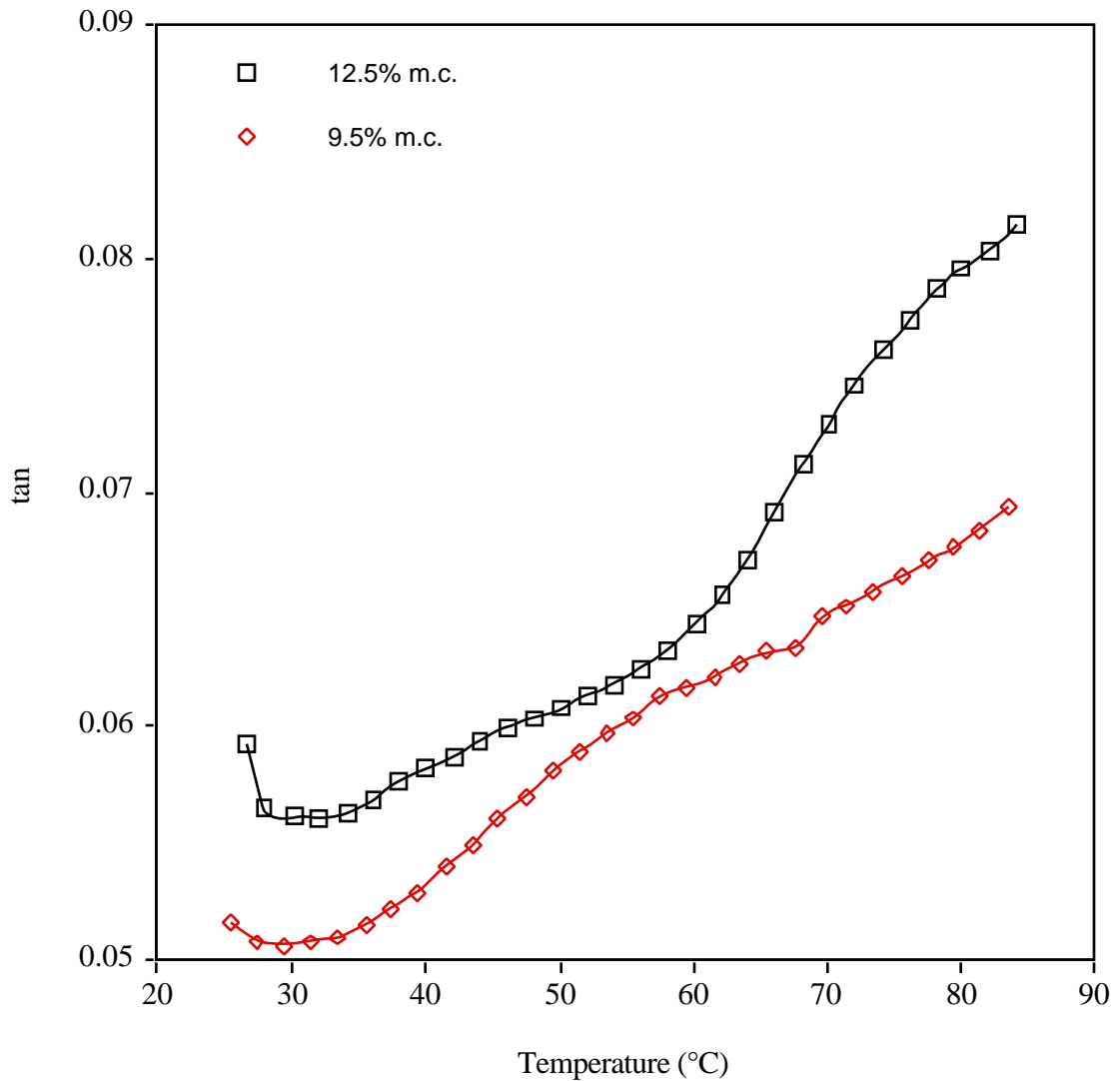


Figure 4.5 Loss tangent for Douglas-fir at 12.5 and 9.5% moisture contents.

The results obtained are consistent with those of Kelly et al. (1987): For yellow-poplar, the transition at 5 and 7% m.c. correspond to lignin whereas the transition at 9% m.c. is attributed to hemicellulose. At 12 and 9% m.c. the transitions in southern pine and Douglas-fir are attributed to hemicellulose. This is a cause of concern for two reasons: (1) wood is clearly thermorheologically complex with two transitions; (2) the transitions are close to the short-term test temperature and moisture content ranges.

4.1.2 Creep Tests

The advantages of using the DMA for creep tests are speed, unattended operation, automatic data collection and reliability. The following parameters recommended by a colleague (Chang, 1991) who used the DMA extensively were used:

- 15 min creep, 45 min recovery
- Time to equilibrate the temperature: 1 min
- Temperature increments: 10°C
- Span: varied between 25 and 40 mm

At first, tests were conducted on unpainted samples which quickly lost moisture. Consequently, the creep curves could not be superposed beyond the second temperature increment. Then some samples were painted with aluminum paint and tested. Due to the long duration of the tests, moisture still escaped and the creep curves could not be superposed. Two examples are shown in figures 4.6 and 4.7 for yellow-poplar at 5 and 7% moisture content, respectively.

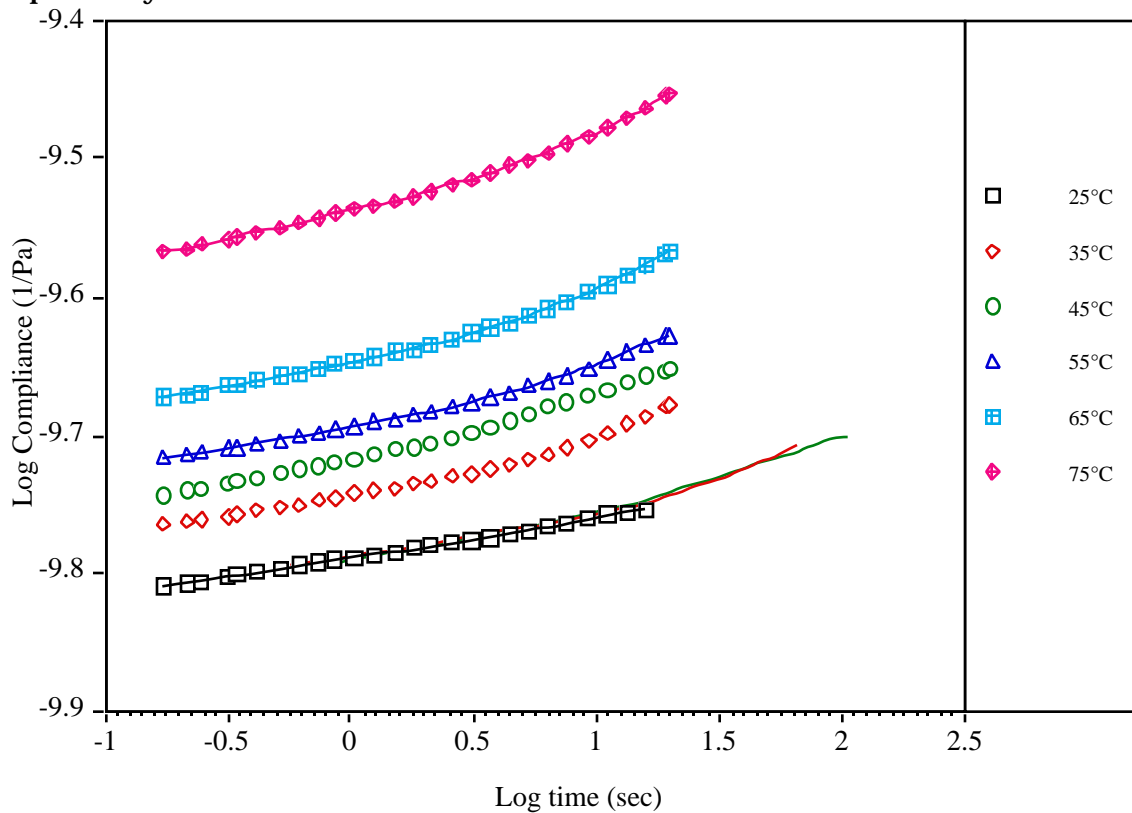


Figure 4.6 Compliance curves for yellow-poplar at 5% moisture content.

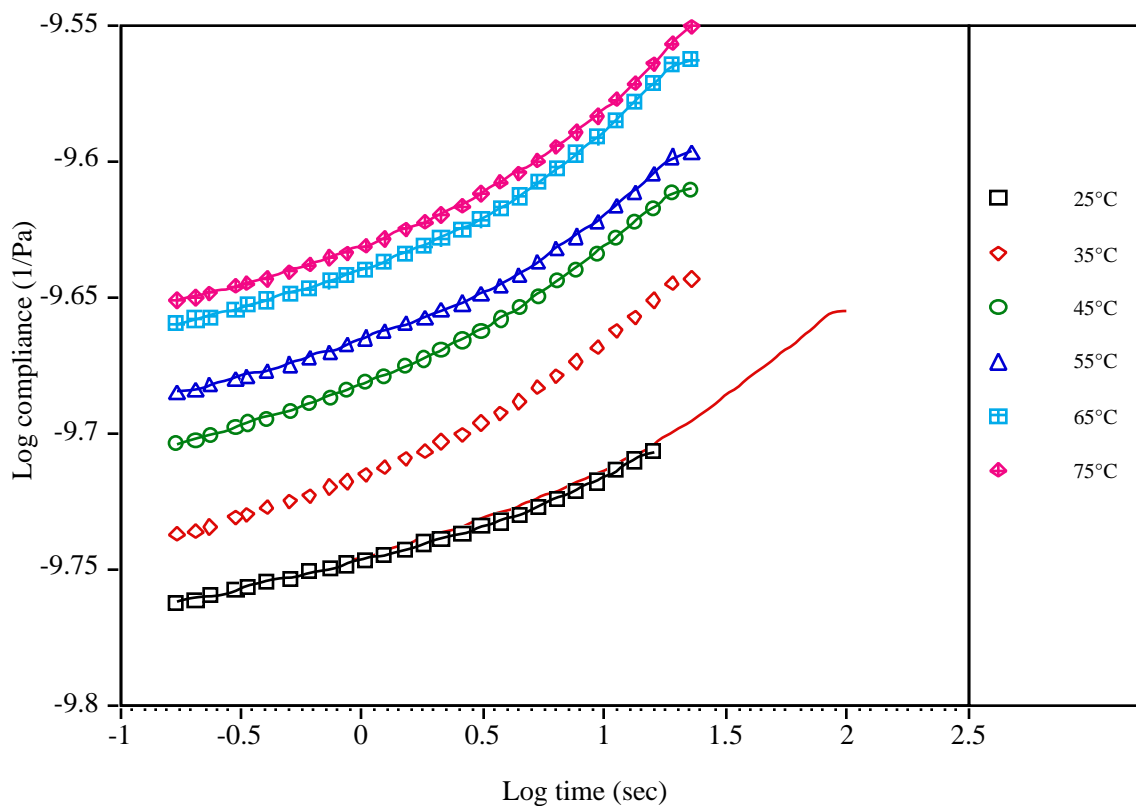


Figure 4.7 Compliance curves for yellow-poplar at 7% moisture content.

The DMA is a useful tool for detecting transitions in polymers and for conducting creep tests for TTSP. However, the lack of humidity control makes it inadequate for wood. The fixed frequency tests revealed that the wood is undergoing a transition between 60 and 80°C at moisture contents between 5% and 10%. Superposition of the creep test curves was not possible beyond 40°C for most tests; although the loss of moisture is a major factor, the presence of transitions can also be a factor.

4.2 Short-Term Creep Tests

The short-term creep tests were the most challenging part of the research. Several problems were encountered and attempts to correct them were made. This led to overall improvements of the results. Short-term creep results were discussed by Tissaoui et al. (1992) and Bond (1993).

4.2.1 Difficulties

The main problems were maintaining a constant temperature and relative humidity, maintaining a constant moisture content from one test to the next,

applying the load in a consistent manner, and the possible creep of the strain gage adhesive.

Environment

It was noticed that the data was not smooth, especially at the higher temperatures. Variations in the temperature and relative humidity were suspected. To check this hypothesis, the temperature and relative humidity were monitored during each test and it was found that the temperature and relative humidity were fluctuating; this led to a change in the moisture content of the samples during the test. To maintain a constant temperature and relative humidity, a new environmental chamber with thicker insulation and a better access door was built. Aluminum paint was applied for added protection especially at the higher temperatures. The result was a marked reduction in temperature and relative humidity fluctuation although slight variation still occurred at the highest temperatures of 70 and 80°C, especially when the target moisture content was 12%.

Moisture content

In order to apply TTSP, it is necessary to maintain a constant moisture content when increasing the temperature between tests. Three dummy samples were placed in the testing chamber to determine the moisture content. The Hailwood-Horobin model (Simpson 1971) was used to approximate the required relative humidity to maintain the desired moisture content. However, adjustments had to be made until the moisture content was stable. This process took from two to four days which added to the time required to complete the tests.

Load application

It is important to apply the load consistently from one test to the next. In some of the tests, the weight rotated or was applied faster than in others. This led to inconsistent results especially for tests that last for short periods of time (hours); problems included fluctuation of the data and variation in the initial compliance. Great efforts were made to insure that the load was released at the same rate with minimum disturbance.

Strain gages

Unless the strain gage adhesive (an epoxy) is cured at a higher temperature than the specimen will be subjected to, it can creep leading to errors in strain measurements (especially at the higher temperatures). To eliminate this problem, the samples were placed in an oven at 95°C for about 15 minutes. It was also suggested by the gage manufacturer that a pre-coat of adhesive be applied prior to installing the strain gages. This however did not change the results.

4.2.2 Creep in tension

Creep experiments in tension were conducted on southern yellow pine, Douglas-fir, and yellow-poplar samples. Figure 4.7 shows the compliance

curves and the master curve obtained by superposition for a yellow-poplar sample at 6% moisture content. The extrapolated data from five hour tests corresponds to about 75 days. The horizontal shift factors follow an Arrhenius relation since the relation between the temperature and the horizontal shift factors is linear as shown in Figure 4.8; the corresponding activation energy is 92.5 kJ/mole.

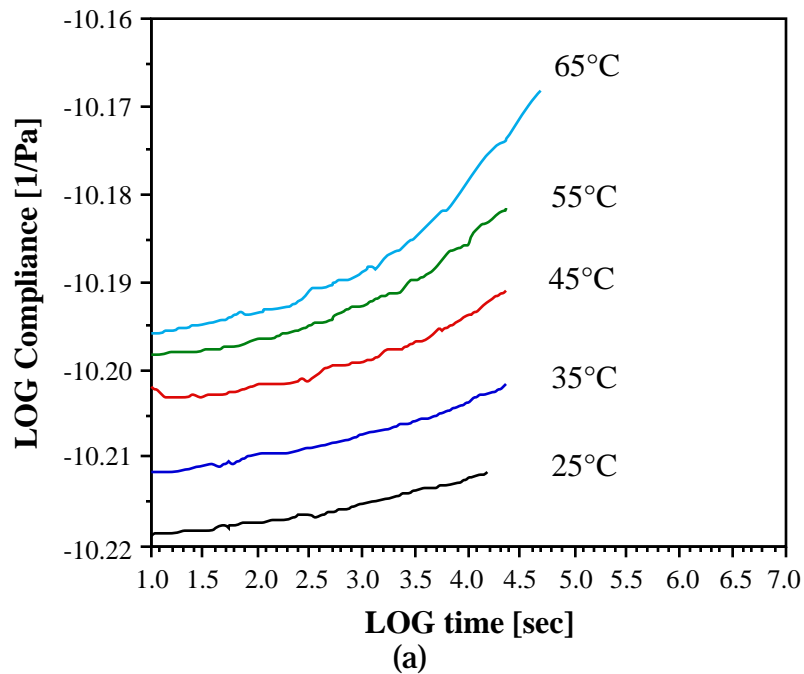
The master curve was fitted to the power law equation using a nonlinear fitting procedure (SAS Institute INC., 1989). The resulting parameters were:

$$D_0 = 6.0475 \times 10^{-11} \text{ Pa}^{-1}$$

$$b = 1.047 \times 10^{-3} \quad \text{sec}^{-k}$$

$$k = 0.273$$

Figure 4.9 shows the master curve and the curve corresponding to the power law equation.



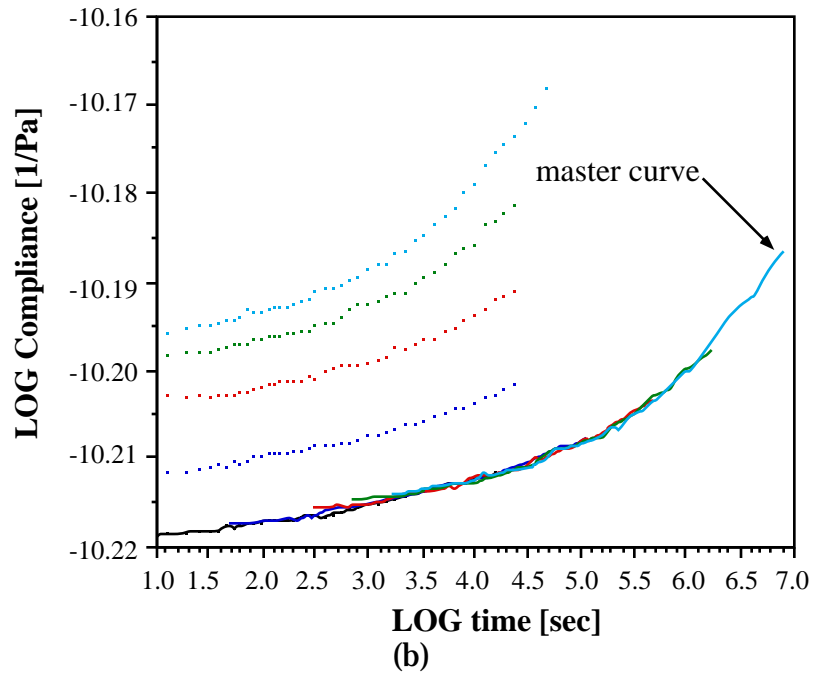


Figure 4.8 (a) Compliance and (b) master curves for yellow-poplar at 6% moisture content (tension).

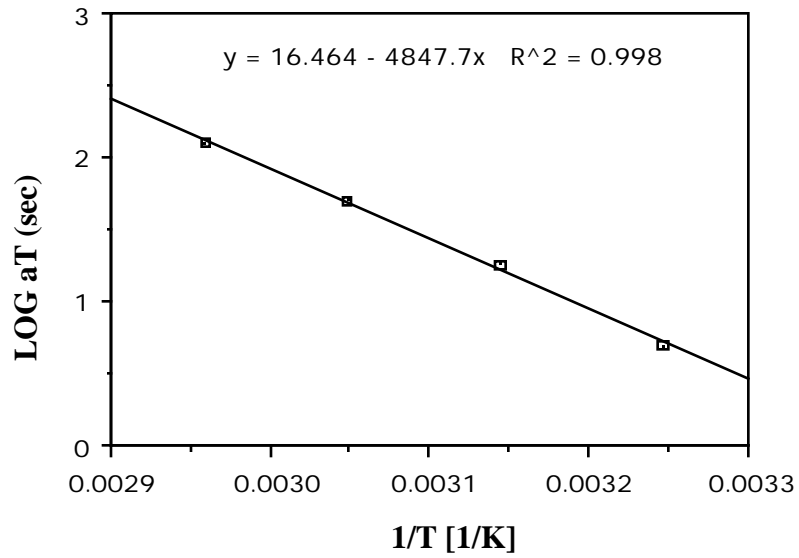


Figure 4.9 Horizontal shift factors (tension).

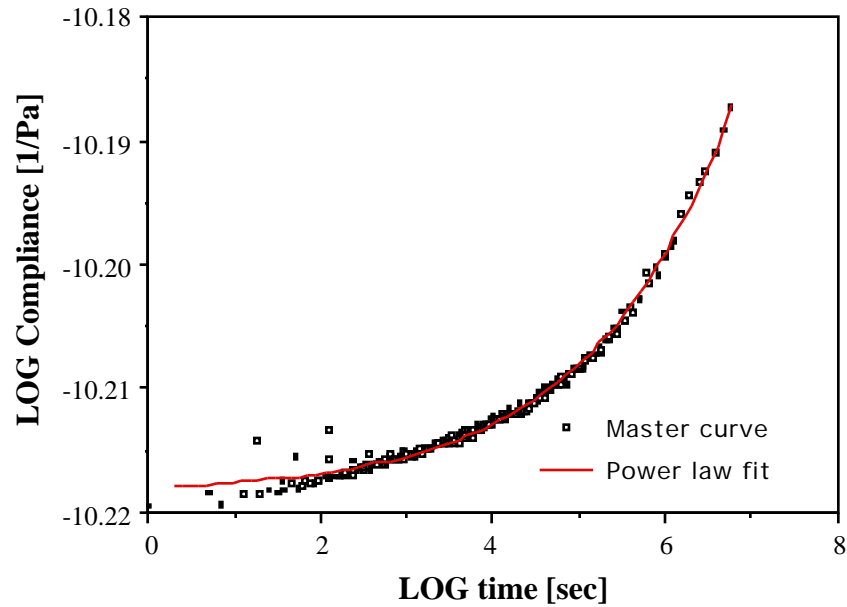


Figure 4.10 Master curve and power law fit (tension).

Creep test on southern pine, Douglas-fir, and yellow-poplar in tension at 6% m.c.

As shown in figure 4.11, the environmental conditions remain constant throughout the creep tests. The creep could be superposed at all temperatures except for the curves at 65°C for southern pine. The compliance and master curves are shown in figures 4.12, 4.14, and 4.16, and the shift factors are plotted in figures 4.13, 4.15, and 4.17. The activation energies were 74.6, 128.0, and 90.7 kJ/mole for southern pine, yellow-poplar and Douglas-fir, respectively. The master curves were fit to the power law equation and the parameters are shown in table 4.3.

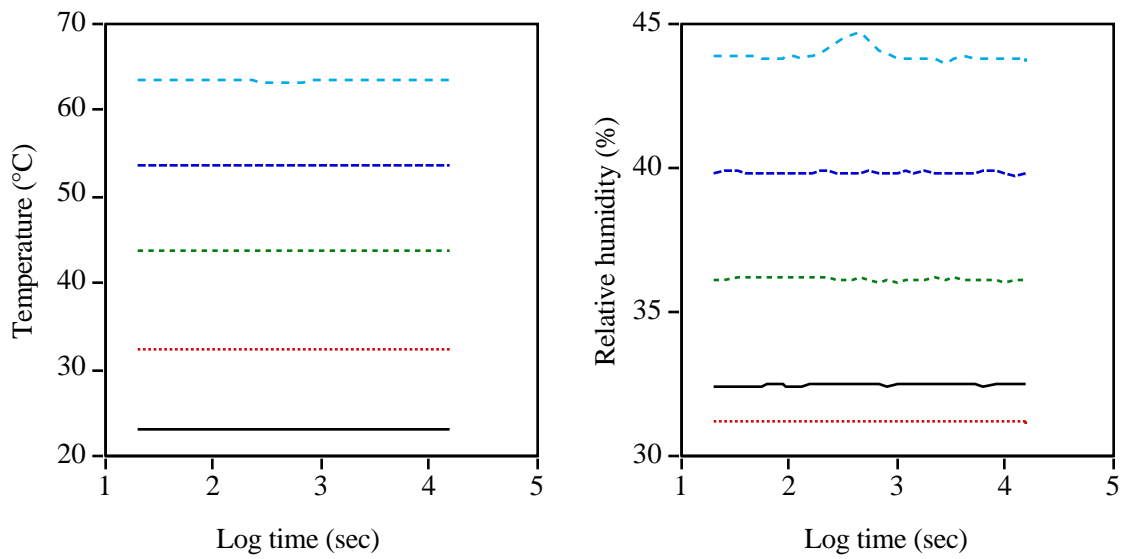


Figure 4.11 temperature and relative humidity during the test.

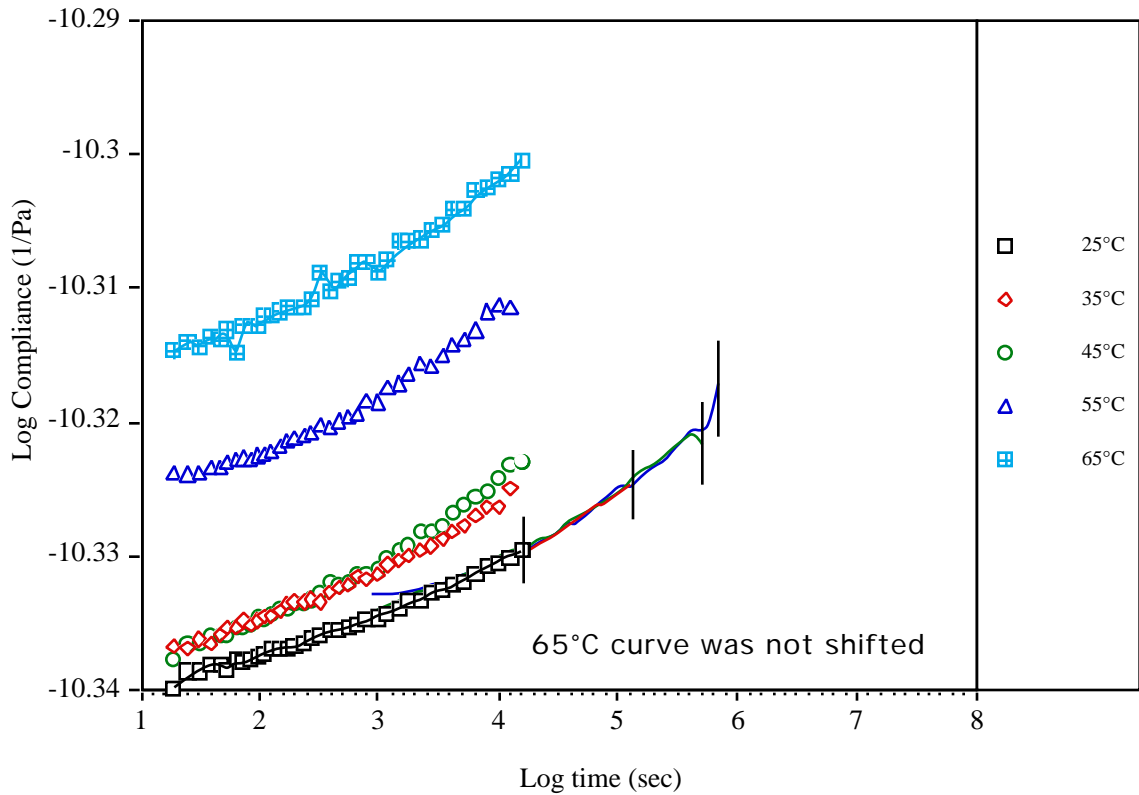


Figure 4.12 Compliance and master curves for southern pine at 6% moisture content (tension).

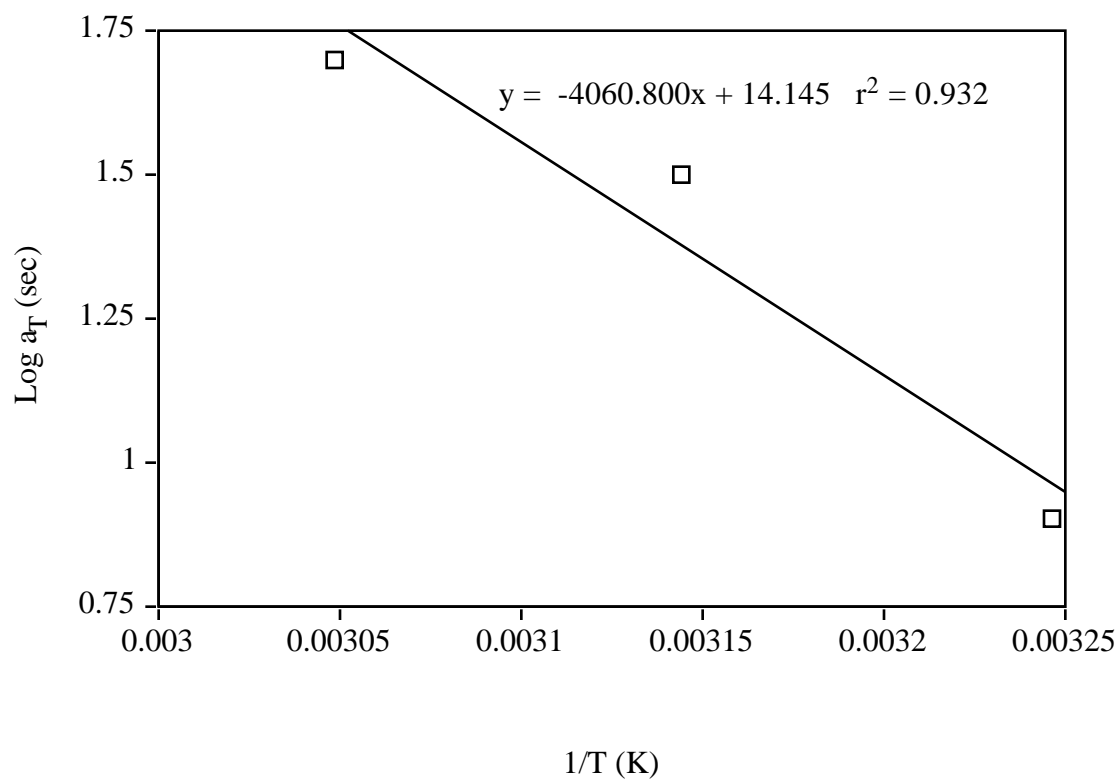


Figure 4.13 Horizontal shift factors for southern pine, DH=74.6 kJ/mole.

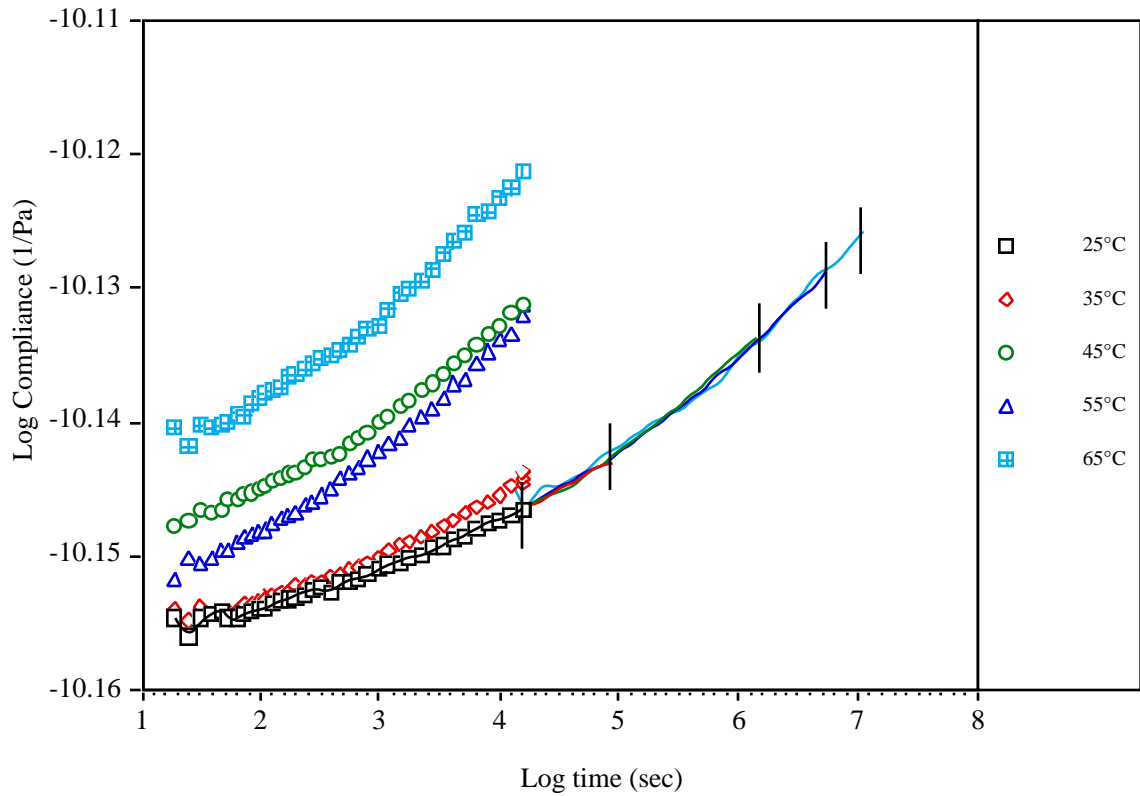


Figure 4.14 Compliance and master curves for yellow-poplar at 6% moisture content (tension).

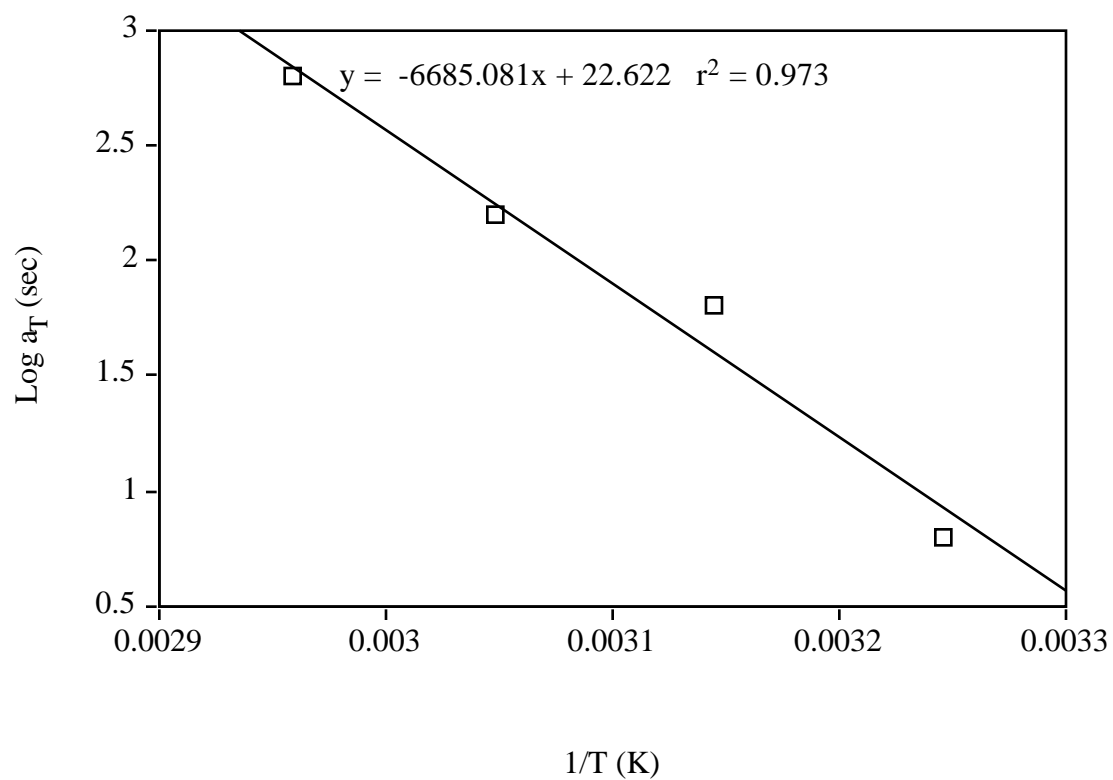


Figure 4.15 Horizontal shift factors for yellow-poplar, DH=128.0 kJ/mole.

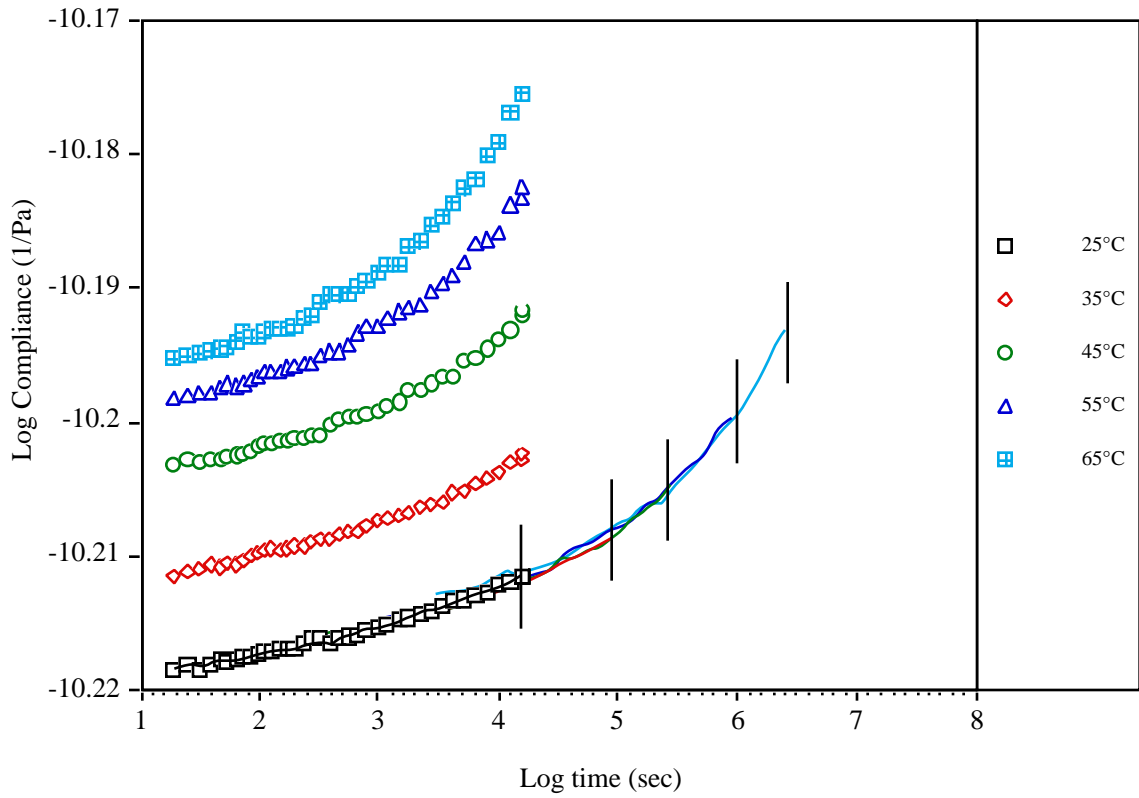


Figure 4.16 Compliance and master curves for first at 6% moisture content (tension).

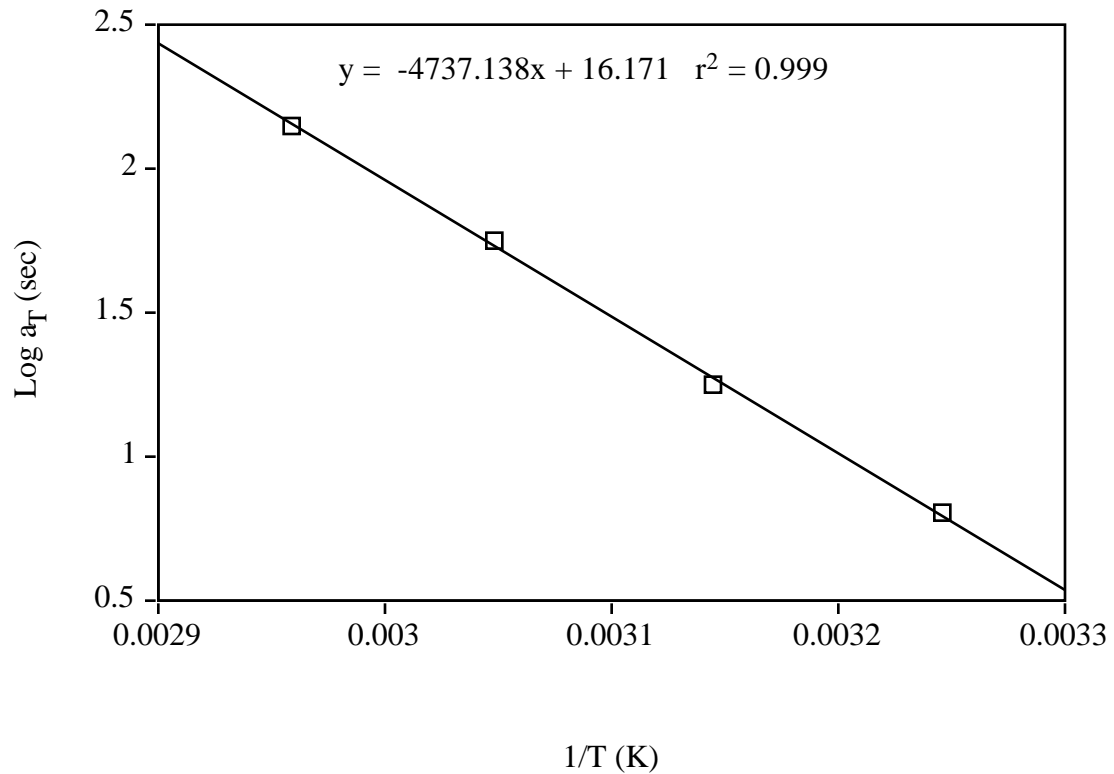


Figure 4.17 Horizontal shift factors, DH=90.7 kJ/mole.

Table 4.3 Power law parameters for southern pine, yellow-poplar, and Douglas-fir at 6% moisture content in tension.

	D_0 (Pa ⁻¹)	b (sec ^k)	k
Southern pine	4.503×10^{-11}	0.0117	0.1256
Douglas-fir	6.049×10^{-11}	0.00135	0.2546
yellow-poplar	6.918×10^{-11}	0.00779	0.1497

4.2.3 Creep in compression

Creep in compression was conducted on southern yellow pine, Douglas-fir, and yellow-poplar samples. Figure 4.18 shows the compliance curves and master curve for a Douglas-fir sample at 9% moisture content. The horizontal shift factors (figure 4.19) follow an Arrhenius relation as indicated by the linear relation between the shift factors and the temperature. The corresponding activation energy is 20.0 Kcal/mole.

The compliance curves for the Douglas-fir sample at 20, 30, 50, and 60°C were superposed to obtain a master curve which was then fitted to the power law equation; the parameters are:

$$D_0 = 8.374 \times 10^{-11} \text{ Pa}^{-1}$$
$$b = 2.53 \times 10^{-3} \text{ sec}^{-k}$$
$$k = 0.248$$

Figure 4.20 shows the master curve from the experimental data as well as the curve from the power law equation. The master curve extrapolated the short term creep data to about 30 days from 4 six hour tests; compliance curves at 70 and 80°C would provide more extrapolation of the data; however, unstable environmental conditions prevented the collection of the creep data.

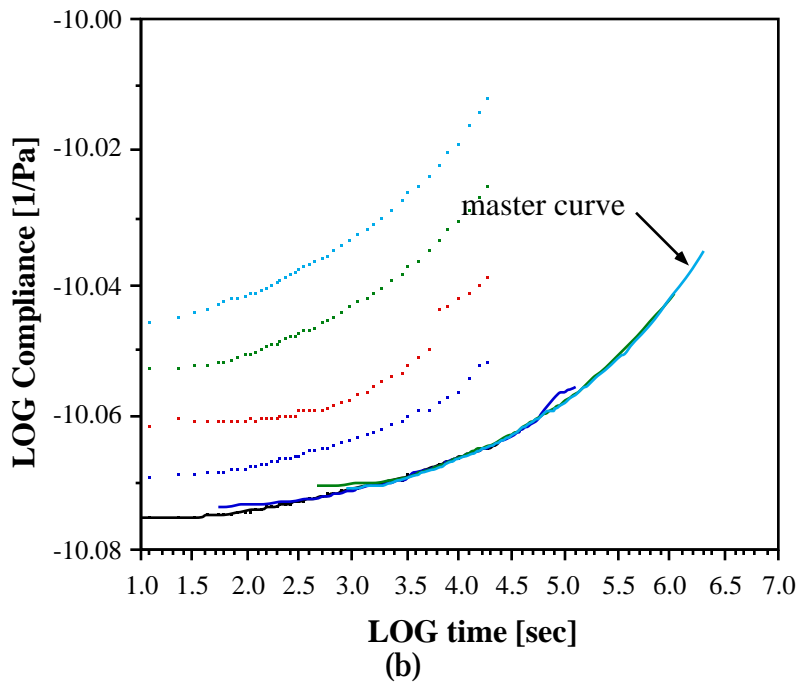
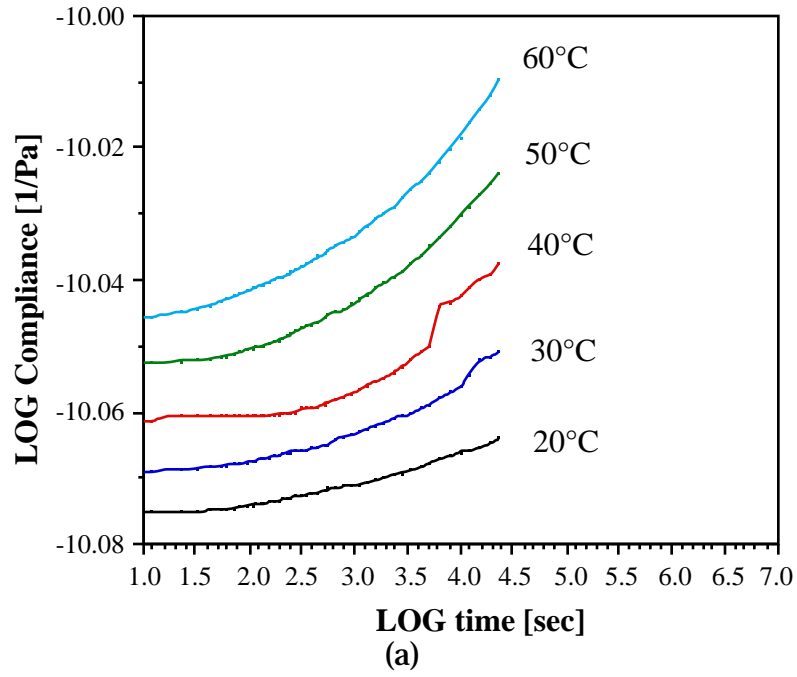


Figure 4.18 (a) Compliance and (b) master curves for Douglas-fir at 9% moisture content (compression).

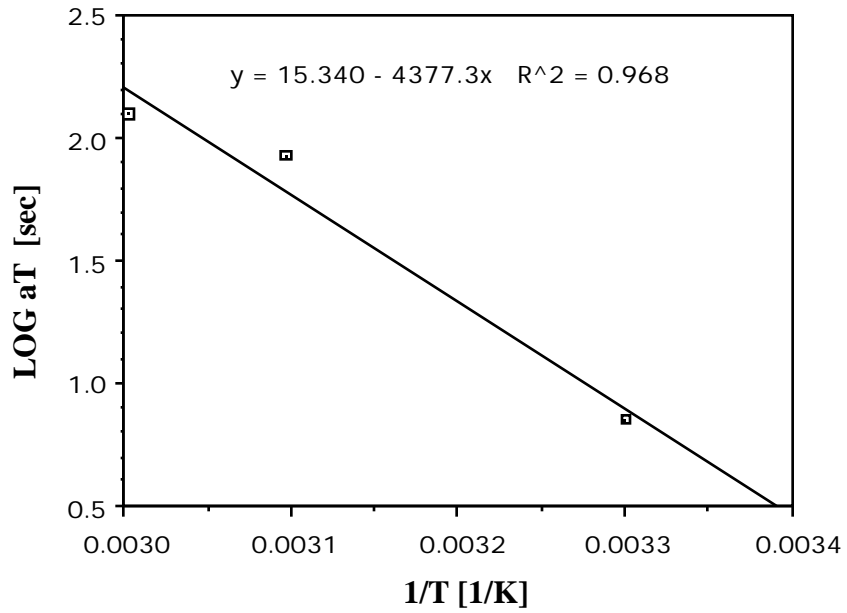


Figure 4.19 Horizontal shift factors (compression).

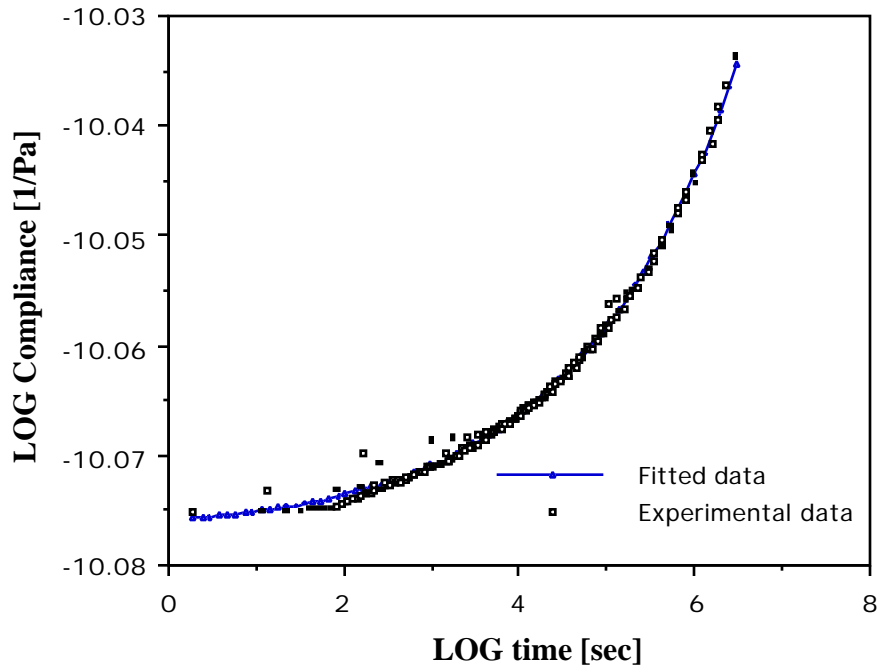


Figure 4.20 Master curve and power law fit (compression).

Creep test on southern pine, Douglas-fir, and Parallam™ in compression at 6% m.c.

Figure 4.21 shows that the environmental conditions remain constant throughout the creep tests. Except for the curves at 70 and 80°C, the curves could be superposed to form a master curve. The compliance and master curves are shown in figures 4.22, 4.24, and 4.26, and the shift factors are plotted in figures 4.23, 4.25, and 4.27. The activation energies were 108.7, 109, and 129 kJ/mole for southern pine, Douglas-fir, and Parallam™, respectively. The master curves were fit to the power law equation and the parameters are shown in table 4.4.

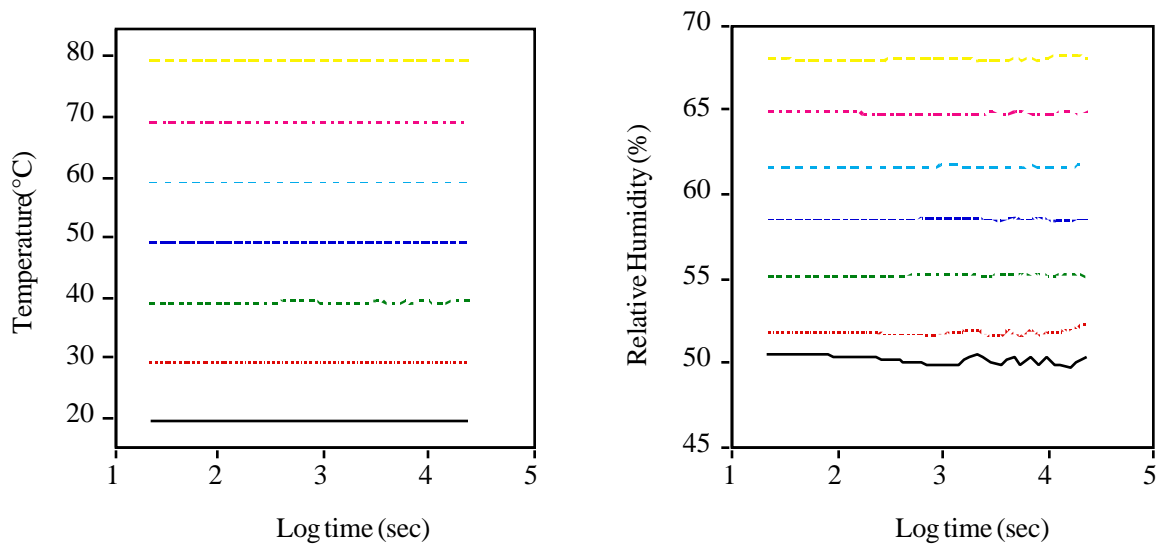


Figure 4.21 Temperature and relative humidity during the test.

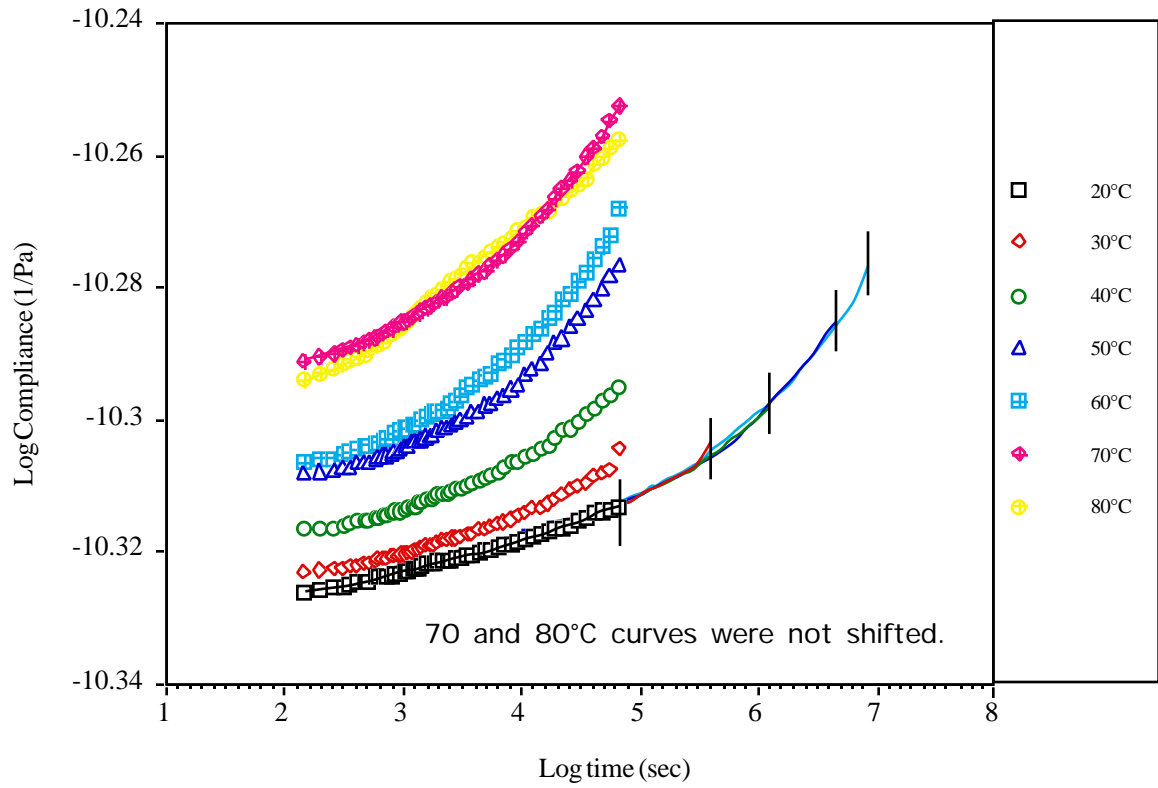


Figure 4.22 Compliance and master curves for southern pine at 9% moisture content (compression).

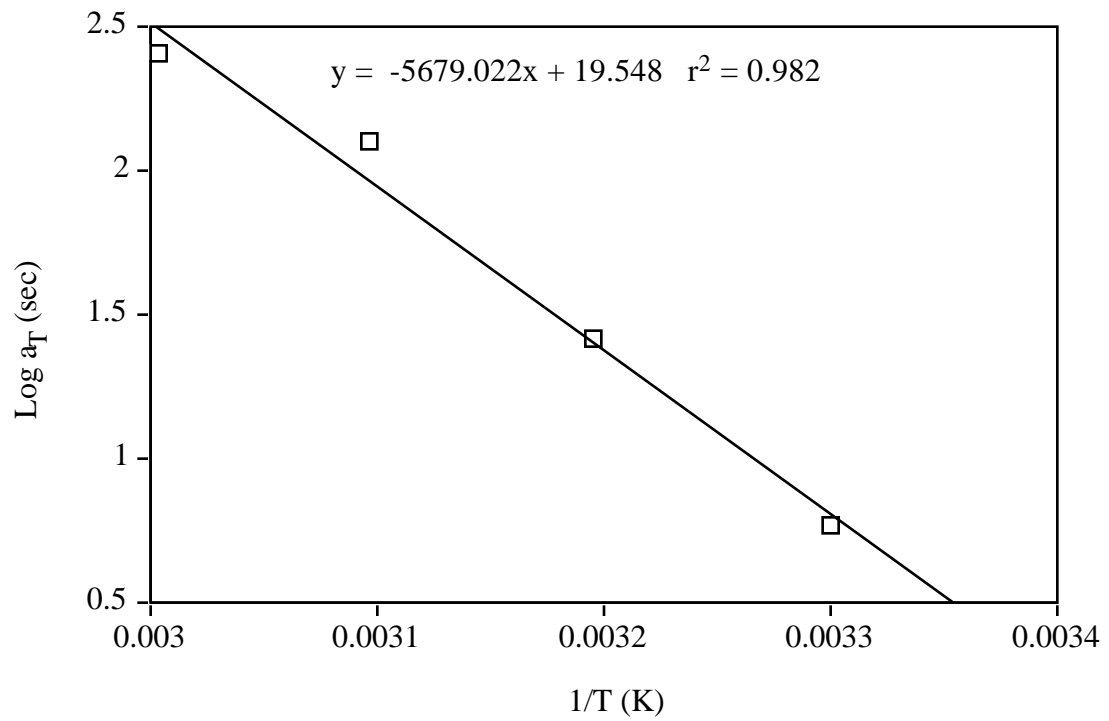


Figure 4.23 Horizontal shift factors for southern pine at 9% moisture content, $\Delta H = 108.7$ kJ/mole.

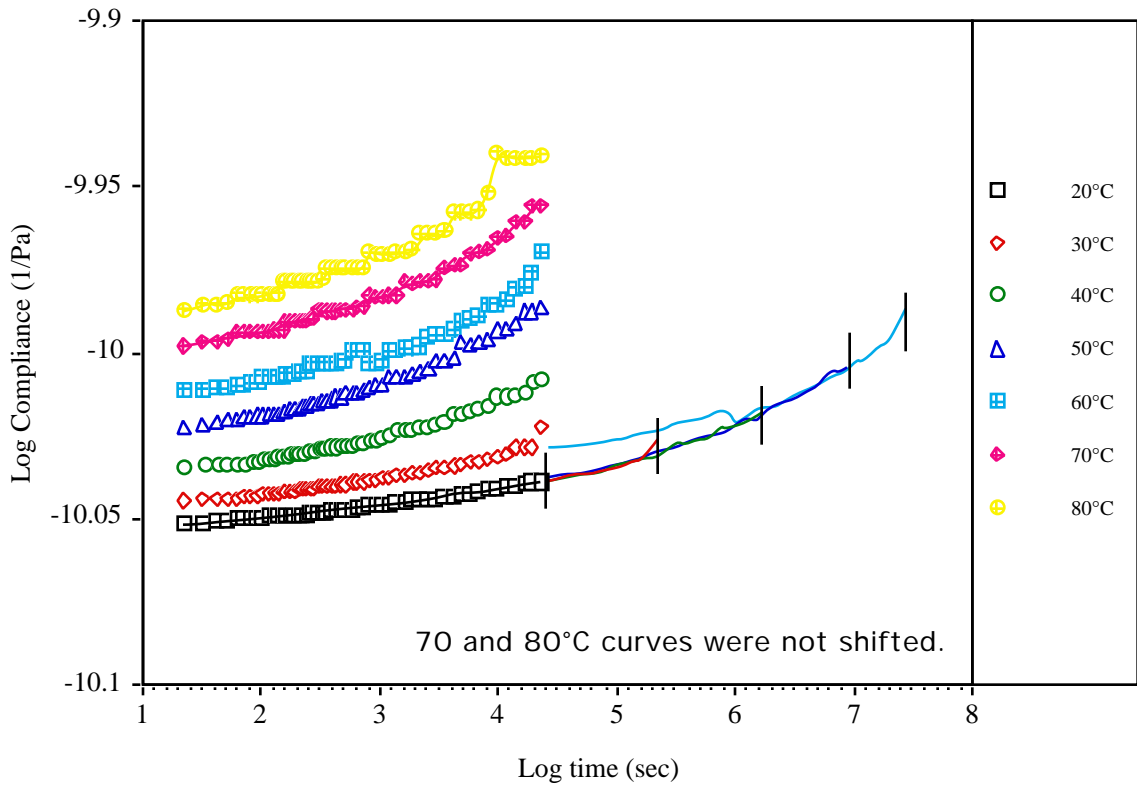


Figure 4.24 Compliance and master curves for Douglas-fir at 9% moisture content (compression).

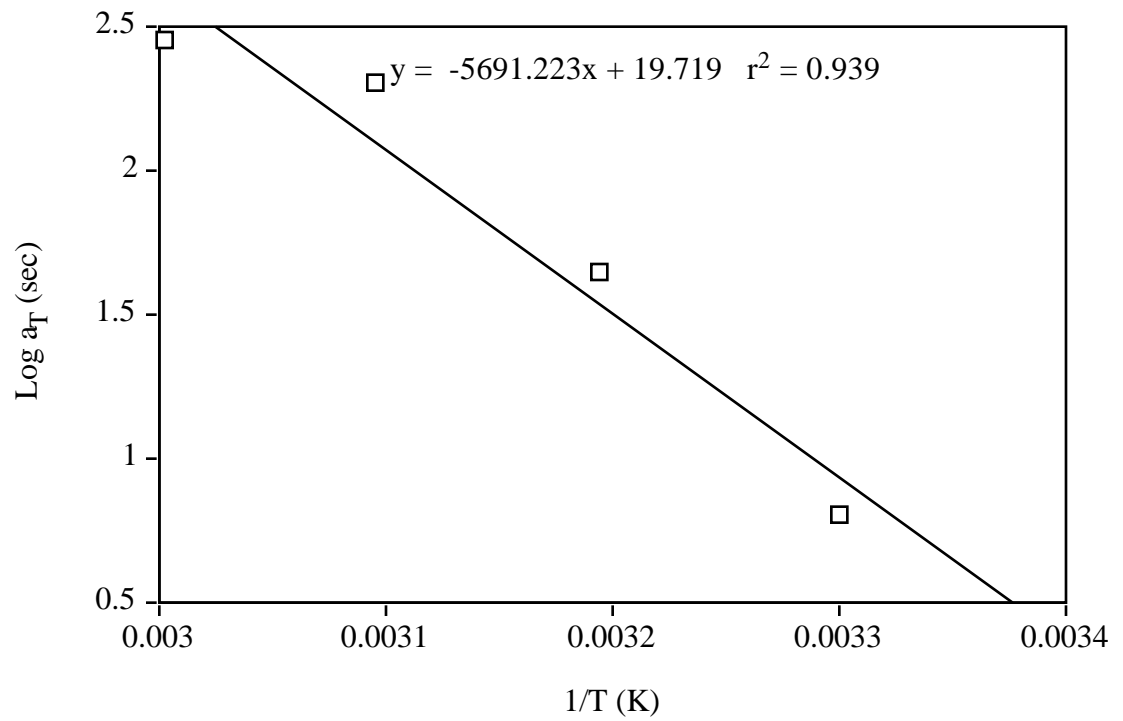


Figure 4.25 Horizontal shift factors for Douglas-fir at 9% moisture content, $\Delta H = 109.0$ kJ/mole.

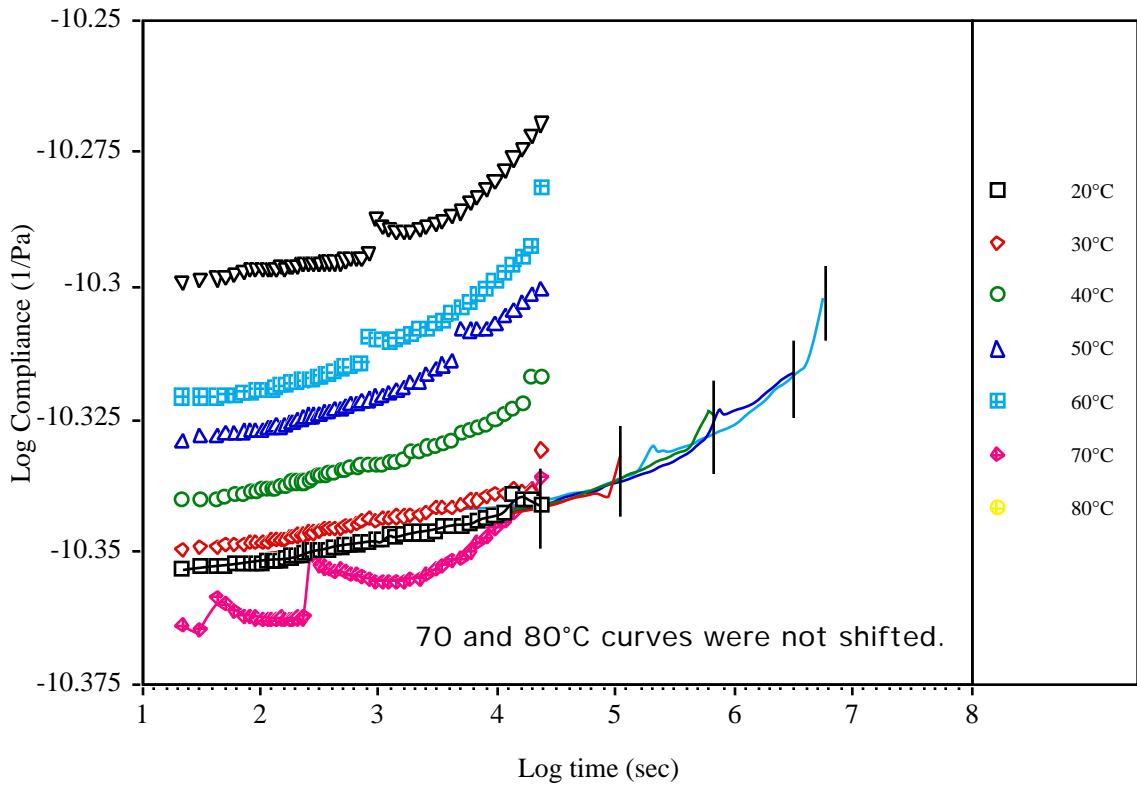


Figure 4.26 Compliance and master curves for Parallam™ at 9% moisture content (compression).

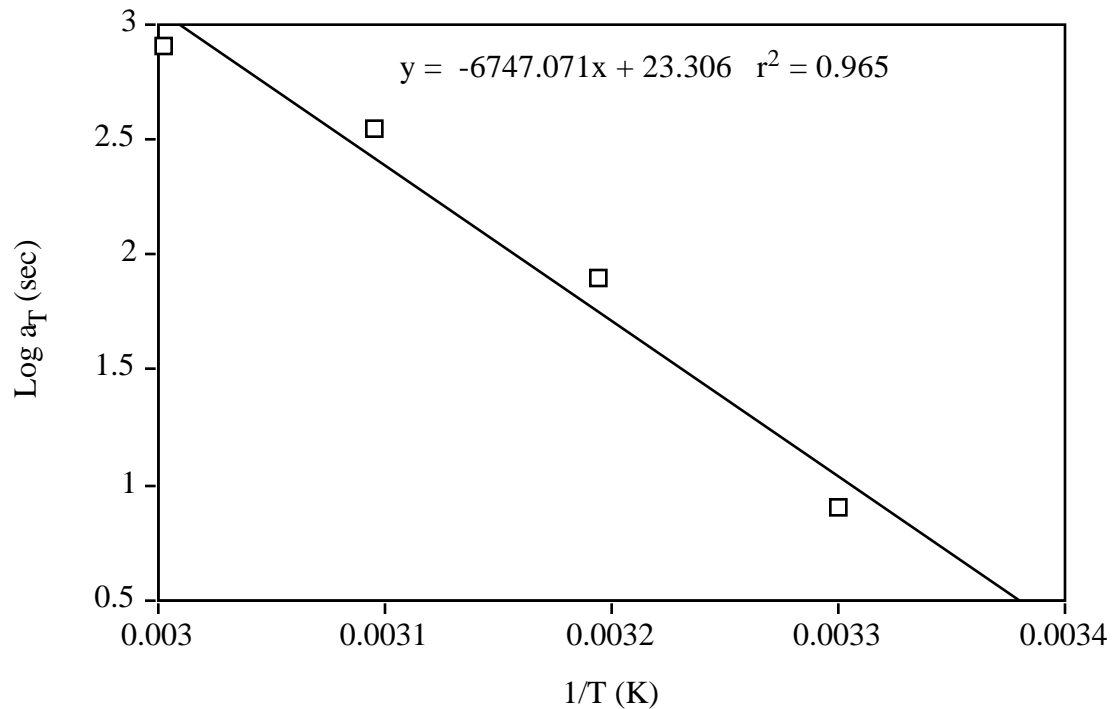


Figure 4.27 Horizontal shift factors for Parallam™ at 9% moisture content, $\Delta H= 129.2$ kJ/mole.

Table 4.4 Power law parameters for southern pine, Douglas-fir, and Parallam™ at 6% moisture content.

	D_0 (Pa ⁻¹)	b (sec ^{-k})	k
Southern pine	4.697×10^{-11}	0.00411	0.2163
Douglas-fir	8.815×10^{-11}	0.00472	0.2083
Parallam™	4.418×10^{-11}	0.00403	0.2006

Superposition of the compliance curves was possible at temperatures below 60°C; however, it was not possible to superpose most of the curves at 70 and 80°C. The activation energies obtained were within published results (Gamalath, 1991). Once the master curves were constructed, the power law equation parameters were determined, the exponents were within the range proposed by Nielsen, 1984.

4.2.4 Time-moisture superposition creep test

The purpose of the test was to investigate the applicability of time-moisture superposition to wood in tension. The tests were conducted at a constant temperature of 40°C to allow faster moisture equilibration. The relative humidity was changed from one test to the next to induce an increase in the moisture content. The initial moisture content was 5%; the subsequent moisture contents were 6, 7, 9, and 17%. Condensation led to the sharp increase from 9 to 17% moisture content in the last test. The creep test was 6 hours long, and recovery lasted 30 hours to allow the specimens to reach equilibrium moisture content. The moisture contents of dummy samples were recorded before and after each test and were nearly identical. The samples tested were yellow-poplar, kiln-dried southern yellow pine, and air-dried southern yellow pine.

Results

The compliance and master curves for the three samples are shown in figure 4.28 for the yellow-poplar, figure 4.29 for kiln-dried southern yellow pine, and figure 4.30 for air-dried southern yellow pine. For the yellow-poplar, it was possible to superpose the compliance curves with some vertical shifting. For the southern pine, it was not possible to superpose the curves at the lower moisture contents (zero or negative horizontal shift); also, larger vertical shifts were necessary.

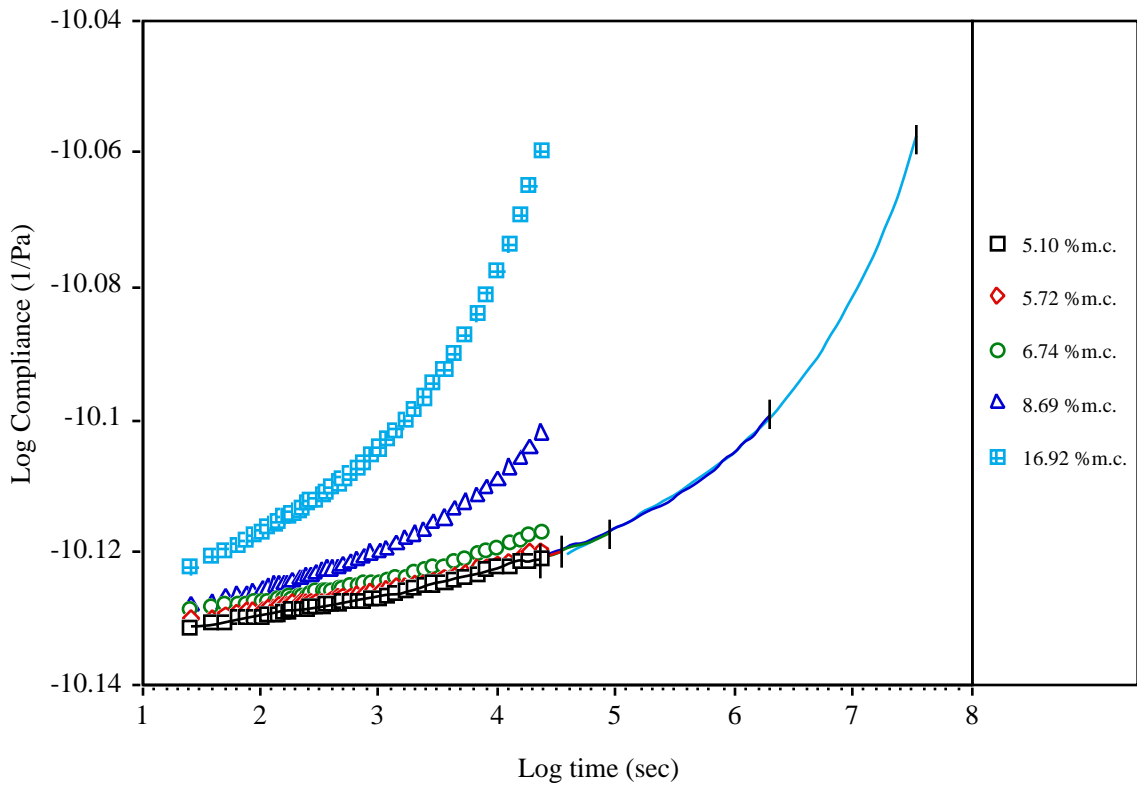


Figure 4.28 Compliance and master curves for the yellow-poplar sample

($M_{c_{ref}} = 5.10\%$).

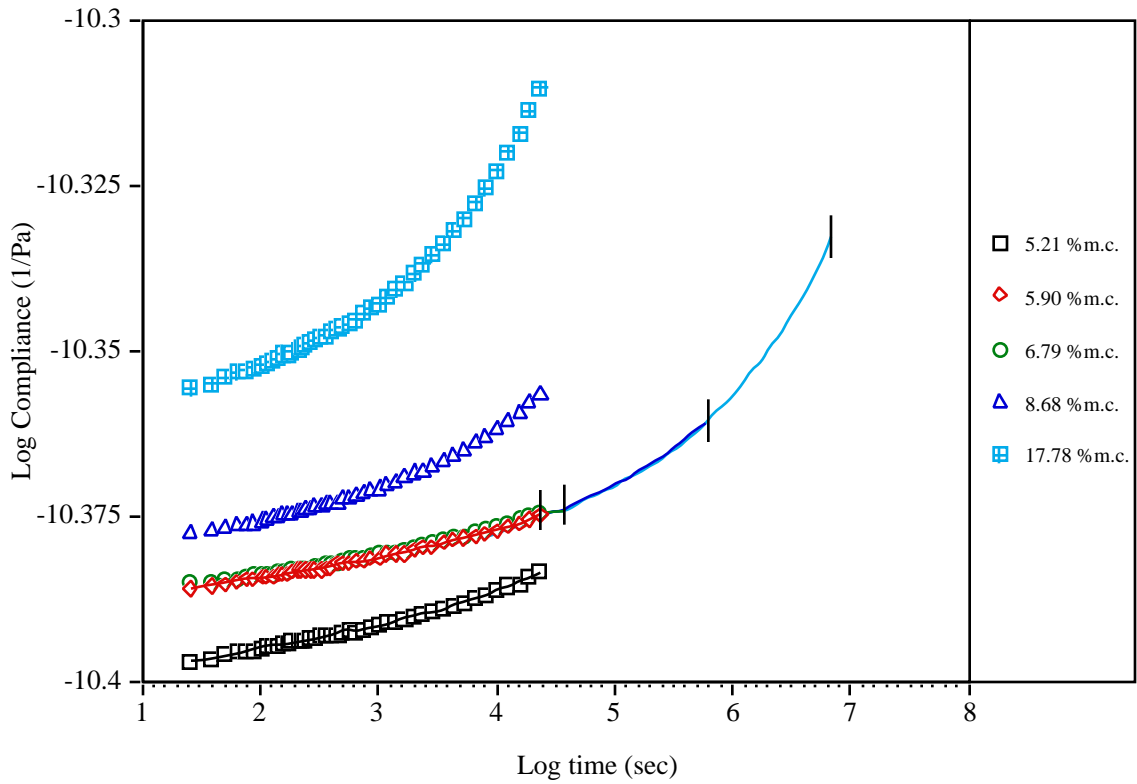


Figure 4.29 Compliance and master curves for the kiln dried southern yellow pine sample ($M_{c_{ref}} = 5.21\%$).

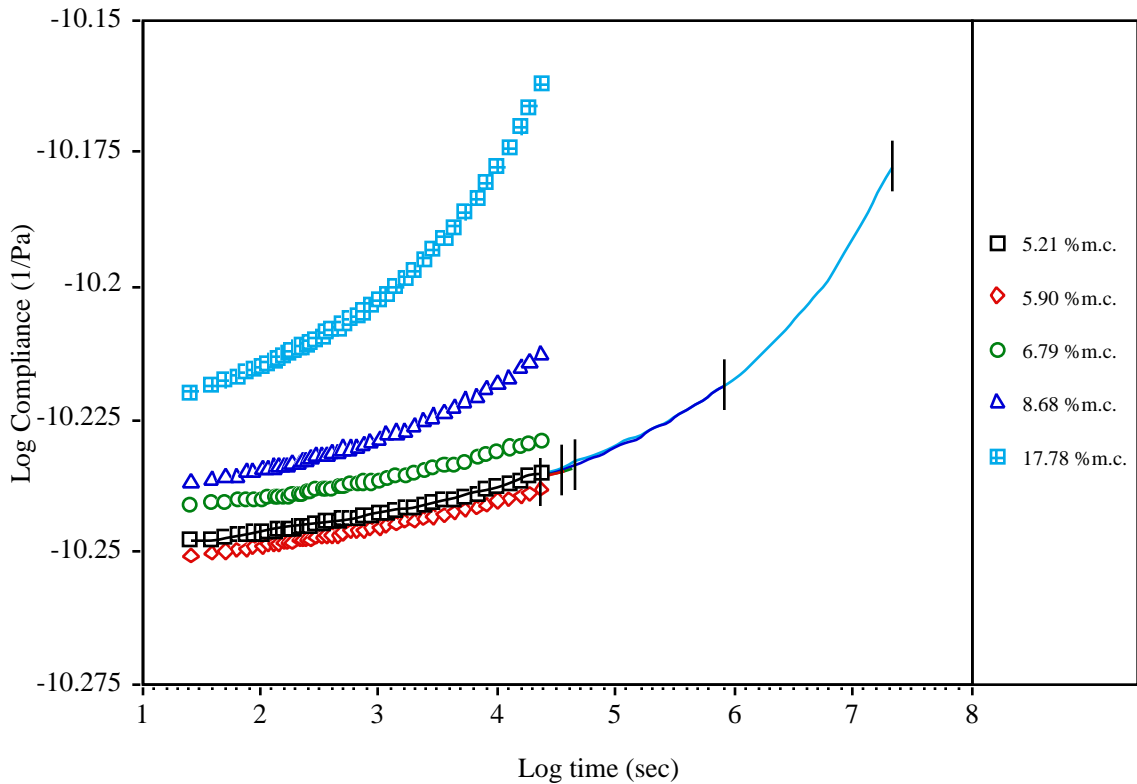


Figure 4.30 Compliance and master curves for the air dried southern yellow pine sample ($M_{c_{ref}} = 5.21\%$)..

The yellow pine master curve was fitted to the power law equation, the equation parameters were:

$$D_0 = 7.495 \times 10^{-11} \text{ (1/Pa)}$$

$$b = 0.0017 \text{ s}^{-k}$$

$$k = 0.273$$

Except for the lower moisture contents, it was possible to superpose the compliance curves at different moisture contents. However, the results should be compared with those from time-temperature superposition and long-term creep to validate them.

4.3 Long-Term Creep Tests

Due to the failure at the grips of one of the tension specimens, the long-term creep test had to be restarted. About 4 months later we had to return one of the borrowed strain indicators, as a result, we stopped taking creep strain readings for all tension specimens and 2 yellow-poplar compression specimens. There was also a brief failure of the environmental conditioning unit which did not seem to affect the results.

The collected data were fit to the power law equation and the three parameters were determined. A summary is presented in tables 4.5 and 4.6 for tension and compression respectively.

Table 4.5 Power law equation parameters for tension from long-term testing.

	D_0 (1/Pa)	$b(\text{sec}^{-k})$	k
Southern pine*	1.30119×10^{-10}	0.005262	0.2417
Southern pine*	1.21509×10^{-10}	0.0002563	0.3809
Southern pine*	1.38392×10^{-10}	5.546×10^{-6}	0.5582
Yellow-poplar*	1.26713×10^{-10}	0.0002103	0.4085
Yellow-poplar*	1.05821×10^{-10}	4.776×10^{-5}	0.4816

* data was collected for four months.

Table 4.6 Power law equation parameters for compression from long-term testing.

	D_0 ()	b	k
Southern pine	7.073×10^{-10}	0.01743	0.1187
Southern pine	8.041×10^{-10}	0.01545	0.1374
Southern pine	7.419×10^{-10}	0.00729	0.1590
Yellow-poplar	1.311×10^{-10}	0.00718	0.1825
Yellow -poplar	2.284×10^{-10}	0.01484	0.1404
Yellow -poplar*	1.374×10^{-10}	0.01151	0.1471
Yellow -poplar*	1.562×10^{-10}	7.573×10^{-5}	0.4503
Douglas-fir	1.181×10^{-10}	0.04336	0.08614
Douglas-fir	1.217×10^{-10}	0.01743	0.1271
Douglas-fir	1.363×10^{-10}	0.02293	0.1212
Douglas-fir	1.353×10^{-10}	0.03784	0.0856

* data was collected for four months

4.3.1 Creep in tension

The long-term creep curves for southern pine and yellow-poplar in tension are shown in figures 4.31 and 4.33 respectively. To better compare the results, the compliance was normalized and plotted again in figures 4.32 and 4.34. The southern pine samples showed more variability in the results than yellow-poplar.

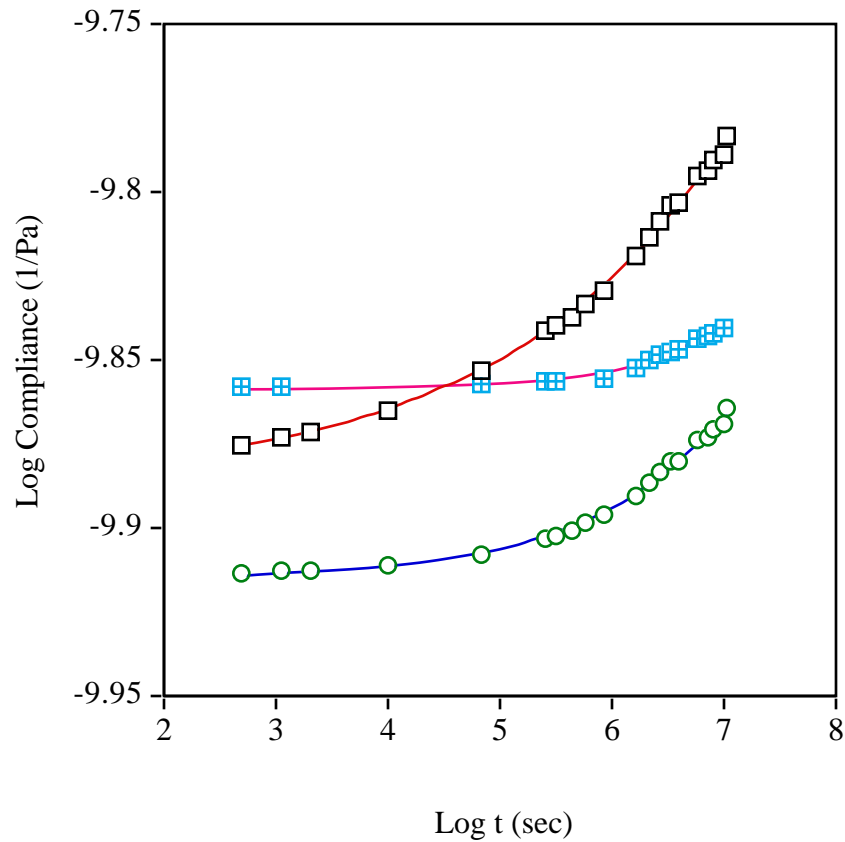


Figure 4.31 Actual (symbols) and power law fit (solid line) for three southern pine specimens in tension.

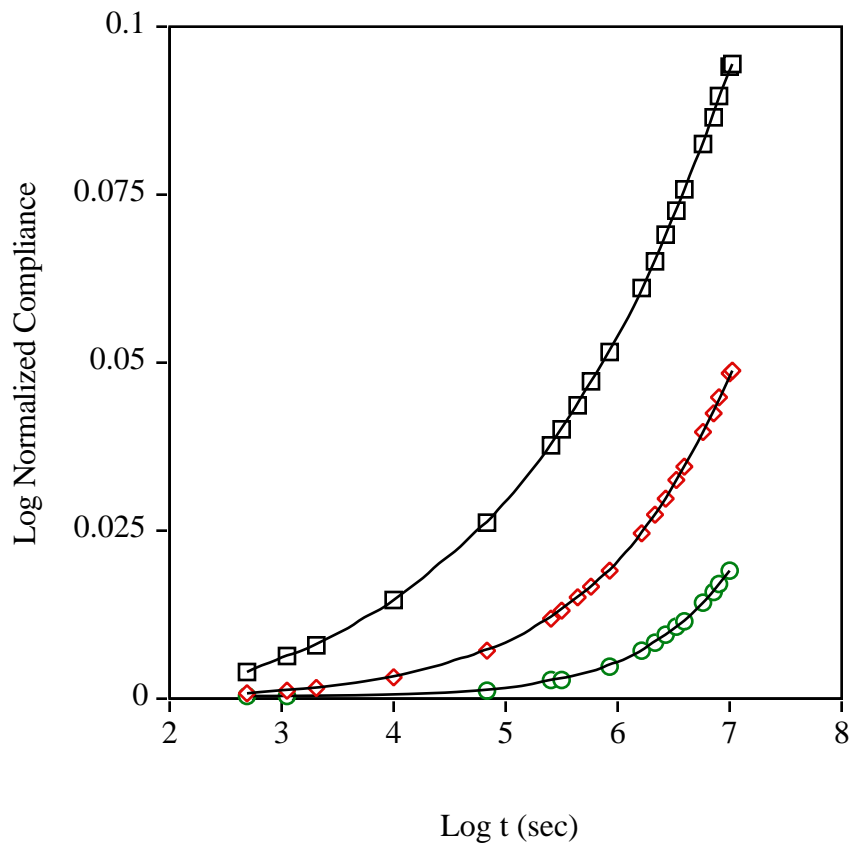


Figure 4.32 Normalized compliance curves for three southern pine specimens in tension.

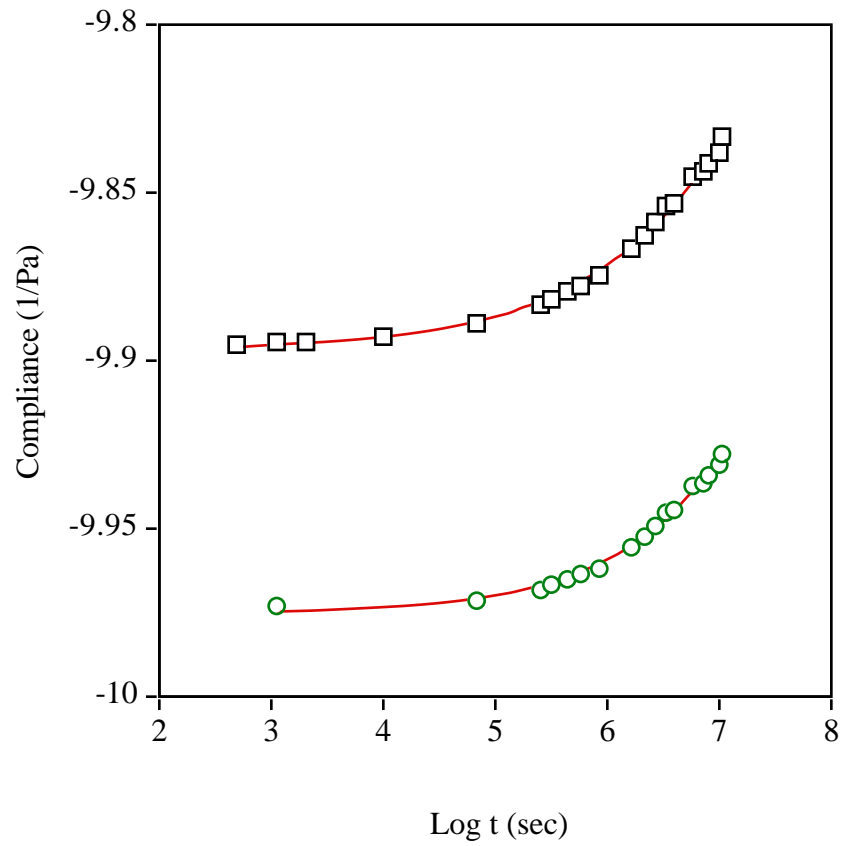


Figure 4.33 Actual (symbols) and power law fit (solid line) for two yellow-poplar specimens in tension.

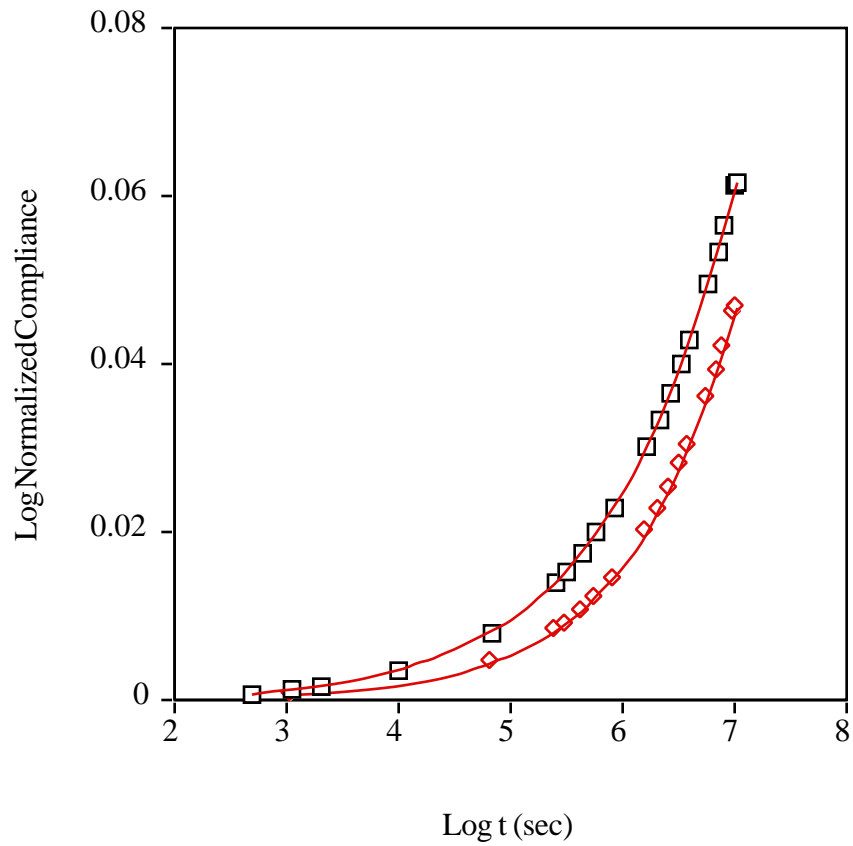


Figure 4.34 Normalized compliance curves for two yellow-poplar specimens in tension.

4.3.1 Creep in compression

The creep curves for southern pine, yellow-poplar, and Douglas-fir are shown in figures 4.35, 4.37 and 4.39, the normalized curves are shown in figures 4.36, 4.38, and 4.40. The normalized curves are consistent.

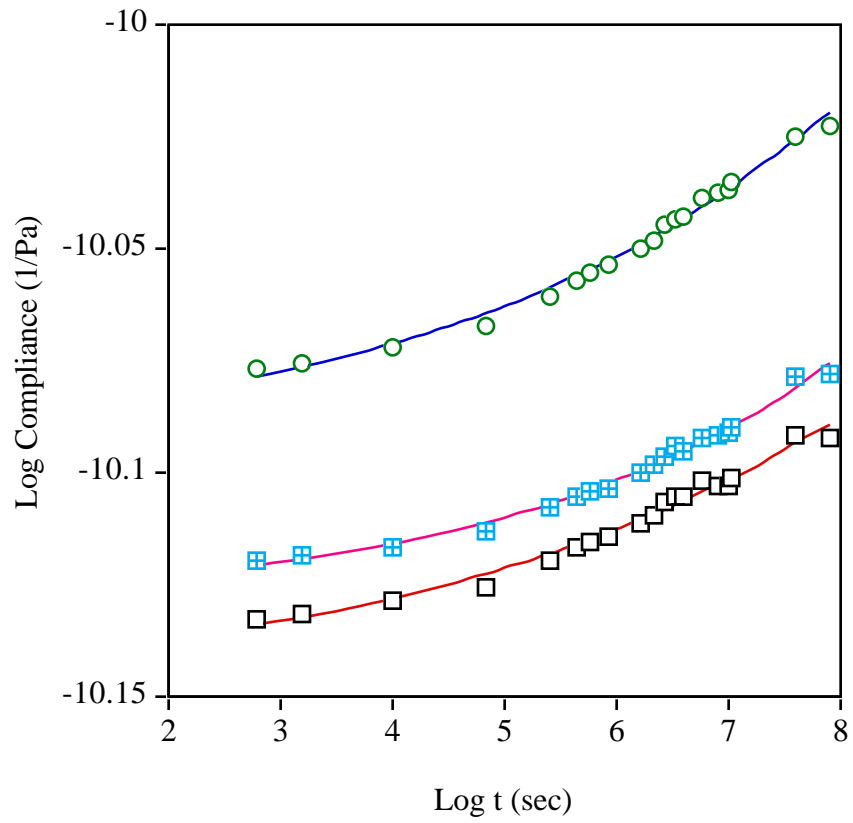


Figure 4.35 Actual (symbols) and power law fit (solid line) for three southern pine specimens in compression.

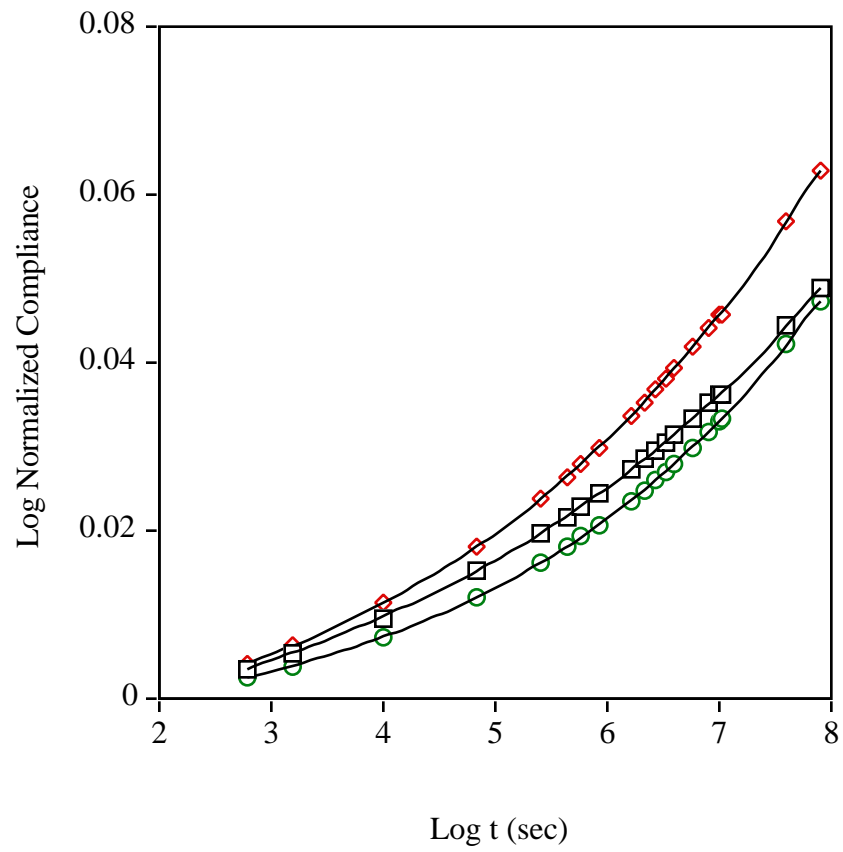


Figure 4.36 Normalized compliance curves for three southern pine specimens in compression.

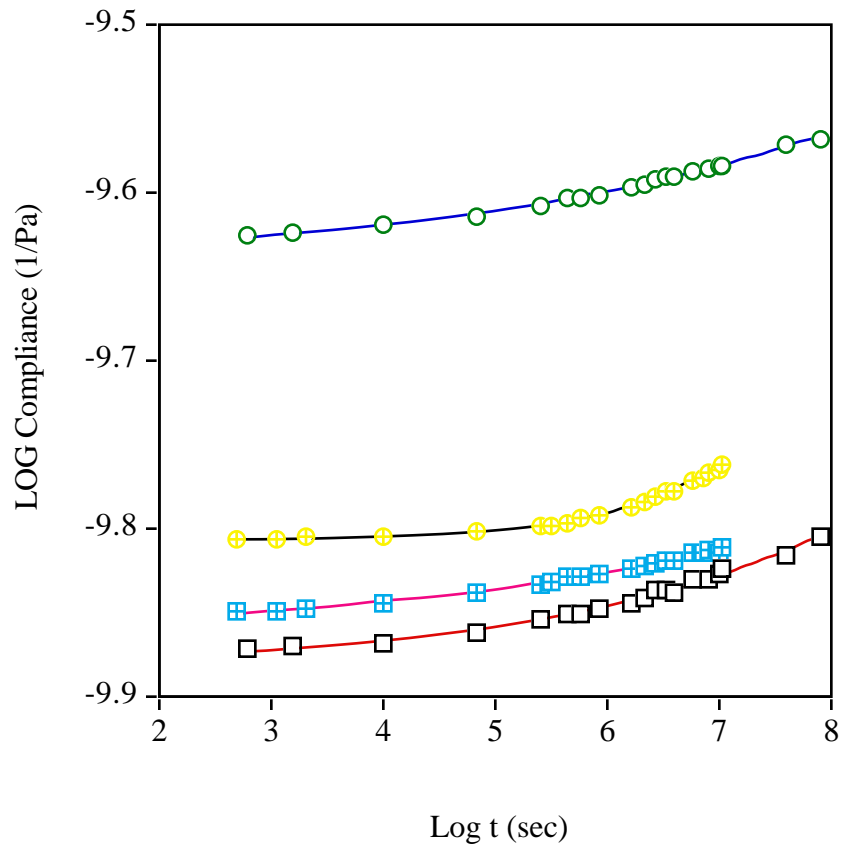


Figure 4.37 Actual (symbols) and power law fit (solid line) for four yellow-poplar specimens in compression.

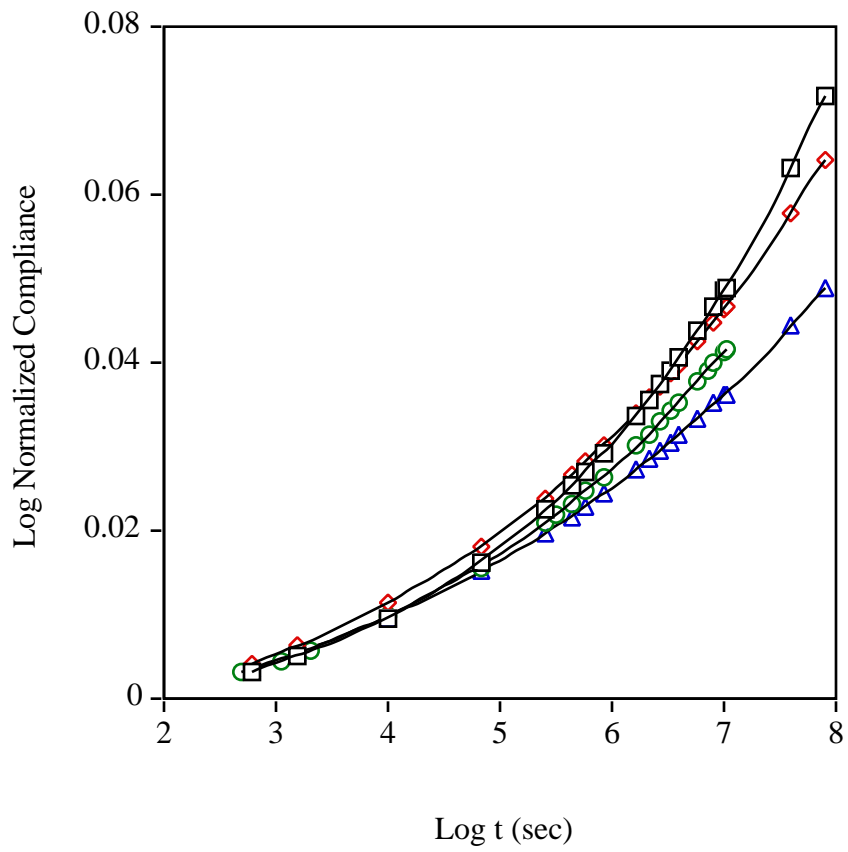


Figure 4.38 Normalized compliance curves for four yellow-poplar specimens in compression.

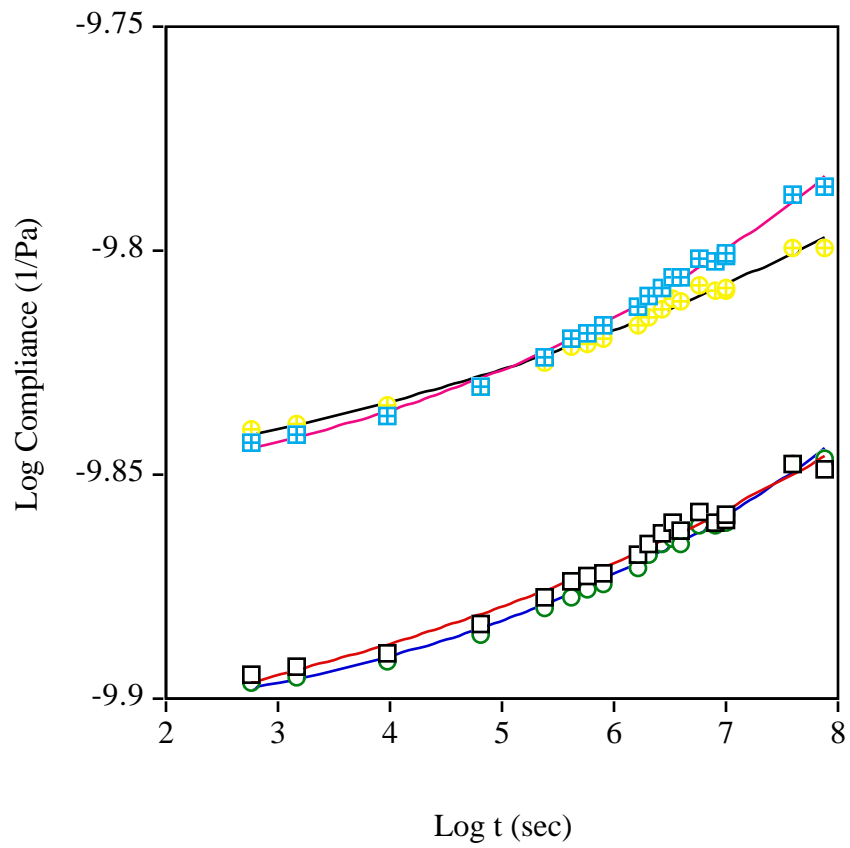


Figure 4.39 Actual (symbols) and power law fit (solid line) for four Douglas-fir specimens in compression.

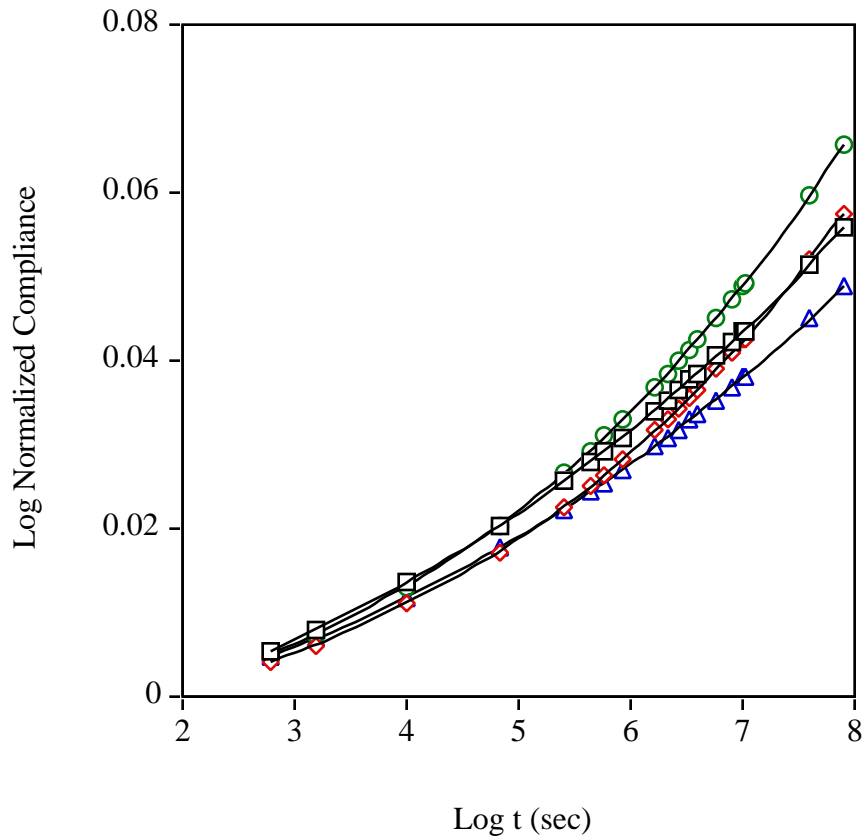


Figure 4.40 Normalized compliance curves for four Douglas-fir specimens in compression.

Figure 4.41. shows the normalized creep curves for tension and compression for yellow-poplar and southern pine. At short times, wood creeps in compression at a larger rate, however, at longer times the tensile creep's rate exceeds that for compression.

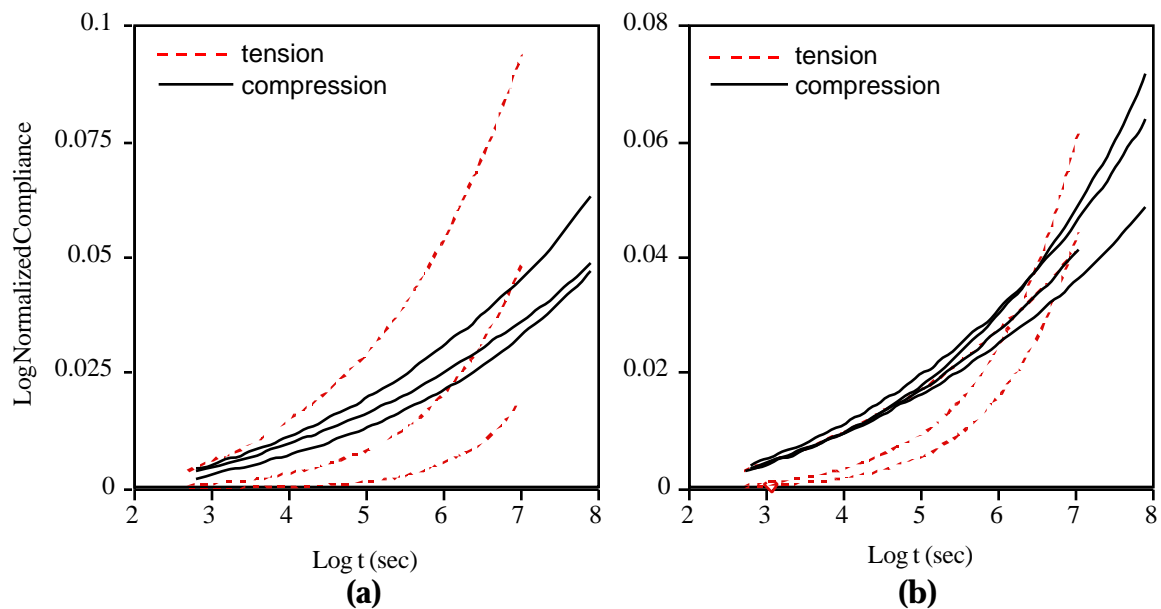


Figure 4.41 Comparison of the long-term creep in compression and in tension for (a) southern pine and (b) yellow-poplar.

4.4 Verification of the creep models

Obtaining a master curve is not a guarantee that the compliance predicted is valid. An analytical approach and comparison with the long-term creep results are used to validate the predicted compliance.

4.3.2 Analytical Criterion for the application of TTSP to wood

According to Hermida and Povolo (1994), if two curves are related by scaling (vertical and horizontal shifting) then their derivatives are also related by scaling in the horizontal direction only. If we can apply this criterion to wood then we have a method to determine the applicability of TTSP to wood that is independent of operator error or bias.

The power law used to fit our creep curves is

$$D = D_0(1 + bt^k)$$

or

$$\log D = \log \left(D_0 (1 + bt^k) \right)$$

In order to get the slope of the individual creep curves we take the derivative of the above equation with respect to $\log t$

$$\frac{d \log D}{d \log t} = \frac{bkt^k}{1 + bt^k}$$

The procedure for determining whether two curves can be superposed is as follows: First the two curves are fitted to the power law equation; then the derivative of each curve is computed and plotted. If the curves can be superposed by horizontal shifting then superposition is valid.

Time-temperature superposition. Figure 4.42 shows the results of a creep test in tension at temperatures of 20, 30, 40, 50, 60 and 70°C. The curves were shifted horizontally and vertically to construct the master curve.

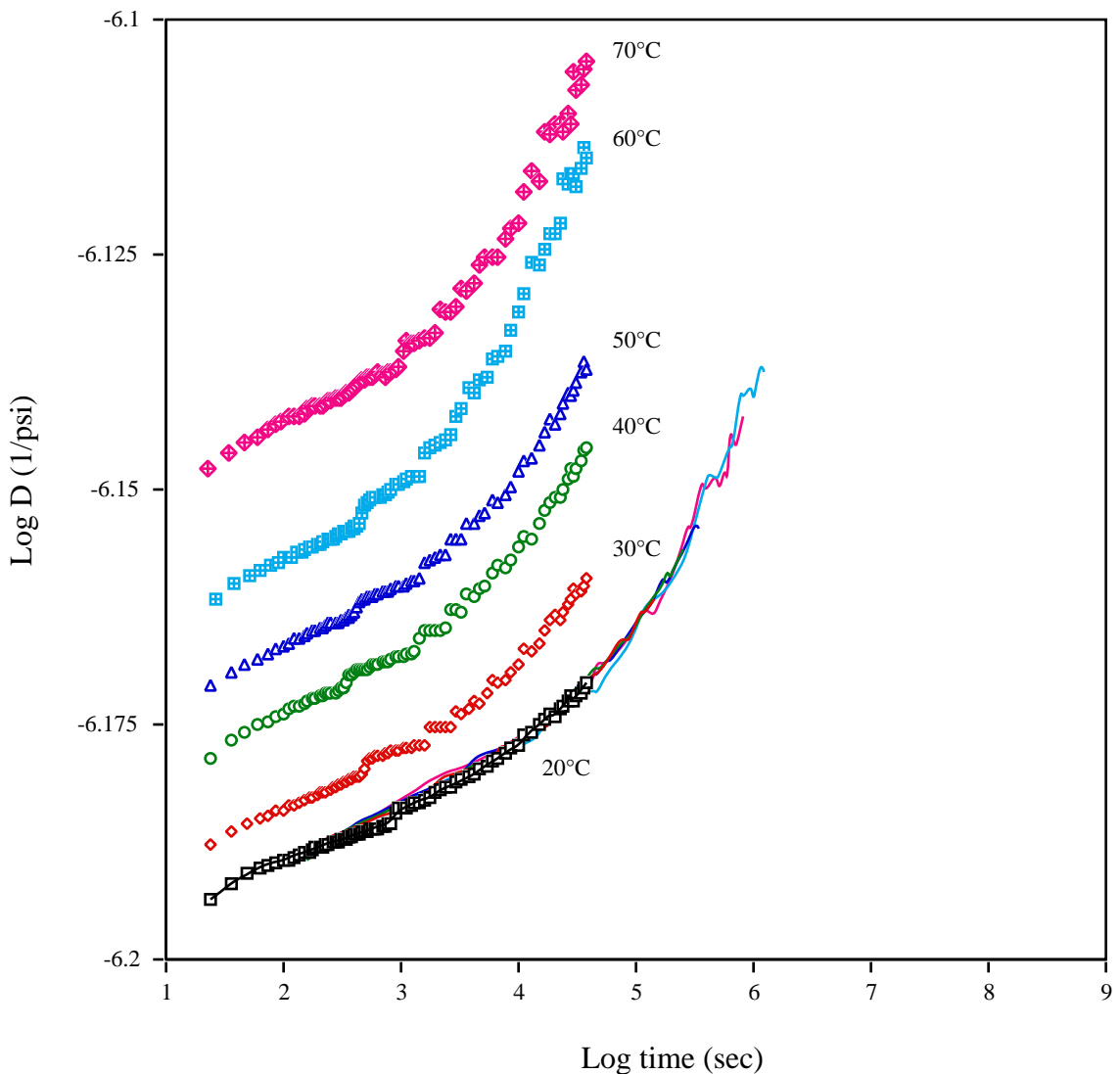


Figure 4.42 Creep curves for yellow-poplar in tension at 9% moisture content.

The curves were then fitted to the power law equation and the derivatives were computed. Figure 4.43 shows the fit and figure 4.44 shows the derivatives.

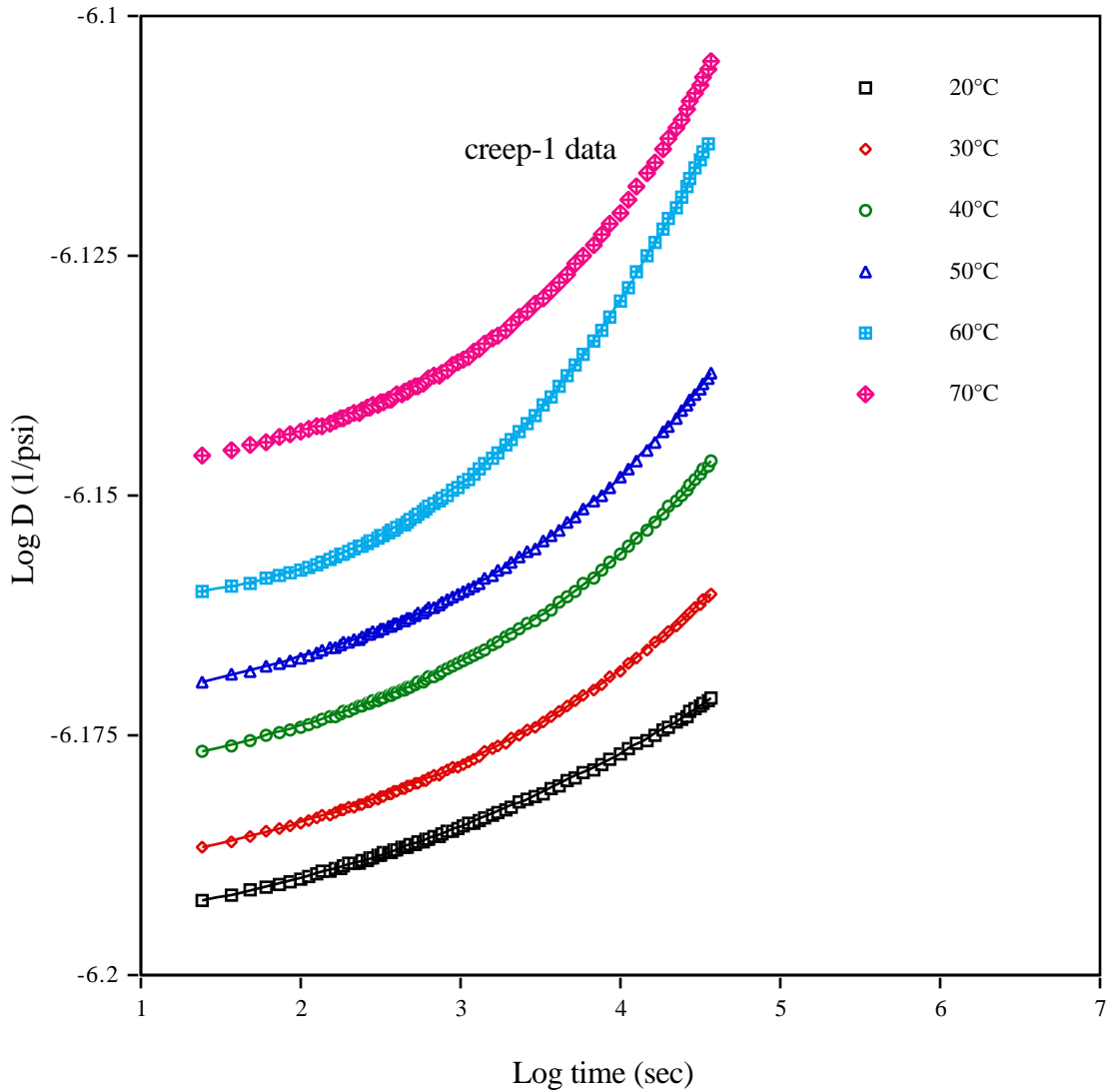


Figure 4.43 Fitted creep curves for yellow-poplar (TTSP).

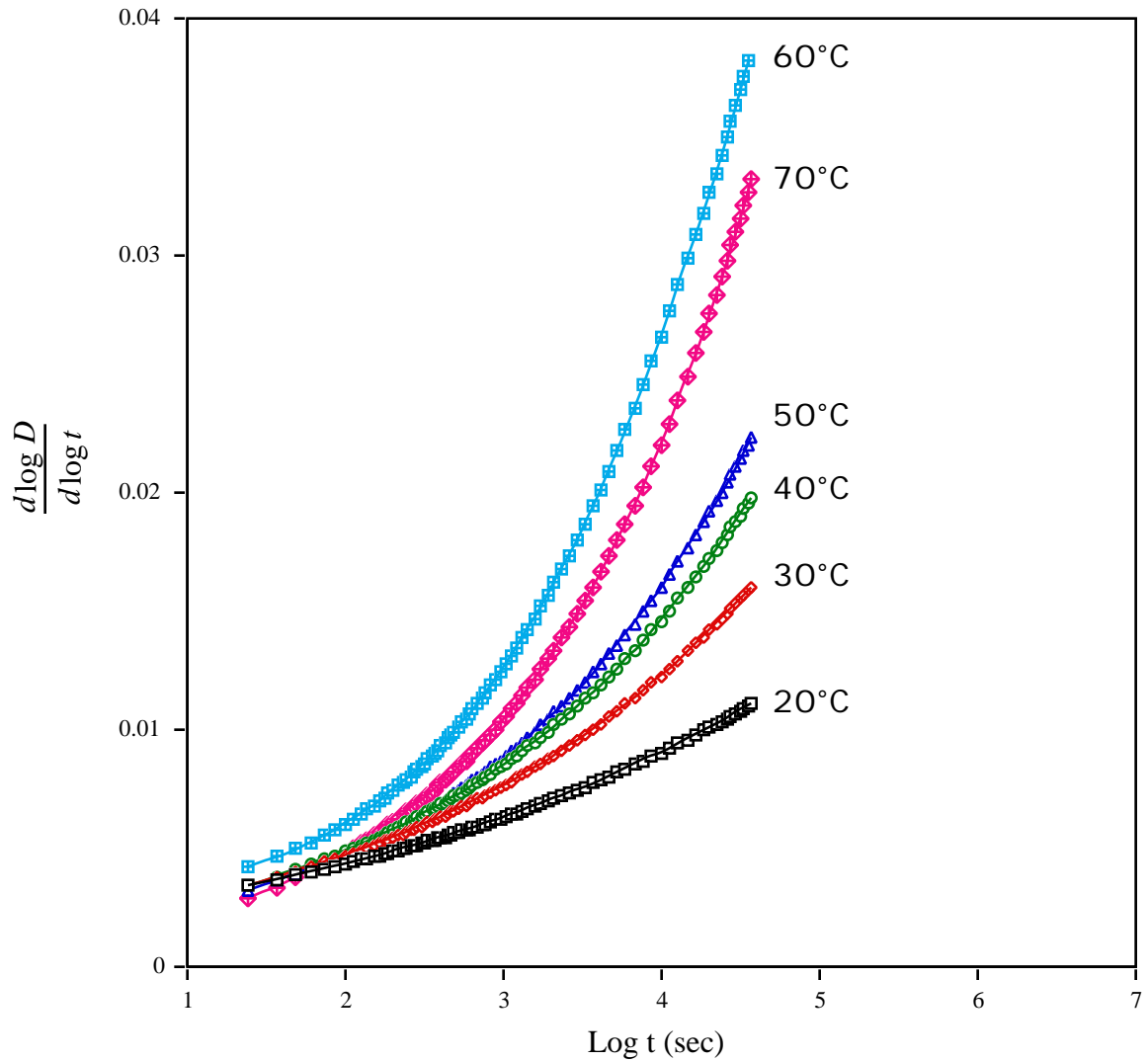


Figure 4.44 $\frac{d \log D}{d \log t}$ vs. $\log t$ for yellow-poplar (TTSP).

It was not possible to superpose the curves in figure 4.44 by horizontal shifting alone; according to the hypothesis, the curves are not related by scaling.

Time-moisture superposition. Figure 4.45 shows the creep and master curves for a yellow-poplar sample in tension at a temperature of 40°C and moisture contents varying between 5.1% and 16.9% moisture content. The curves at the lower moisture contents (5.1% and 5.7%) could not be superposed while the curves at the higher moisture contents could be superposed.

Figure 4.46 shows the derivatives of the creep curves. It was not possible to superpose the curves at 5.1, 5.7 and 6.7 % moisture content by horizontal

shifting. However, the curves at 8.7 and 16.9% moisture contents were superposed successfully.

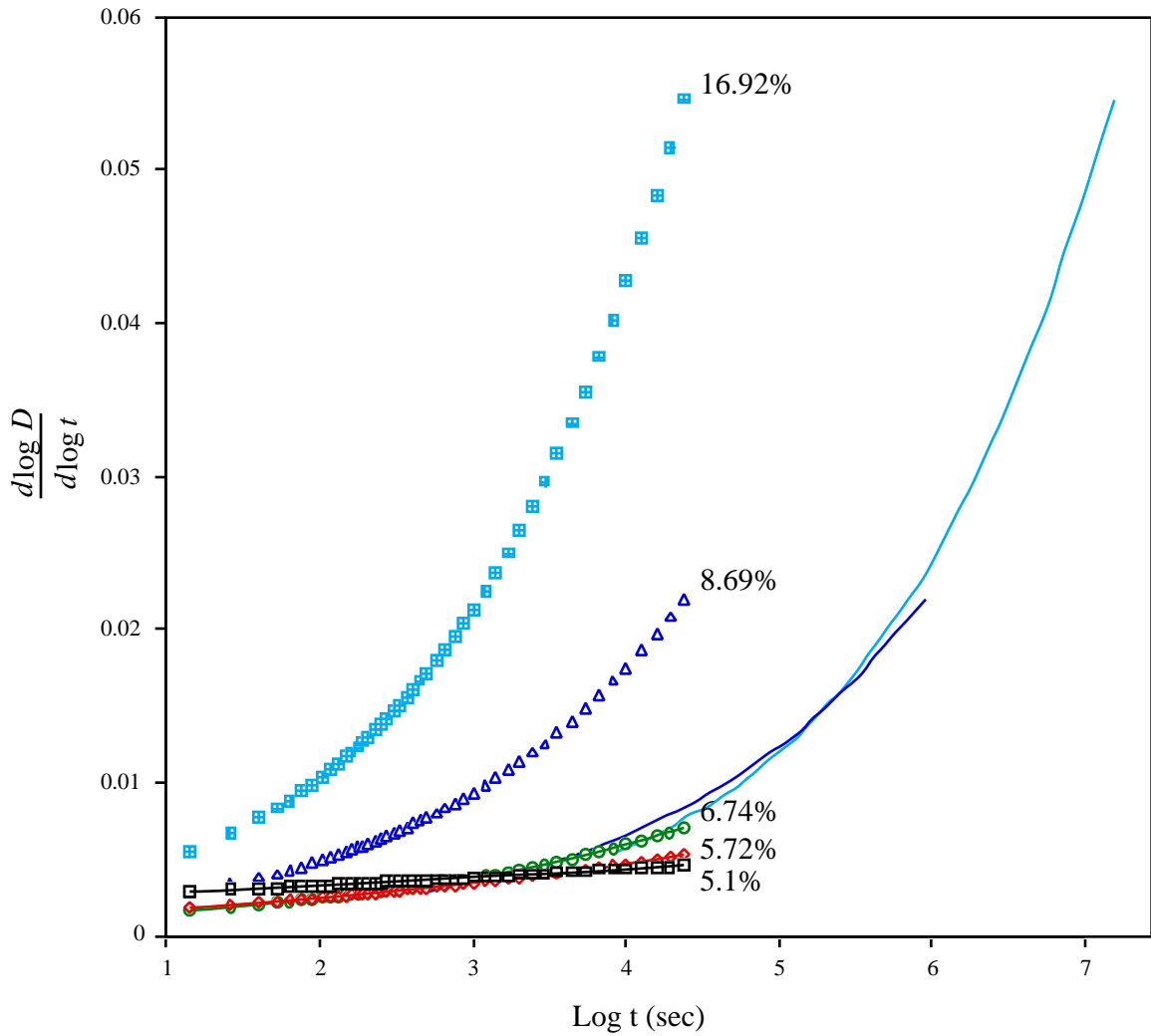


Figure 4.45 $\frac{d \log D}{d \log t}$ vs. $\log t$ for yellow-poplar (TMSP).

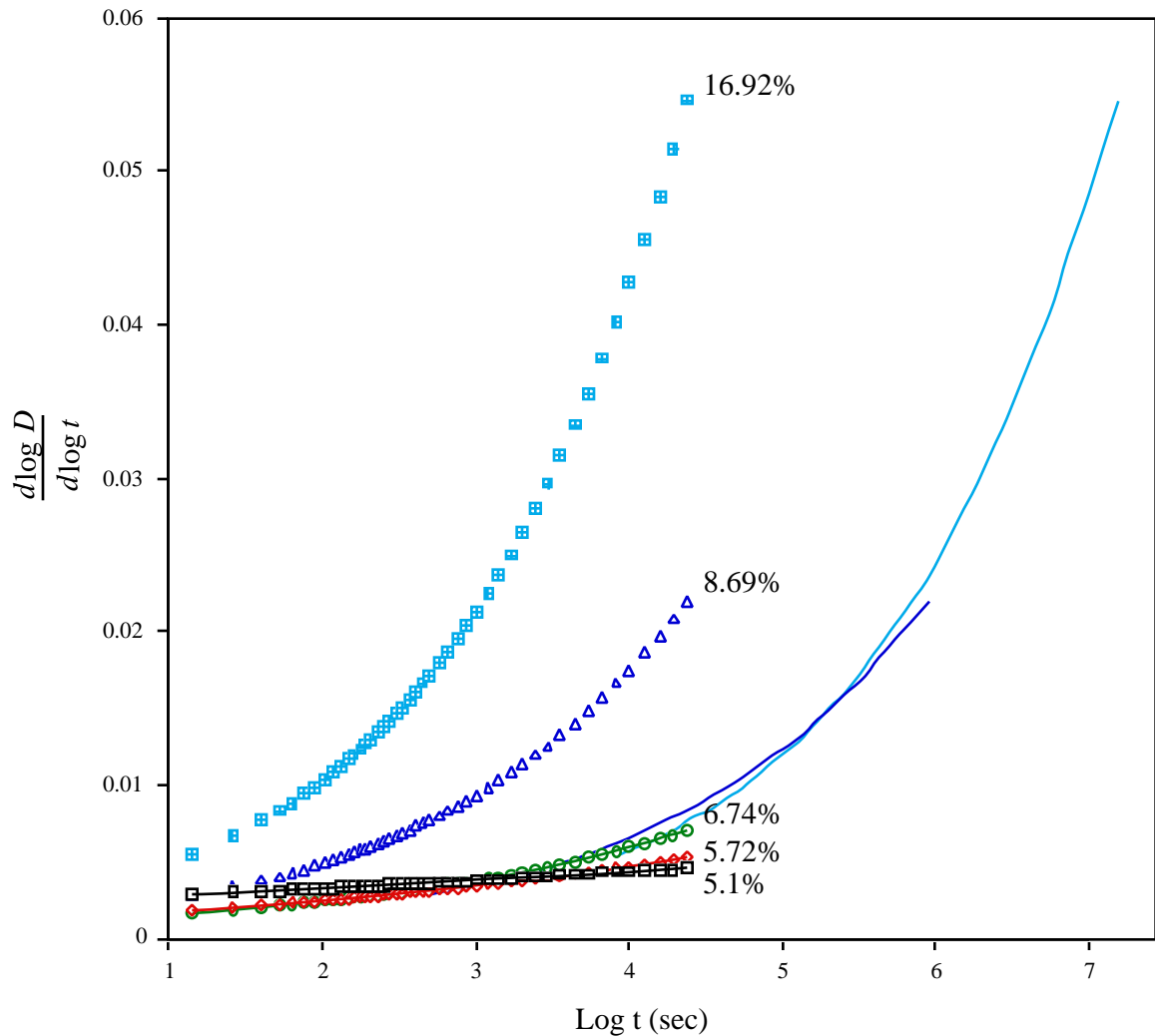


Figure 4.46 $\frac{d \log D}{d \log t}$ vs. $\log t$ (TMSP).

The analytical criterion is a convenient and consistent method to check if TTSP or TMSP is applicable for a set of curves. A computer program can be written to automatically compute the shift factor for several points. If the shift factor is the same for all points (within a predetermined margin of error), then superposition is applicable. In the above examples, it was not possible to superpose the derivative curves without vertical shifting (except at high moisture contents for TMSP). This would raise the question whether the master curves obtained by manual shifting are valid.

4.3.3 Comparison between short-term and long-term results

Since the long-term tests were conducted at 12% moisture content, the master curves from short-term tests at 6 and 9% moisture contents would have to be shifted to match. This is true for a yellow-poplar sample in tension (figure 4.48), but is not the case for a southern pine sample in compression (figure 4.49). From the limited master curves, it can be concluded that the predicted creep curves correlate reasonably well with the long-term creep results.

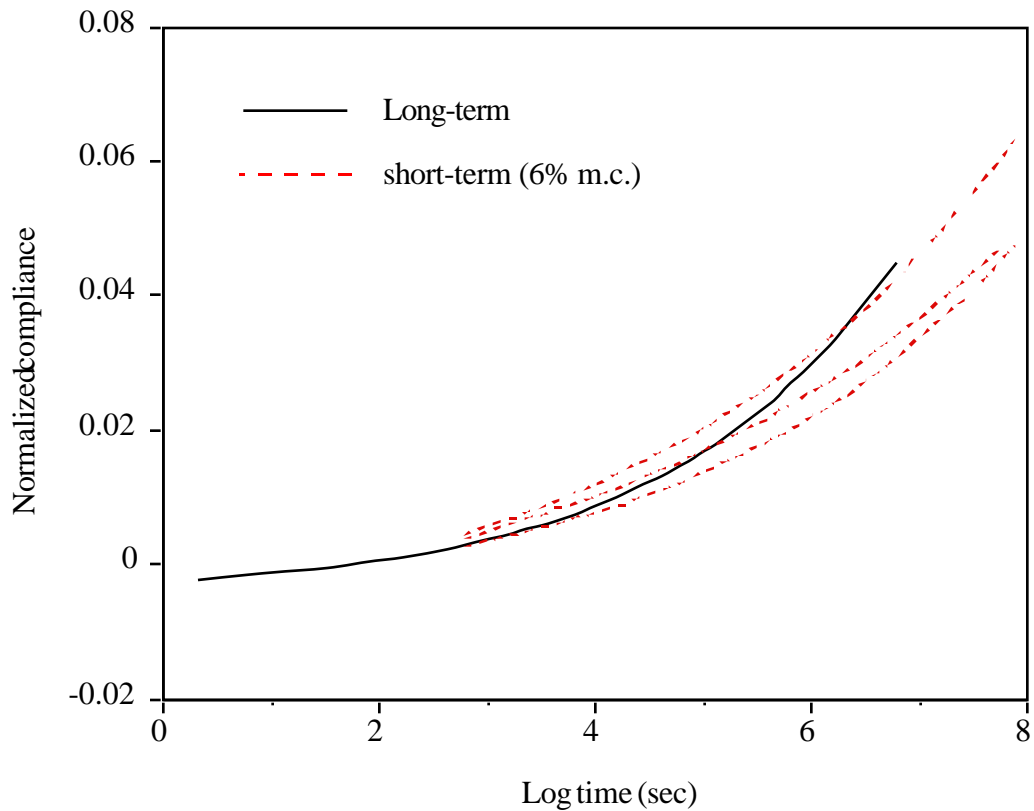


Figure 4.47 Normalized short-term and long-term compliance curves for southern pine in compression.

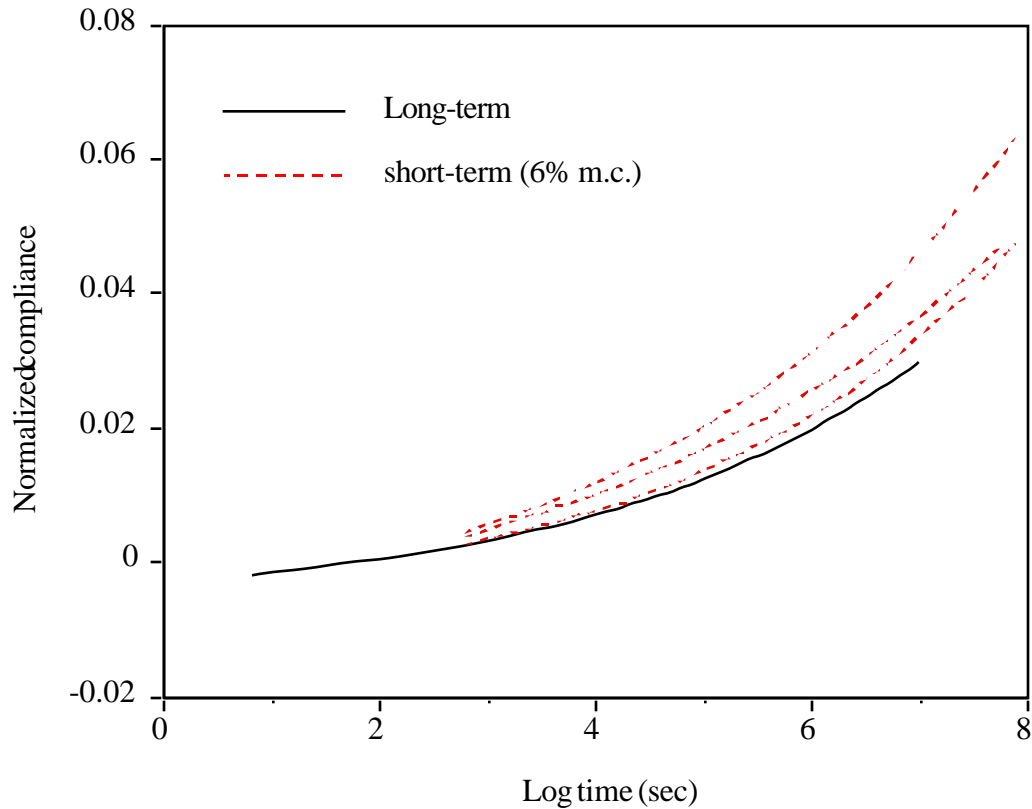


Figure 4.48 Normalized short-term and long-term compliance curves for yellow-poplar in tension.

4.4 Finite Element Analysis

A general-purpose finite element program, ABAQUS, was used to analyze various simple and complex wood structures such as beams, trusses, arches, and domes.

In order to conduct creep analysis in ABAQUS, the user needs to supply a creep model which can be defined in the input data file or in a user subroutine.

4.4.1 Creep model using time hardening model

A power law in time can be used to define the creep rate as

$$\dot{\epsilon}^{cr} = A \tilde{q}^n t^m \quad (4.1)$$

where $\dot{\epsilon}^{cr}$ is the uniaxial equivalent creep strain rate, \tilde{q} is the Mises or Hill's equivalent stress (Hill's for anisotropic materials), and A , n , and m are constants ($A, n > 0, -1 < m \leq 0$).

The creep behavior is defined in the input file as follows:

```

*MATERIAL, NAME = A1
*ELASTIC
E,
*CREEP, LAW = TIME
A, n, m

```

To model anisotropic creep, the potential option is used to define the ratios used to scale the stress values in each directions:

```

*MATERIAL, NAME = A1
*ELASTIC
E, n
*CREEP, LAW = TIME
A, n, m
*POTENTIAL
R11, R22, R33, R12, R13, R23

```

4.4.2 Creep model with user subroutine

An alternative to using the power law to define the creep rate is using a subroutine which is invoked at each integration point. The creep law has the general form

$$\dot{\epsilon}^{cr} = g^{cr}(p, q, \tilde{\epsilon}^{cr}, \text{time}, \dots) \quad (4.2)$$

where $\dot{\epsilon}^{cr}$ is the uniaxial equivalent creep strain rate, p is the equivalent pressure stress $p = -\frac{1}{3}(\sigma_{11} + \sigma_{22} + \sigma_{33})$, q is the Mises or Hill's equivalent stress (Hill's for anisotropic materials), and $\tilde{\epsilon}^{cr}$ is the uniaxial equivalent creep.

The subroutine must define the increments of inelastic creep as functions of the variables in the g^{cr} function.

The subroutine has the following format:

```

SUBROUTINE CREEP(DECRA, DESWA, ECO, ESWO, P, QTILD, TEMP, DTEMP,
1 PREDEF, DPRED, TIME0, DTIME, STATEV, CMNAME, LEXIMP)
C
C IMPLICIT REAL*8(A-H,O-Z)
C
C CHARACTER*8 CMNAME
C
C      coding to define DECRA
C
C RETURN
END

```

Required variables:

DECRA(1): $\tilde{\epsilon}^{cr}$, uniaxial equivalent creep strain increment.

Variables needed if implicit integration is used:

DECRA(2): $\dot{\epsilon}^{cr}$ / $\tilde{\epsilon}^{cr}$

DECRA(4): $\dot{\epsilon}^{cr}$ / p

DECRA(5): $\dot{\epsilon}^{cr}$ / q

Example:

If $\dot{\epsilon}^{cr} = A \tilde{q} t^m$ then

$$\epsilon^{cr} = \frac{1}{m+1} A \tilde{q} t^{(m+1)} \quad \text{at time} = t$$

$$\epsilon^{cr} = \frac{1}{m+1} A \tilde{q} (t + \Delta t)^{(m+1)} \quad \text{at time} = t + \Delta t$$

Therefore

$$\epsilon^{cr} = \text{DECRA}(1) = \frac{1}{m+1} A \tilde{q} [(t + \Delta t)^{(m+1)} - t^{(m+1)}]$$

and

$$\begin{aligned} \dot{\epsilon}^{cr} / \tilde{q} &= \text{DECRA}(5) = \frac{1}{m+1} A [(t + \Delta t)^{(m+1)} - t^{(m+1)}] \\ &= \frac{1}{\tilde{q}} \text{DECRA}(1) \end{aligned}$$

The visco procedure

In order to conduct creep analysis in ABAQUS, the visco procedure is used; the required data input lines are:

*STEP, NLGEOM, INC=200

*VISCO, CETOL=., EXPLICIT

initial time increment, time period, minimum time increment, maximum time increment

4.4.3 Incorporation of the creep law from experimental analysis

The compliance obtained from the creep experiments is fitted to a power law of the form

$$D = D_0 (1 + b t^k) \tag{4.3}$$

The creep strain can be defined as

$$\epsilon^{cr} = \int_0^t b t^k \tag{4.4}$$

Since $\epsilon_0^{cr} = D_0$

$$\epsilon^{cr} = D_0 b t^k \tag{5.5}$$

and the creep strain rate is

$$\dot{\epsilon}^{cr} = k D_0 b t^{(k-1)} \tag{5.6}$$

This equation can be used to obtain the constants A, n, and m used in the creep law definition in ABAQUS. The constants are:

$$A = k D_0 b, \quad n = 1, \quad m = k - 1$$

If a user subroutine is used

$$\text{DECRA}(1) = \frac{1}{m+1} A \text{QTILD} [(\text{TIME0} + \dots)^{(m+1)} - \text{TIME0}^{(m+1)}]$$

$$\text{DECRA}(5) = \text{DECRA}(1) / \text{QTILD}$$

where

$$\text{QTILD} = \tilde{q}$$

TIME0 = time at the beginning of step
DTIME = time increment

4.4.4 Creep analysis checking

In order to check the creep model used in ABAQUS, the strain measured in one of the tension experiments (yellow-poplar, 40°C, 12% EMC) is compared to that from an ABAQUS finite element analysis. The procedure is as follows:

1) Use nonlinear fitting to obtain the creep parameters; the constants are:

$$D_0 = 5.3732 \times 10^{-7} \text{ psi}^{-1}$$

$$b = 7.0047 \times 10^{-3}$$

$$k = 0.3313$$

which leads to

$$A = 1.2468 \times 10^{-9}$$

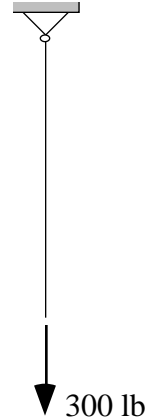
$$n = 1$$

$$m = -0.6687$$

2) Use ABAQUS to obtain the creep strain for a period of time comparable to the duration of the test.

Input file

```
*HEADING
  TRUSS ANALYSIS FOR CREEP
  TISSAOUI
*NODE, SYSTEM=R
  1, 0.0, 0.0,
  2, 7.0 , 0.0
*ELEMENT,TYPE=C1D2 ,ELSET=EALL
  1 1 2
*SOLID SECTION, ELSET=EALL, MATERIAL=WOOD
  0.133632
*MATERIAL, NAME=WOOD
*ELASTIC
  1.86108E6,0.3
*CREEP, LAW=TIME
  1.246826339E-9, 1.0, -0.6687286
*BOUNDARY
  1,1,3
  2,2,3
*STEP, NLGEOM, INC=50
*STATIC, PTOL=0.005,DIRECT
  0.0333, 1.
*CLOAD
  2, 1, 300.0
*PRINT, RESIDUAL=NO
*EL PRINT, SUMMARY=NO, FREQ=2
S,E
*NODE PRINT, SUMMARY=NO
U,RF,CF
*END STEP
*STEP, NLGEOM, INC=200
*VISCO, CETOL=0.02E-6
  1.0, 22000.0
*PRINT, RESIDUAL=NO
*EL PRINT, SUMMARY=NO, FREQ=2
S,CE
*EL FILE, FREQ=1
S,CE,E
*NODE PRINT, SUMMARY=NO
U
*NODE FILE
U
*END STEP
```



As shown in figure 4.49, the strain obtained using ABAQUS is nearly identical to that from the creep experiment.

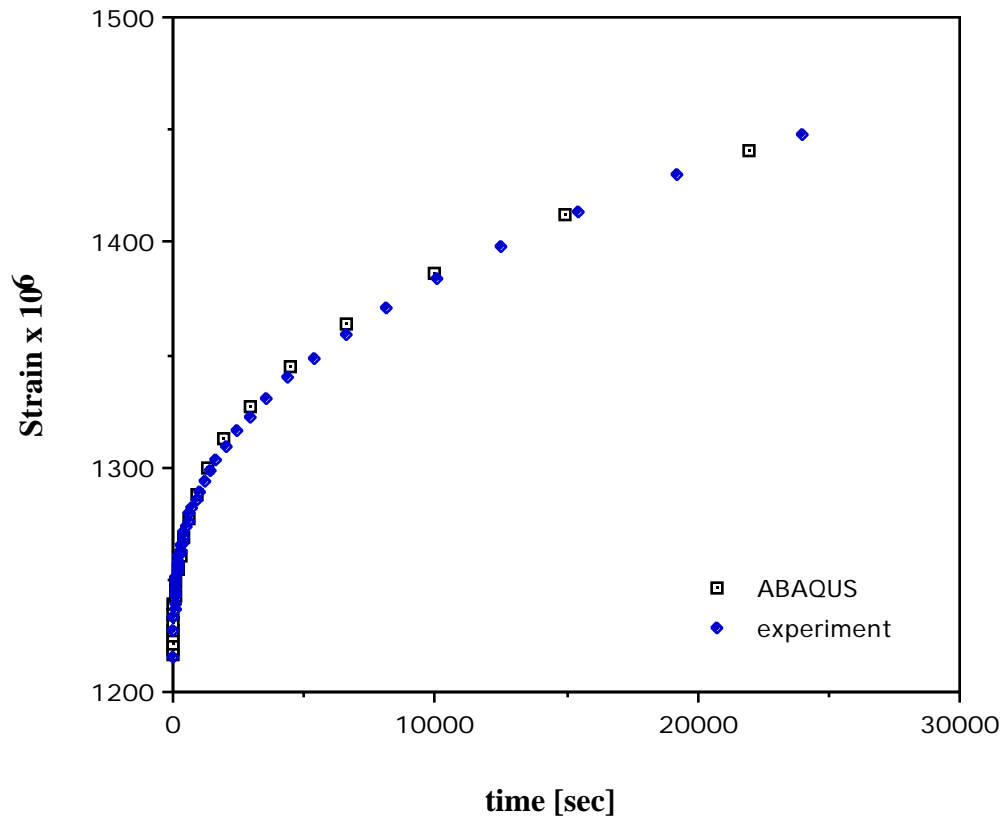


Figure 4.49 ABAQUS and experimental results for a truss element in tension.

4.4.5 Analysis of a truss for creep

In order to compare long-term creep (50 years) to short-term creep (1 year), a roof truss (figure 4.50) is analyzed using ABAQUS. Gamalath's (1991) creep model is used:

$$\frac{D_{cr}}{D_0} = P_1 t^{P_2} \quad (6.6)$$

where

$$P_1 = 0.0749 - 2.291 \times 10^{-8} E \quad (\text{from regression analysis})$$

$$P_2 = 0.3358 \quad (\text{average})$$

The parameters for ABAQUS are:

$$A = P_1 P_2 D_0$$

$$n = 1$$

$$m = 1 - P_2$$

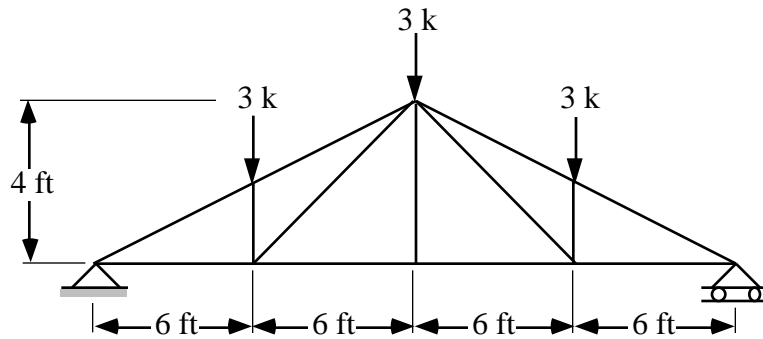


Figure 4.50 Roof truss.

Input file

```
*HEADING
TRUSS ANALYSIS FOR CREEP
TISSAOUI
*NODE, SYSTEM=R
  1, 0.0, 0.0,
  2, 72.0, 24.0
  3, 144.0, 48.0
  4, 216.0, 24.0
  5, 288.0, 0.0
  6, 144.0, 0.0
*ELEMENT,TYPE=C1D2 ,ELSET=EALL
  1  1  2
  2  2  3
  3  3  4
  4  4  5
  5  2  6
  6  4  6
  7  1  6
  8  5  6
  9  3  6
*SOLID SECTION, ELSET=EALL, MATERIAL=WOOD
30.25
*MATERIAL, NAME=WOOD
*ELASTIC
2.43140E6,0.3
*CREEP, LAW=USER
*BOUNDARY
1,1,3
5,2,3
6,3
2,3
3,3
4,3
5,3
*STEP, NLGEOM, INC=50
*STATIC, PTOL=0.005,DIRECT
0.0333, 1.
*CLOAD
2, 2, -3000.0
3, 2, -3000.0
4, 2, -3000.0
*PRINT, RESIDUAL=NO
*EL PRINT, SUMMARY=NO, FREQ=10
S,E
*NODE PRINT, SUMMARY=NO
U,RF,CF
*END STEP
*STEP, NLGEOM, INC=200
*VISCO, CETOL=0.02E-6
1.0, 4.4E5
*PRINT, RESIDUAL=NO
*EL PRINT, SUMMARY=NO, FREQ=17
S,E
*EL FILE, FREQ=10
S,
*NODE PRINT, SUMMARY=NO
U,RF,CF
*NODE FILE
U
*END STEP
```

Figure 4.51 shows the displacement at the midpoint of the bottom chord while figure 4.52 shows the percent change in creep $\frac{u - u_0}{u_0} \times 100$. After 16 years, the creep displacement is equal to the instantaneous displacement. It is equal to 150 % of the initial displacement after 50 years.

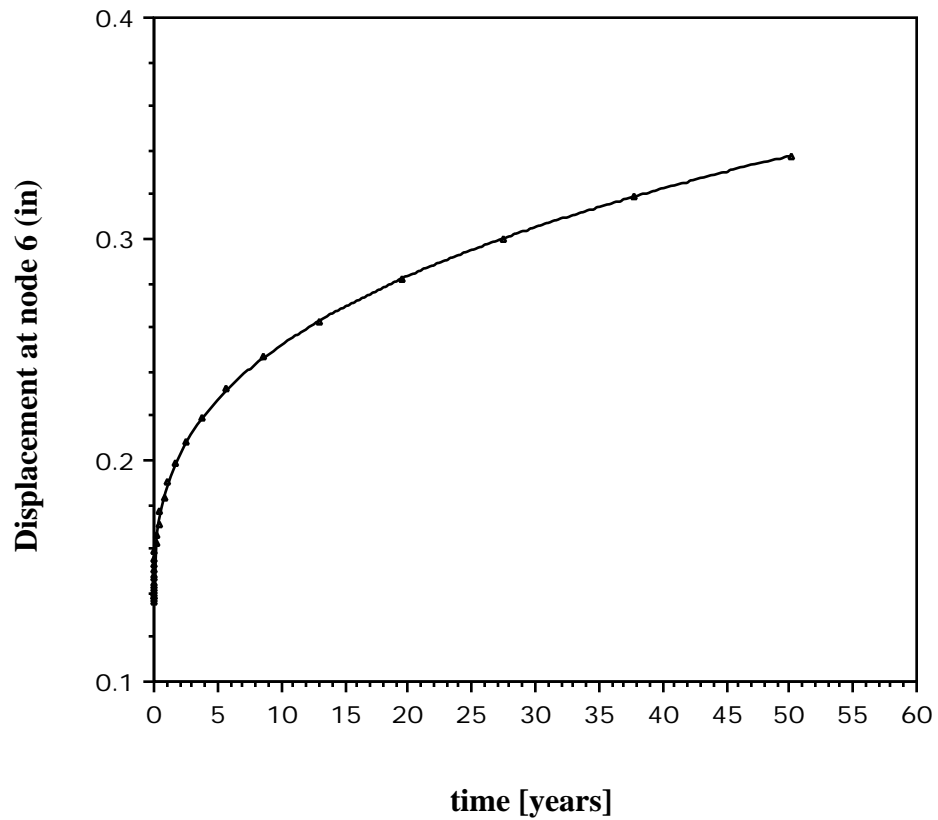


Figure 4.51 Displacement at middle of bottom chord

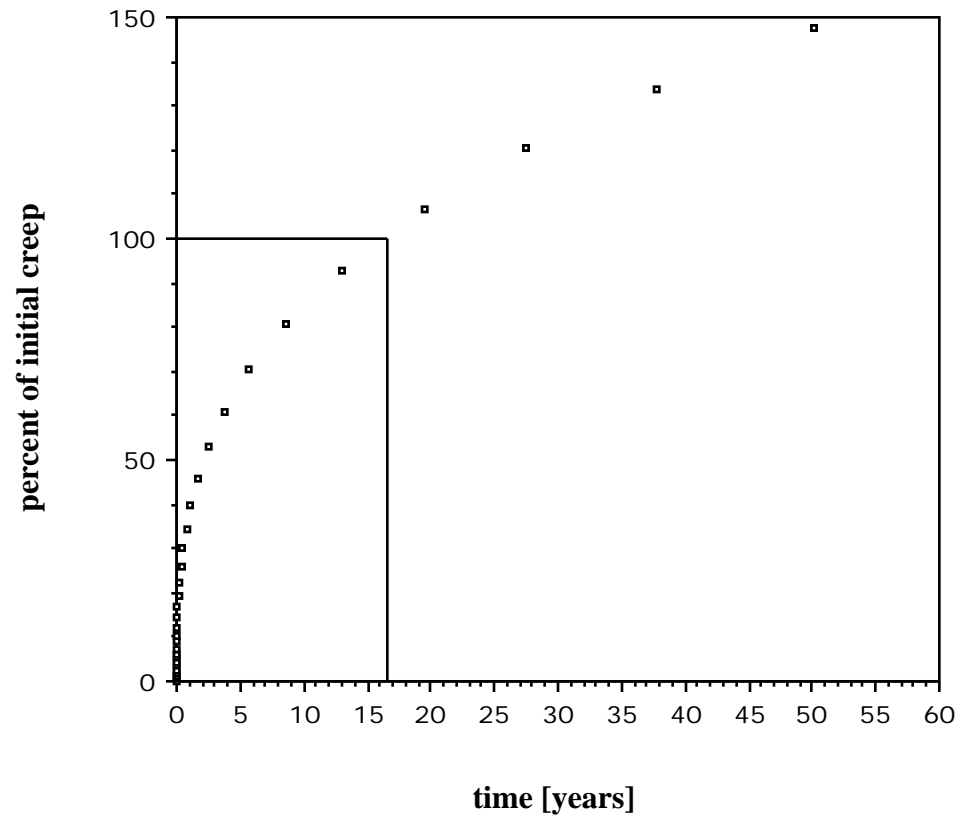


Figure 4.52 Creep deflection as a percentage of elastic deflection.

4.4.6 Finite element analysis for stability

To illustrate the use of finite element analysis to determine the effect of creep on stability, a small arch and a three-hinged arch are analyzed.

Analysis of an arch

The arch in figure 4.53 is prone to snap through buckling due to its shallow geometry. As figure 4.54 shows, the short term buckling load is about 190 lb. When 50% of the short term load is applied, the arch becomes unstable after about 70 years as shown in figure 4.55.

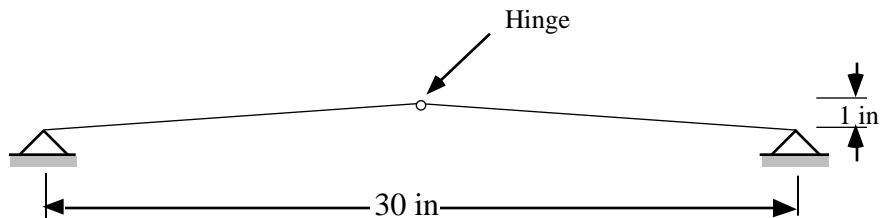


Figure 4.53 Geometry of the A-frame (cross sectional area = 1 in²).

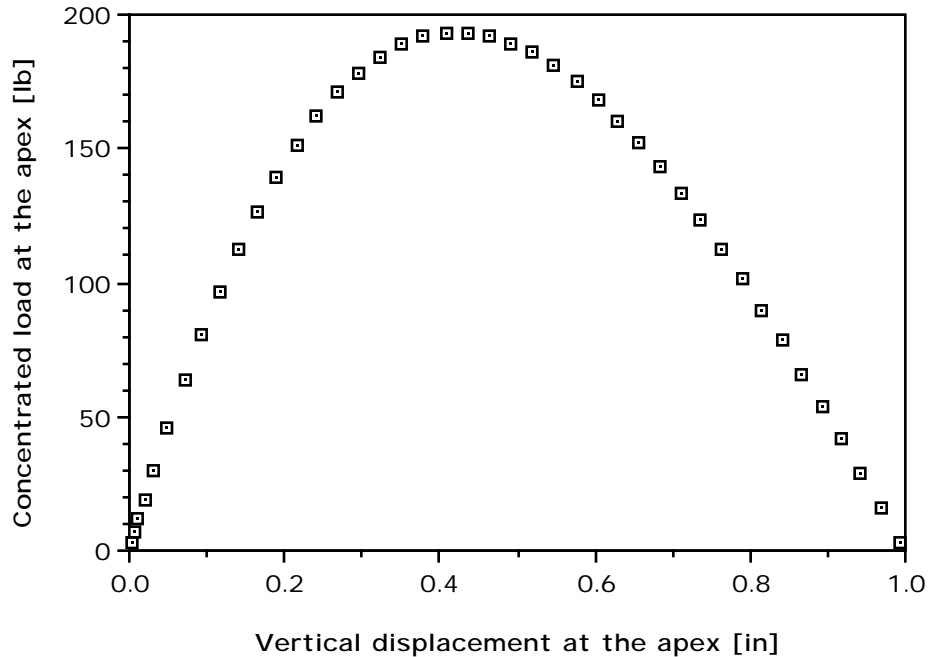


Figure 4.54 Load deflection path at the apex.

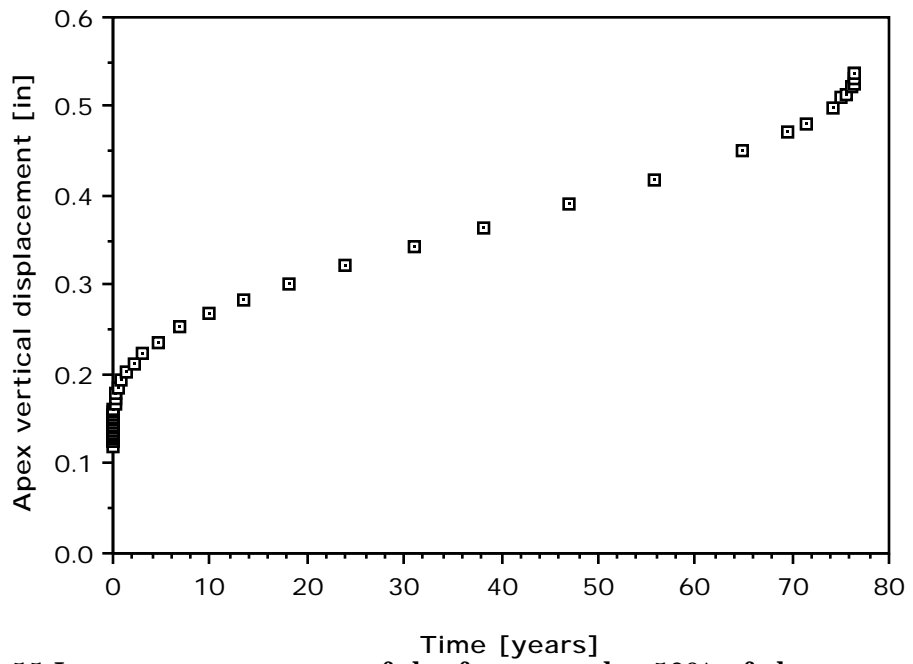


Figure 4.55 Long term response of the frame under 50% of short term critical load.

Creep of a three hinged arch

Figure 4.56 shows a three hinged arch that was used as a design example by Faherty and Williamson (1989). The design loads were 400 lb/ft dead load and 480 lb/ft snow load. The arch cross section is 6.75 x 27 in. ABAQUS was used to determine the long-term behavior of the arch. The creep law proposed by Nielsen (1992) was used. Figure 4.57 shows the deflection at the apex vs. time for dead load in combination with uniform snow load and snow over half the arch. The arch does not become unstable after 50 years, this is due to the large safety factor against buckling. The short term critical loads and deflections are:

Uniform snow load: $P_{cr} = DL + 4.88 LL$
 $_{cr} = 16.26$ in at apex

Half snow load: $P_{cr} = DL + 6.791 LL$
 $_{cr} = 30.16$ in at apex

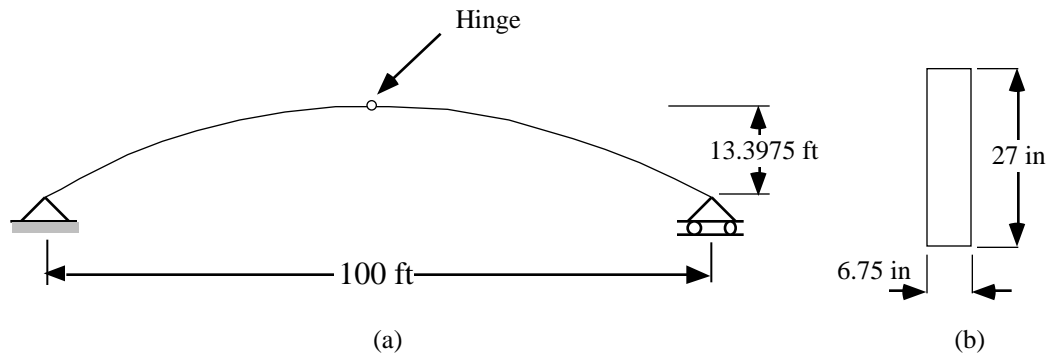


Figure 4.56 (a) Geometry and (b) cross section of three hinged arch

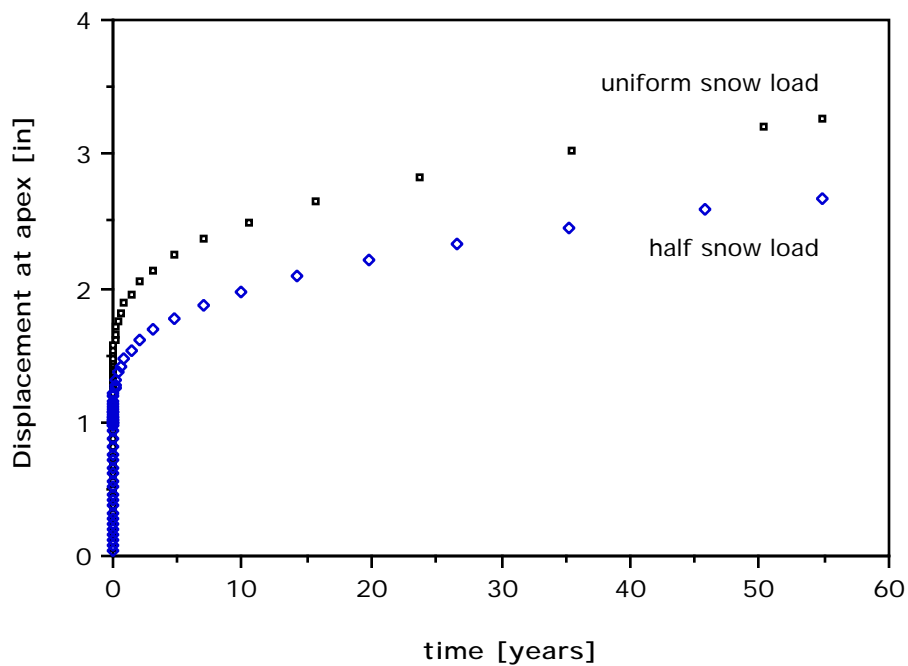


Figure 4.57 Creep displacements at the apex.

Creep of the Church of the Nazarene Varax Dome

The Varax dome dimensions are shown in figure 4.58 The dome consists of seven identical sectors and is supported by fourteen columns. At the perimeter, a steel ring with a cross-sectional area of 5 in² provides additional support (Tissaoui, 1991). The dome consists of 77 beams (5.125 x 12 in), 112 purlins (3.125 x 7.5 in), and 14 edge beams (3.125 x 22 in). The beams are

connected using the Varax connector. The dome is covered with 2-in tongue-and-groove wood decking which is not included in this model to simplify the analysis. The design loads for the dome are 15 psf dead load and 25 psf snow load.

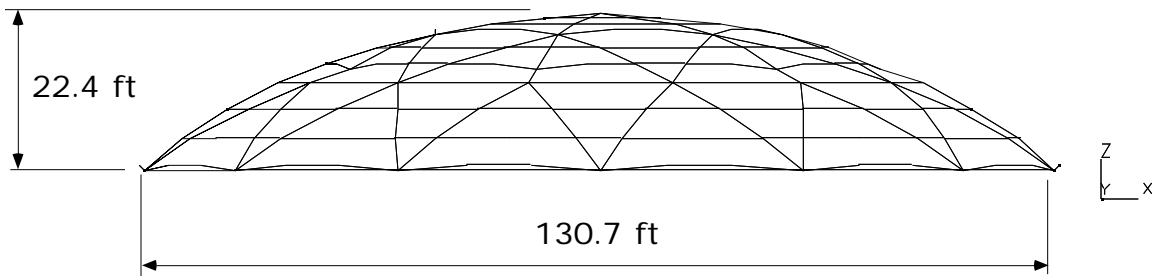
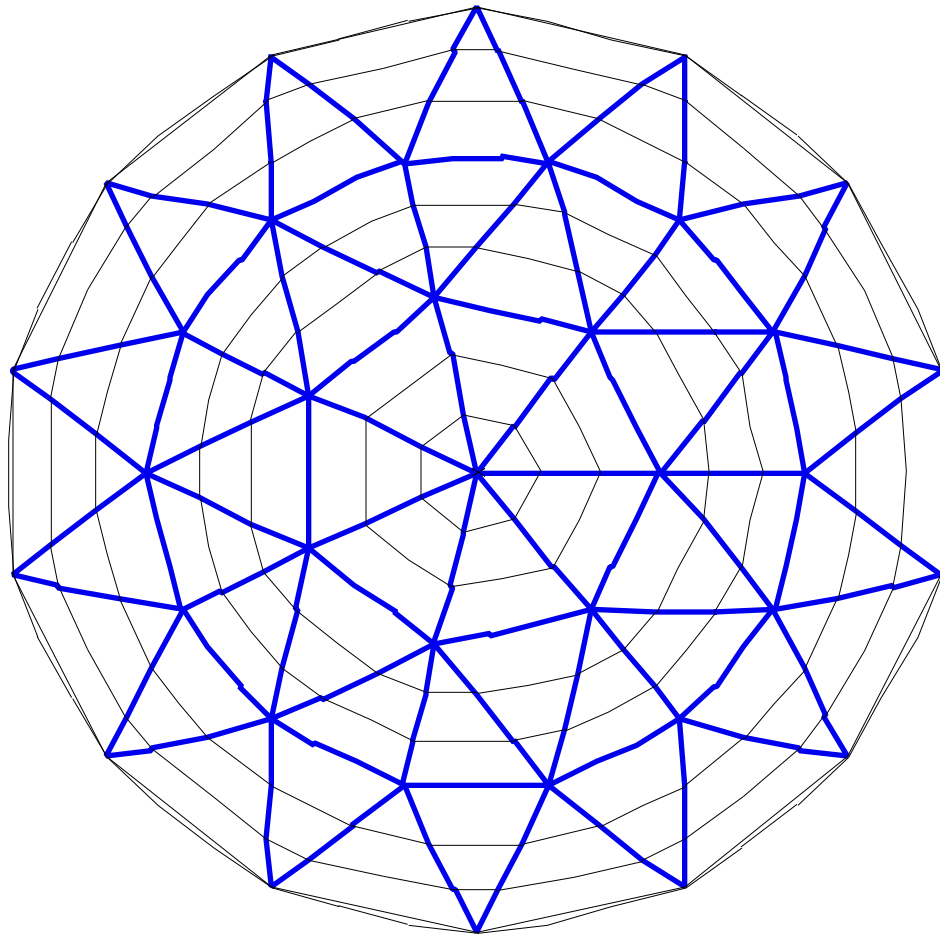


Figure 4.58 Varax dome geometry.

From static nonlinear analysis, it was determined that the critical load factor for the live load is equal to 3.32. The vertical displacement at the apex was between 2.5 and 3.0 in. The buckled shape is shown in figure 4.59.

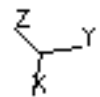
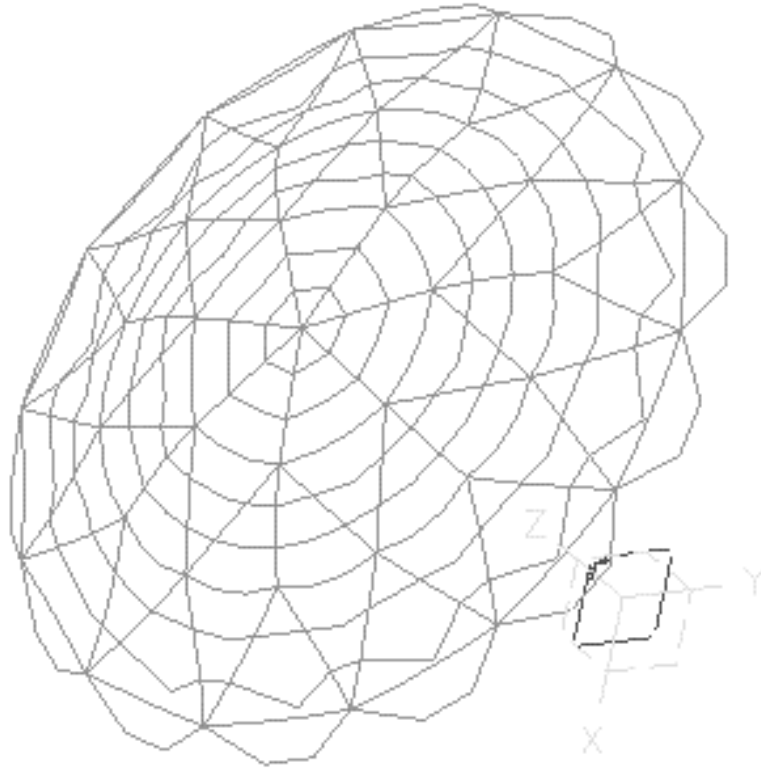


Figure 4.59 Buckled shape of the dome

Creep analysis was conducted for 50 years, using creep laws from Gamalath (1991), LeGovic (1987), and the equations from our long-term tests. The parameters used are shown in table 4.7.

Table 4.7 Creep parameters used in finite element analysis of the Varax dome.

	Le Govic	Gamalath	long-term (southern pine)
D_0 (in ² /lb)	4.045×10^{-7}	4.113×10^{-7}	5.545×10^{-7}
b sec ^k	0.0388	0.0192	0.0154
k	0.112	0.3358	0.1373

The snow load was applied for the entire 50 years which, although unrealistic, is a worst case assumption which may reveal potential instability. Figure 4.60 shows the vertical displacement at the apex. In the worst case, the displacement doubled, but no instability was detected.

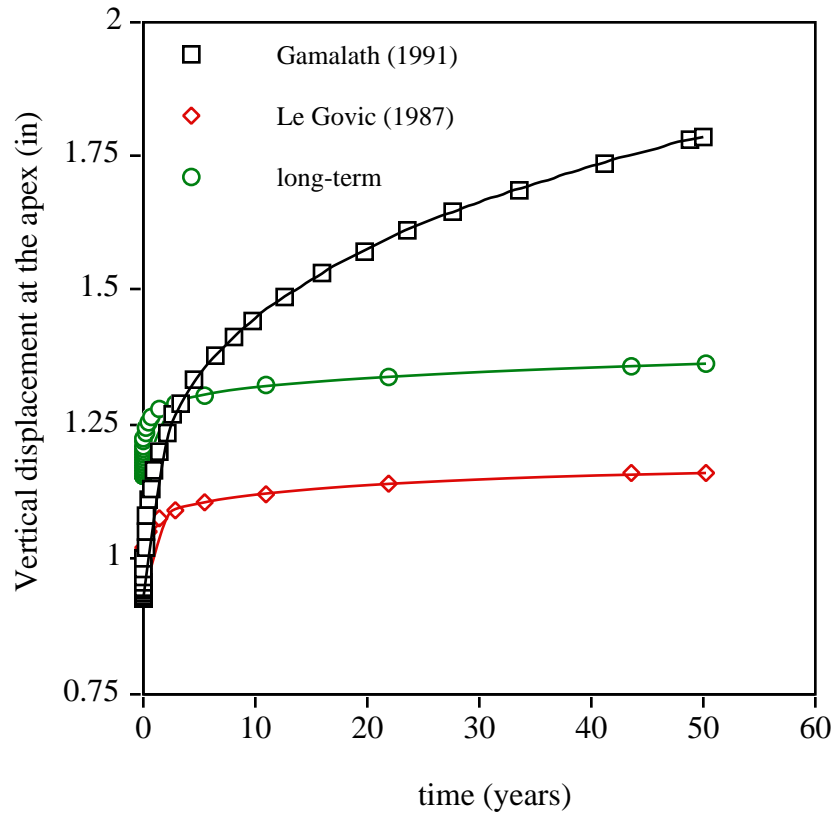


Figure 4.60 Vertical displacement at the dome apex.

From the above results, it is clear that creep will not lead to instability during the design life of the Varax dome.

5. CONCLUSIONS AND RECOMMENDATIONS

5.1 Conclusions

The application of the principle of time-temperature superposition was only possible at temperatures below 65°C, and the resulting creep curves did not extend beyond 2 years. As was determined from the dynamic tests and from the literature (Kelly et al, 1987), wood undergoes two distinct transitions due to lignin and hemicellulose. These transitions depend on the moisture content. This would make wood thermorheologically complex having two or more phases; additionally, if the lignin and hemicellulose depend differently on temperature, one would expect wood to exhibit different responses depending on where it is in the time/temperature/moisture content scale. The breakdown of TTSP for thermorheologically complex polymers is well documented (Fesko and Tschoegl 1971, 1974, Lim et al., 1971). TTSP is not applicable to a block copolymer unless one of the components dominates the behavior. When neither component dominates, each contributes differently to the behavior and the curves cannot be superposed. Between 6 and 12% moisture content, wood undergoes transitions due to either or both hemicellulose and lignin between 65 and 80°C. During and after this transition, the behavior changes and TTSP can no longer be applied. Therefore, TTSP can be only be applied at temperatures below 70°C, the resulting horizontal shift factors follow an Arrhenius relation with activation energies between 75 and 130 kJ/mole. The response can be extended further than 2 years by extending the creep test at 60°C to a week or more.

It was not possible to determine whether Parallam™ is more susceptible to creep than solid wood. This can be attributed to the small size of the samples used.

The power law equation for creep can be used in finite element analysis to model the long term behavior of wood structures. Serviceability and instability problems can be predicted. From finite element analysis of the Varax dome subjected to dead and snow loads, it can be concluded that creep does not lead to instability during the design life.

5.2 Recommendations

- At the maximum temperature (60 or 65°C), the test should be conducted for two days to a week to obtain a master curve that extends for more than a decade. Then the sample should be tested again at the lowest temperature to check for damage, as was done by Colby (1989).

- Creep experiments on wood are very sensitive to temperature and relative humidity changes, and rate of loading. Also the tests are time consuming and require daily monitoring. Automating the tests would make the task easier and less demanding. The tests can be automated by using a computer to control loading and unloading of the samples, temperature and relative humidity increases, monitoring of the moisture contents of the samples, and data collection and manipulation.
- A computer program can be written or purchased to automatically superpose the individual creep curves. This would lead to elimination of operator bias, also more data can be processed in less time.
- The dynamic behavior at a wide range of temperatures and frequencies and at different moisture contents should be studied further.
- Larger samples of Parallam™ and other structural lumber composites should be tested to determine if they are more susceptible to creep.

6. REFERENCES

ABAQUS, General-Purpose Finite Element System, Hibbit, Karlsson and Sorensen, Inc., 100 Medway Street, Providence, RI 02906, USA.

American Institute of Timber Construction, Timber Construction Manual, third editions, John Wiley & Sons, Inc., New York, 1985.

Aklonis, J. J., and MacKnight, W. J. , Introduction to Polymer Viscoelasticity, John Wiley and Sons, 1983.

Bathe, K. J. , Finite Element Procedures in Engineering Analysis, Prentice-Hall, Englewood Cliffs, N.J., 1982.

Bodig, J., and Jayne, B. A., Mechanics of Wood and Wood Composites, Van Nostrand Reinhold Company, 1982.

Bodig (ed.), J. , Reliability-Based Design of Engineered Wood Structures, Kluwe Academic Publishers, 1992.

Bond, B. H., Development of Tension and Compression Creep Models for Wood Using the Time-Temperature Superposition Principle. Thesis (M.S.)--Virginia Polytechnic Institute and State University, 1993.

Boyle, J. T., and Spence, J., Stress Analysis of Creep, Butterworths, 1983.

Britvec, S. J., The Stability of Elastic Systems, Pergamon Press Inc, 1973.

Bushnell, D., "A Strategy for the Solution of Problems involving Large Deflections, Plasticity, and Creep," International Journal for Numerical Methods in Engineering, Vol. 11, 1977, pp. 683-708.

Chan, E. C. Y., "Nonlinear Geometric, Material, and Time Dependent Analysis of Reinforced Concrete Shells with Edge Beams," Ph.D. Dissertation, University of California, Berkeley, 1983.

Chang, Y.S., Personal communication, 1991.

Clauser, W. S., "Creep of Small Wood Beams Under Constant Bending Load," Forest Products Laboratory, Forest Service U.S.D.A., Report No. 2150, 1959.

Colby, R. H., "Breakdown of time-temperature superposition in Miscible Polymer Blends," Polymer, 1989, Vol. 30, pp. 1275-1278.

Davidson, R. W. , "The Influence of Temperature on Creep in Wood," Forest Products Journal, 1962, pp377-381

Desh, H. E. , Timber, its Structure, Properties and Utilisation, Timber Press, 1981.

Dinwoodie, J. M. , Wood: Nature's Cellular, Polymeric, Fibre-Composite, The Institute of Metals, 1989.

Emri, I. and Pavsek V., "On the Influence of Moisture on the Mechanical Properties of Polymers," Materials Forum, 1992, vol. 16, pp. 123-131.

Faherty, K. F. , Williamson, T. G. , Wood Engineering and Construction Handbook, McGraw Hill-Inc, 1989.

Ferry, J. D. , Viscoelastic Properties of Polymers, John Wiley and Sons, 1980.

Fesko, T. G. and Tschoegl, N. W. , "Time-Temperature Superposition in Thermorheologically Complex Materials," Journal of polymer science. Part C, Polymer letters, 1971, No. 35, pp. 51-69

Fesko, T. G. and Tschoegl, N. W. , "Time-Temperature Superposition in Styrene/Butadiene Block Copolymers," International Journal of Polymeric Materials, 1974, Vol. 3, pp. 55-79

Findley, W. N., "Creep Characteristics of Plastics," Proc. Symposium on Plastics, American Society for Testing and Materials, Philadelphia, PA, 1944, pp118-34.

Gamalath, S. , "Long Term Creep Modeling of Wood Using Time-Temperature Superposition Principle," Ph.D. Dissertation. Wood Science and Forest Products, Virginia Polytechnic Institute & State University, Virginia, USA, 1991.

Greenbaum, G. A. , and Rubinstein, M. F. , "Creep Analysis of Axisymmetric Bodies using Finite Elements," Nuclear Engineering and Design, Vol. 7, 1968, pp. 379-397.

Gressel, P. , "Prediction of Long-Term Deformation Behavior from Short-Term Creep Experiments," Holz als Roh- und Werkstoff, Vol. 42, 1984, pp. 293-301.

Hermida, E. B. and Povolo F., "Analytical-Numerical Procedure to Determine if a Set of Experimental Curves Can Be Superimposed to Form a Master Curve," Polymer Journal, Vol. 26, No. 9 pp 981-992 (1994).

Holzer, S. M. ,Loferski, J. R. , and Dillard, D. A. , "A Review of Creep in Wood: Concepts Relevant to Develop Long-Term Behavior Predictions for Wood Structures," Wood and Fiber Science, 21(4), 1989, pp. 376-392.

Huet, C. , and Navi, P. , "Multiparabolic Multitransition Model for Thermo-Viscoelastic Behavior of Wood," Mechanics of Wood and Paper Materials, AMD-Vol 112, 1990, pp. 17-24.

Irvine, G. M., "The Glass Transition of Lignin and Hemicellulose and their Measurement by Differential Thermal Analysis," Tappi Journal, May, 1984, pp. 118-121.

Kabir, A. F., "Nonlinear Analysis of Reinforced Concrete Panels, Slabs and Shells for Time dependent Effects," Ph.D. Dissertation. Civil Engineering, University of California, Berkeley, USA, 1976.

Kelly, S. S., Rials, T. G. , and Glasser, W. G , "Relaxation Behaviour of the Amorphous Components of Wood," Journal of Material Science, 1987, pp 22:617-624

Kraus, H. , Creep Analysis, Wiley, 1980.

Le Govic, C. , Felix, B. , Hadj Hamou, A. , Rouger, F. , and Huet, C. , "Evidence for an Equivalence Between Time and Temperature and Modeling Creep in Wood," Actes du 2e colloque. Sciences et industries du bois, Nancy, 22-24 avril, 1987, pp I:349-356.

Le Govic, C. , Felix, B. , Benzaim, A. , and Rouger, F. , "Creep Behavior of Wood as a Function of Temperature: Experimental Study, Modelling and Consequences for Design Codes," Proceedings of the Second Pacific Timber Engineering Conference, University of Auckland, New Zeland, 28-31 August, 1989, pp. 273-277.

Lim, C. K., Cohen, R.E., and Tschoegl, N. W., "Time-Temperature Superposition in Block Copolymers," Advances in Chemistry Series, ACS Monograph No. 99, 1971, pp. 397-417.

McCrum, N. G. ,and Morris, E. L. , "On the Measurement of the Activation Energies for Creep and Stress Relaxation," Proc. Roy. Soc., 1964, Vol. 281

Mendelson, A. , and Hirschberg, M. H. , and S. S. Manson, "A General Approach to the Practical Solution of Creep Problems," Journal of Basic Engineering, ASME, Vol. 81, 1959, pp. 585-598.

Nakayasu, H. , Markovitz, H., Plazek, D. J., "The frequency and Temperature Dependence of the Dynamic Mechanical Properties of a High Density Polyethylene," Transactions of The Society of Rheology, 1961, pp. 261-283.

National Design Specifications for Wood Construction, National Forest Products Association, 1986, Washington, D.C.

Neal, D. W. , "Restoration of Navy LTA (Lighter than Air) Hangars," Evaluation and Upgrading of Wood Structures: Case Studies, Proceedings Structures Congress '86, ASCE, September 1986, pp. 1-12.

Nickell, R. E. , "Thermal Stress and Creep," in Structural Mechanics Computer Programs, W. D. Pilkey et al., editors, University Press of Virginia, Charlottesville, 1974, pp. 103-122.

Nielsen, L. F. , "Power Law Creep as Related to Relaxation Elasticity, Damping, Rheological Spectra, and Creep Recovery - with Special Reference to Wood," IUFRO Timber Engineering Group Meeting, Xalapa, Mexico 1984.

Nielsen, L. F. , "Lifetime of Wood as Related to Strength Distribution," Reliability-Based Design of Engineered Wood Structures, Bodig, J. (ed.), Kluwe Academic Publishers, 1992.

Nilson, A. H. , et al., Finite Element Analysis of Reinforced Concrete, American Society of Civil Engineers, 1982.

Onogi, S., Sasaguri, K., Adachi, T., Ogihara, S., "Time-Humidity Superposition in Some Crystalline Polymers," Journal of Polymer Science, 1962, Vol. 58, pp. 1-17.

Oviatt, A. E. Jr., "Moisture Content of Glulam Timbers in Use in the Pacific Northwest," Pacific Northwest Forest and Range Experiment Station, Forest Service, U.S.D.A., 1968.

Plazek, D. J., "Temperature Dependence of the Viscoelastic Behavior of Polystyrene," The Journal of Physical Chemistry, 1965, v 69 pp 480-487.

Povolo, F., and Fontelos, N. , "Procedure to Determine if a set of Experimental Curves are Really Related by Scaling," Res Mechanica, Vol. 22, 1987, pp. 185-198.

Sakata, I. , and Senju, R. , "Thermoplastic Behavior of Lignin with Various Synthetic Plastisizers," Journal of Applied Polymer Science, 19pp19:2799-2810

Salmèn, N. L., "Viscoelastic Properties of in Situ Lignin Under Water-Saturated Conditions," Journal of Material Science, 1975, pp10:3090-3096

Schniewind, A. P., "Recent Progress in the Study of the Rheology of Wood." Wood Science and Technology, Vol 2, 1968, pp 188-206.

Sharma, M. G. , "Theories of Phenomenological Viscoelasticity Underlying Mechanical Testing," Testing of Polymers, Schmitz, J. V. (ed.), Interscience Publishers, 1965, pp. 147-199.

Simpson, W. T., "Equilibrium Moisture Content Prediction for Wood." Forest Products Journal, 1971, Col. 21, pp 48-49.

Snyder, M. D. and Bathe, K. J. , "A Solution Procedure for Thermo-Elastic-Plastic and Creep Problems," Nuclear Engineering and Design, Vol. 64, 1981, pp. 49-80.

Takayanagi, M. , "Viscoelastic Behavior of Crystalline Polymers," Fourth International Congress on Rheology, Vol. 1, Interscience, New York, 1965, pp. 161-187

Tissaoui, J., "Stability Analysis of the Church of the Nazarene Varax Dome", M.S. Thesis. Civil Engineering, Virginia Polytechnic Institute & State University, Virginia, USA, 1991.

Tissaoui, J., Loferski, J. R., Holzer, S. M., Dillard, D. A., Bond, B. H.,

"Long-term creep law for wood in compression and tension parallel to grain," Mechanics of Cellulosic Materials, American Society of Mechanical Engineers, Applied Mechanics Division, v 145, pp 33-38

Van Der Put, T. A. C. M. , "Deformation and Damage Processes in Wood," Delft University Press, 1989.

Yen, S. , and Williamson, F. L. , "Accelerated Characterization of Creep Response of an Off-Axis Composite Material," Composites Science and Technology, Vol. 38, 1990, pp. 103-118.

Williams, J. G., Stress Analysis of Polymers, John Wiley and Sons, 1980.

Wolcott, M. P., "Modeling Viscoelastic Cellular Materials for the Pressing of Wood Composites," Ph.D. Dissertation. Materials Engineering Science, Virginia Polytechnic Institute & State University, Virginia, USA, 1989.

Wood Handbook, United States Department of Agriculture, U.S. Forest Products Laboratory, Agriculture Handbook No. 72, U.S. Government Printing Office, Washington, D.C., 1987.

Zienkiewicz, O. C., The finite Element Method in Engineering Science, McGraw-Hill, London, 1971

Zienkiewicz, O. C. , and Corneau, I. C. , "Viscoplasticity-Plasticity and Creep in Elastic Solids - A United Numerical Approach," International Journal for Numerical Methods in Engineering, Vol. 8, 1974, pp. 821-845.

Zienkiewicz, O. C. , and Watson, M. , "Some Creep Effects in Stress Analysis with Particular Reference to Concrete Pressure Vessels," Nuclear Engineering and Design, Vol. 4, 1966, pp. 406-412.

Vita

Jacem Tissaoui was born in Jendouba, Tunisia on December 5, 1967. He finished high school in 1985 after which he came to the United States to pursue a Bachelor of Science degree in Civil Engineering at Penn State. After graduating in 1989, he attended Virginia Tech where he obtained a Master of Science degree in Civil engineering and continued to pursue a PhD degree. He was married in 1992 to Luz and had a son, Yassine in 1994. After graduating he plans to go home to Tunisia.